
Andreas Schadschneider
Götz S. Uhrig

Strongly Correlated Systems in Solid State Physics

Version: March 12, 2004

Sommersemester 2003

Contents

I	Introduction	3
I.1	Strongly correlated systems	3
I.2	The Hubbard model and its relatives	3
I.2.1	Derivation of the Hubbard model	3
II	Exact solution of one-dimensional spin models	7
II.1	Heisenberg model	7
II.2	Solution of the XY model	8
II.2.1	Diagonalization of quadratic forms	11
II.2.2	Spectrum of the XY model	13
II.2.3	Summary	15
II.3	Bethe-Ansatz for the XXZ model	17
II.3.1	Symmetries and invariant subspaces	17
II.3.2	The Bethe-Ansatz	18
II.4	Relation between classical and quantum systems	25
II.4.1	Spin models	26
II.4.2	Vertex models	27
II.4.3	Partition function and transfer matrix	30
II.4.4	Commuting transfer matrices	32
II.4.5	Transfer matrix and conserved quantities	33
II.4.6	The Yang-Baxter equation	37
II.4.7	Trotter-Suzuki decomposition	39
II.5	Algebraic Bethe Ansatz	41
II.6	Spectrum and structure of excitations in the XXZ model	47
II.6.1	Isotropic ferromagnet	47
II.6.2	Isotropic antiferromagnet	52
II.6.3	Anisotropic XXZ model	61
II.6.4	Magnetic field effects	65
A	Exercises	69

B Supplementary material	73
B.1 Phase diagram of the 6-vertex model	73
B.2 More on strings	75
B.3 Inversion relations	76

Chapter I

Introduction

I.1 Strongly correlated systems

What are “strongly correlated systems”? One of the goals of this course is to try answering this question. There is no accepted precise definition, but for starters we give a somewhat vague description. In the following it hopefully becomes clear that strongly correlated systems are “more than just the sum of their parts”. Typically the systems we are dealing with are made up of a large number of simple elements, e.g. localized spin-1/2. But through their mutual interaction these simple elements can lead to rather complex behaviour, especially various kinds of orderings as magnetic order (ferromagnetic or antiferromagnetic) or superconductivity. Often there are even phase transitions between different ordered states as parameters like the interaction strengths are varied.

I.2 The Hubbard model and its relatives

Before we start to discuss some specified models and introduce the methods for their investigation we try to give a rather general justification for the class of Hamiltonians that we will be the focus of this course. Here we try to identify the essential degrees of freedom which allows to simplify the description by obtaining an effective Hamiltonian for them.

I.2.1 Derivation of the Hubbard model

We start from the very general Hamiltonian describing the interactions between electrons in the potential $U_{ion}(\mathbf{r})$ created by a static lattice of ions. Here we have already neglected the motion of the ions since we are mainly interested in the interactions of electrons and (localized) spins. Therefore dynamic lattice effects like phonons will play almost no role in the things to come.

The electrons interact via Coulomb repulsion $V_{ee}(\mathbf{r} - \mathbf{r}') \propto \frac{1}{|\mathbf{r} - \mathbf{r}'|}$. In the language of second quantization the Hamiltonian for this system of ions and electrons reads

$$\begin{aligned}
\mathcal{H} &= \mathcal{H}_{kin} + \mathcal{H}_{int} \\
&= \sum_{\sigma} \int d^3r \psi_{\sigma}^{\dagger}(\mathbf{r}) \left[-\frac{\hbar^2}{2m} \nabla^2 + U_{ion}(\mathbf{r}) \right] \psi_{\sigma}(\mathbf{r}) \\
&\quad + \sum_{\sigma, \sigma'} \int d^3r \int d^3r' \psi_{\sigma}^{\dagger}(\mathbf{r}) \psi_{\sigma'}^{\dagger}(\mathbf{r}') V_{ee}(\mathbf{r} - \mathbf{r}') \psi_{\sigma'}(\mathbf{r}') \psi_{\sigma}(\mathbf{r})
\end{aligned} \tag{I.2.1}$$

with field operators $\psi_{\sigma}^{\dagger}(\mathbf{r})$.

According to Bloch's theorem the free electronic band $\epsilon_{\mathbf{k}} = \frac{\hbar^2 k^2}{2m}$ splits under the influence of the periodic potential U_{ion} in an infinite number of bands with Bloch functions $u_{\mathbf{k}\alpha}$. Basically Bloch functions allow to reduce the problem to a boundary-value problem for the unit cell which then leads for each wave vector \mathbf{k} to a discrete spectrum labeled by the band index α . From these we introduce the *Wannier functions*

$$\phi_{i\alpha}(\mathbf{r}) = \frac{1}{\sqrt{L}} \sum_{\mathbf{k}} e^{-i\mathbf{k}\cdot\mathbf{R}_i} u_{\mathbf{k}\alpha}(\mathbf{r}) \tag{I.2.2}$$

which are localized at site \mathbf{R}_i of the ion lattice. L denotes the number of lattice sites. Since the Wannier functions are related to the Bloch functions by an unitary transformation they are a completely equivalent description of the underlying physics.

We now define creation operators for electrons in a Wannier orbital:

$$c_{i\alpha\sigma}^{\dagger} = \int d^3r \phi_{i\alpha}(\mathbf{r}) \psi_{\sigma}^{\dagger}(\mathbf{r}) \tag{I.2.3}$$

with the inverse relation

$$\psi_{\sigma}^{\dagger}(\mathbf{r}) = \sum_{i,\alpha} \phi_{i\alpha}^*(\mathbf{r}) c_{i\alpha\sigma}(\mathbf{r}). \tag{I.2.4}$$

These operators are fermionic and satisfy the anticommutation relations

$$\{c_{j\alpha\sigma}, c_{l\beta\sigma'}^{\dagger}\} = \delta_{jl} \delta_{\alpha\beta} \delta_{\sigma\sigma'}, \quad \{c_{j\alpha\sigma}, c_{l\beta\sigma'}\} = \{c_{j\alpha\sigma}^{\dagger}, c_{l\beta\sigma'}^{\dagger}\} = 0. \tag{I.2.5}$$

Transforming the Hamiltonian to the Wannier basis one obtains

$$\mathcal{H} = \sum_{ij\alpha\sigma} t_{ij}^{\alpha} c_{i\alpha\sigma}^{\dagger} c_{j\alpha\sigma} + \sum_{ijmn} \sum_{\alpha\beta\mu\nu} \sum_{\sigma\sigma'} v_{ijmn}^{\alpha\beta\mu\nu} c_{i\alpha\sigma}^{\dagger} c_{j\beta\sigma'}^{\dagger} c_{n\mu\sigma'} c_{m\nu\sigma} \tag{I.2.6}$$

with matrix elements

$$\begin{aligned}
t_{ij}^{\alpha} &= \langle i\alpha | \left[-\frac{\hbar^2}{2m} \nabla^2 + U_{ion}(\mathbf{r}) \right] | j\alpha \rangle \\
&= \int d^3r \phi_{i\alpha}^*(\mathbf{r}) \left[-\frac{\hbar^2}{2m} \nabla^2 + U_{ion}(\mathbf{r}) \right] \phi_{j\alpha}(\mathbf{r})
\end{aligned} \tag{I.2.7}$$

and

$$\begin{aligned} v_{ijmn}^{\alpha\beta\mu\nu} &= \langle i\alpha, j\beta | V_{ee}(\mathbf{r} - \mathbf{r}') | m\mu, n\nu \rangle \\ &= \int d^3r \int d^3r' \phi_{i\alpha}^*(\mathbf{r}) \phi_{j\beta}^*(\mathbf{r}') V_{ee}(\mathbf{r} - \mathbf{r}') \phi_{m\mu}(\mathbf{r}) \phi_{n\nu}(\mathbf{r}'). \end{aligned} \quad (\text{I.2.8})$$

Up to now we have not made any approximations (apart from the assumption that the ions are static). (I.2.6) is just the basic Hamiltonian (I.2.1) rewritten in a basis which is more suitable to describe the aspects that we will be interested in.

Following Hubbard [1] we make some simplifying assumptions. First of all we look at the case where only one relevant band α exists. This means that we can drop the summations over α, β etc. as well as the band index itself. Furthermore we assume an s-band. Then t_{ij} is a function of the distance between the sites i and j and has no direction dependence, i.e. $t_{ij} = t(|\mathbf{R}_i - \mathbf{R}_j|)$. The Hamiltonian (I.2.6) is then simplified to

$$\boxed{\mathcal{H} = \sum_{ij\sigma} t_{ij} c_{i\sigma}^\dagger c_{j\sigma} + \sum_{ijmn} \sum_{\sigma\sigma'} v_{ijmn} c_{i\sigma}^\dagger c_{j\sigma'}^\dagger c_{n\sigma'} c_{m\sigma}} \quad (\text{I.2.9})$$

Usually the matrix elements decrease strongly with increasing distance $|\mathbf{R}_i - \mathbf{R}_j|$. Therefore in (I.2.9) we can restrict the interaction to nearest neighbours $\langle ij \rangle$:

$$\boxed{\begin{aligned} \mathcal{H} &= -t \sum_{\langle ij \rangle} \sum_{\sigma} \left(c_{i\sigma}^\dagger c_{j\sigma} + c_{j\sigma}^\dagger c_{i\sigma} \right) + U \sum_i n_{i\uparrow} n_{i\downarrow} + V \sum_{\langle ij \rangle} n_i n_j \\ &\quad + X \sum_{\langle ij \rangle} \sum_{\sigma} \left(c_{i\sigma}^\dagger c_{j\sigma} + c_{j\sigma}^\dagger c_{i\sigma} \right) (n_{i,-\sigma} + n_{j,-\sigma}) + J \sum_{\langle ij \rangle} \mathbf{S}_i \cdot \mathbf{S}_j \\ &\quad + Y \sum_{\langle ij \rangle} \left(c_{i\uparrow}^\dagger c_{i\downarrow}^\dagger c_{j\downarrow} c_{j\uparrow} + c_{j\downarrow}^\dagger c_{j\uparrow}^\dagger c_{i\uparrow} c_{i\downarrow} \right) \end{aligned}} \quad (\text{I.2.10})$$

where the short-hand notation

$$\begin{aligned} t &= -t_{ij}, & U &= v_{iiii}, \\ X &= v_{iiij}, & V &= v_{ijij}, \\ J &= -2v_{ijji}, & Y &= v_{iiji} \end{aligned} \quad (\text{I.2.11})$$

has been introduced. The particle number operators $n_{i\sigma}$, n_i and the spin operators are defined as usual through

$$n_{j\sigma} = c_{j\sigma}^\dagger c_{j\sigma}, \quad n_j = n_{j\uparrow} + n_{j\downarrow}, \quad \mathbf{S}_i = \frac{1}{2} \sum_{\alpha,\beta} c_{i\alpha}^\dagger \tau_{\alpha\beta} c_{i\beta} \quad (\text{I.2.12})$$

with $\tau_{\alpha\beta} = ((\tau^x)_{\alpha\beta}, (\tau^y)_{\alpha\beta}, (\tau^z)_{\alpha\beta})$, where τ^α are the standard Pauli matrices.

(I.2.10) is known as *generalized Hubbard model*. Apart from the *single-particle hopping* term t , which describes the motion of electrons to neighbouring lattice sites, and the (*on-site*) *Coulomb*

interaction U of two electrons at the same site, the Hamiltonian contains additional interaction terms. V is the Coulomb interaction between electrons at neighbour sites. X is called *bond-charge interaction*. It corresponds to a single-particle hopping where the hopping amplitude depends on the occupation numbers of the sites involved. In fact it is proportional to the charge (number of electrons) located at the bond $\langle ij \rangle$ between the sites i and j which motivates the name. J is a *spin-spin interaction* between neighbouring particles and Y is a term describing the *hopping of pairs* of electrons to neighbour sites.

Each lattice site j in the generalized Hubbard model can be in one of four different states: empty, singly-occupied by an electron with spin \uparrow , singly-occupied by an electron with spin \downarrow , and doubly-occupied by two electrons (with spins \uparrow and \downarrow , respectively).

It is helpful to determine some symmetries of the Hamiltonian (I.2.10). It can be checked that it commutes with the following operators:

$$N = \sum_j n_j, \quad M = N_\uparrow - N_\downarrow = \sum_j (n_{j\uparrow} - n_{j\downarrow}), \quad \mathbf{S} = \sum_j \mathbf{S}_j. \quad (\text{I.2.13})$$

This corresponds to the conserveration of the total number N of electrons, the magnetization M and the total spin \mathbf{S} .

Hubbard [1] gave a simple estimate for the matrix elements in the case of transition metals: $t \approx 1 \text{ eV}$, $U \approx 10 \text{ eV}$, $V \approx 2 - 3 \text{ eV}$, $X \approx 0.5 \text{ eV}$ und $J, Y \ll 1 \text{ eV}$. This was taken as motivation to neglect all interaction terms except for the on-site Coulomb repulsion U and the single-particle hopping t which is of course needed to describe the relevant physics correctly. The resulting Hamiltonian is nowadays simply called the *Hubbard model*. However it should be emphasized that at about the same time it was “discovered” independently by Gutzwiller [2] and Kanamori [3].

Chapter II

Exact solution of one-dimensional spin models

In the following we want to discuss various special cases of the general Hamiltonian (I.2.10) for a one-dimensional lattice. This is interesting for several reasons. First of all, in one dimension methods for an exact treatment of such interacting many-body problems exist. It is one goal of this chapter to give an overview of these approaches. From a physical point of view low-dimensional systems can be interesting due to the importance of quantum fluctuations. These compete with tendencies to ordering and lead in many cases to a behaviour very different to that found in higher dimensions. Finally, there are many real substances which — as very good approximation — can be regarded as low dimensional. The most important example are high-temperature superconductors where the important physics takes place in two-dimensional copper-oxide planes. Their discovery has inspired a search for related materials, also in order to determine the mechanism leading to superconductivity. It is believed that the low dimensionality is an essential ingredient. In recent years a variety of materials which can be regarded as effectively one-dimensional chain structures have been synthesized.

II.1 Heisenberg model

We start our discussion of special Hamiltonians with the Heisenberg model and its variants. In the Heisenberg model [4] only the spin exchange term J is non-vanishing. Therefore we deal with a system of *localized spins*, i.e. there are no hopping processes. These kind of models have been introduced to describe magnetic ordering phenomena, e.g. *ferromagnetism* or *antiferromagnetism*.

In the derivation presented in Sec. I.2 we have obtained the isotropic variant of the Heisenberg model. In principle one can imagine a general anisotropic interaction of the form

$$\mathcal{H} = \pm \sum_{j=1}^L [J_x S_j^x S_{j+1}^x + J_y S_j^y S_{j+1}^y + J_z S_j^z S_{j+1}^z] - B \sum_{j=1}^L S_j^z \quad (\text{II.1.1})$$

where we have also allowed for a magnetic field in z -direction. We have written the Hamiltonian (II.1.1) already in a form taking into account the chain structure of the one-dimensional lattice. Usually *periodic boundary conditions* are used to make the system translational invariant. This means that spin operators S_{L+1}^α , which appear in the sum in (II.1.1), are identified with S_1^α .

A remark should be made about the overall sign which we have taken as \pm in (II.1.1). There is no general convention for either choice, instead both are used depending on the purpose. This can be understood best by going back to the isotropic case $J_x = J_y = J_z =: J$. Neglecting quantum mechanics for a moment one sees that for the case $\pm J < 0$ the energy is minimized if neighbouring spins are parallel. This corresponds to *ferromagnetism*. On the other, for $\pm J > 0$ an anti-parallel orientation of spins is favoured, leading to *antiferromagnetism*. Therefore if one wants to study ferromagnetism, the sign is chosen as $-J$ whereas for antiferromagnetic materials $+J$ is used. This has the advantage that the exchange constant J has to be positive in both cases. However, one should be careful when comparing with results from various publications which convention actually has been used.

Apart from the case $J_x = J_y = J_z$ corresponding to the isotropic Heisenberg model, other special cases are worth mentioning. The most general case where all couplings can be different is called *XYZ model*. It is worth pointing out that this case can be solved exactly for vanishing magnetic field $B = 0$ by using the so-called *Bethe-Ansatz*. The solution, i.e. the determination of the energy spectrum and corresponding eigenfunctions, is due to R. Baxter [5, 6] in 1972.

The case $J_x = J_y \neq J_z$ is called *XXZ model*. It is exactly solvable for general values of couplings and magnetic field. We will present the construction of the eigenstates using the Bethe-Ansatz in Sec. II.3. Note that this kind of asymmetry is rather natural for a one-dimensional lattice. One can imagine that the interaction in direction of the chain (along the z -axis) is different from that perpendicular to the chain. A similar argument applies to the two-dimensional variant. Finally, the case $J_z = 0$ is called *XY model*. It is also exactly solvable, even without Bethe-Ansatz. This will be the topic of the next section.

II.2 Solution of the *XY* model

Although the asymmetry of the *XY* model is not the most realistic one, we can learn a lot from the exact solution of this model, not only about techniques but also about the underlying physics. For convenience we rewrite the Hamiltonian of the *XY* model in the form

$$\boxed{\mathcal{H}_{xy} = -\frac{1}{2} \sum_{j=1}^L [(1+\gamma)\sigma_j^x \sigma_{j+1}^x + (1-\gamma)\sigma_j^y \sigma_{j+1}^y + 2B\sigma_j^z]} \quad (\text{II.2.1})$$

in terms of Pauli matrices

$$\sigma^x = \begin{pmatrix} 0 & 1 \\ 1 & 0 \end{pmatrix}, \quad \sigma^y = \begin{pmatrix} 0 & -i \\ i & 0 \end{pmatrix}, \quad \sigma^z = \begin{pmatrix} 1 & 0 \\ 0 & -1 \end{pmatrix} \quad (\text{II.2.2})$$

instead of spin-1/2 operators $S^\alpha = \frac{1}{2}\sigma^\alpha$.

In the following we assume that the magnetic field B , the anisotropy parameter γ and the chain length L satisfy

$$B \geq 0, \quad 0 \leq \gamma \leq 1, \quad L \text{ even.} \quad (\text{II.2.3})$$

Furthermore we will use periodic boundary conditions, i.e.

$$\sigma_{L+1}^\alpha = \sigma_1^\alpha \quad (\alpha = x, y, z). \quad (\text{II.2.4})$$

We now introduce the spin flip operators σ^\pm

$$\sigma^x = \sigma^+ + \sigma^-, \quad \sigma^y = \frac{1}{i} (\sigma^+ - \sigma^-). \quad (\text{II.2.5})$$

The Pauli matrices satisfy the algebra

$$\{\sigma_j^+, \sigma_j^-\} = 1, \quad [\sigma_j^\alpha, \sigma_l^\beta] = 0 \quad \text{for } j \neq l \text{ and } \alpha, \beta = x, y, z, +, -, \quad (\text{II.2.6})$$

where $\{A, B\}$ denotes the anticommutator of operators A, B .

Jordan and Wigner [7] have already in 1928 proposed to express the spin-1/2 operators through proper fermion operators. This means that the commutator in (II.2.6) is changed into an anticommutator so that the algebraic relations obtain an uniform structure ¹. It is obvious to try this using fermions instead of bosons because the Hilbert spaces have the same dimensions. This implies the identification

$$|\uparrow\rangle \longleftrightarrow |1\rangle, \quad |\downarrow\rangle \longleftrightarrow |0\rangle \quad (\text{II.2.7})$$

where $|\uparrow\rangle, |\downarrow\rangle$ are S^z eigenstates in spin language and $|1\rangle, |0\rangle$ the fermion eigenstates where a fermion is present or non-present, respectively.

The *Jordan-Wigner transformation* is then defined by

$$\begin{aligned} \sigma_j^+ &= \exp\left(i\pi \sum_{l=1}^{j-1} c_l^\dagger c_l\right) \cdot c_j^\dagger, \\ \sigma_j^- &= \exp\left(i\pi \sum_{l=1}^{j-1} c_l^\dagger c_l\right) \cdot c_j, \\ \sigma_j^z &= 2c_j^\dagger c_j - 1. \end{aligned} \quad (\text{II.2.8})$$

Here the operators c_j, c_j^\dagger are (spinless) fermion operators satisfying the usual anticommutation relations (Exercise 1)

$$\{c_j, c_l^\dagger\} = \delta_{jl}, \quad \{c_j, c_l\} = \{c_j^\dagger, c_l^\dagger\} = 0. \quad (\text{II.2.9})$$

As usual we define the number operators $n_j = c_j^\dagger c_j$ which have eigenvalues 0 and 1 corresponding to the number of particles at site j .

¹The problem is that such mixed commutator/anticommutator structures do not allow a *canonical* transformation in the usual sense.

The factor

$$F_j := e^{i\pi \sum_{l=1}^{j-1} c_l^\dagger c_l} = (-1)^{\sum_{l=1}^{j-1} n_l} = \prod_{l=1}^{j-1} (1 - 2c_l^\dagger c_l) \quad (\text{II.2.10})$$

commutes with c_j^\dagger and c_j and should be familiar from the definition of fermionic creation/annihilation operators. The exponent counts the number of occupied state “to the left” of the site j . It is just the number of times the operator has to be (anti-)commuted with other creation or annihilation operators to move it into the correct position in the standard ordering. Therefore F_j is ± 1 depending on whether the number of occupied sites to the left is even or odd. This becomes especially obvious in the second representation given in (II.2.10).

An important property that we will need in the following is

$$F_j F_{j+1} = (-1)^{n_j}. \quad (\text{II.2.11})$$

We now can translate the Hamiltonian of the XY model into fermionic language making use of this identity. For $j \neq L$ we have

$$\sigma_j^x \sigma_{j+1}^x = (c_j^\dagger - c_j)(c_{j+1}^\dagger + c_{j+1}) \quad (\text{II.2.12})$$

$$\sigma_j^y \sigma_{j+1}^y = (c_j^\dagger + c_j)(c_{j+1} - c_{j+1}^\dagger). \quad (\text{II.2.13})$$

Here the identity

$$(c_j^\dagger + c_j)(-1)^{n_j} = c_j^\dagger - c_j \quad (\text{II.2.14})$$

has been used which is easily verified for the basis states $|0\rangle$ and $|1\rangle$.

The boundary terms $\sigma_L^\alpha \sigma_1^\alpha$ have to be treated separately. For the first term we have

$$\sigma_L^x \sigma_1^x = (-1)^{\sum_{j=1}^{L-1} n_l} (c_L^\dagger + c_L)(c_1^\dagger + c_1). \quad (\text{II.2.15})$$

We now define the operator

$$P := (-1)^{\sum_{j=1}^L n_l} = (-1)^N = \prod_{l=1}^L (-\sigma_l^z) \quad (\text{II.2.16})$$

where $N = \sum_{j=1}^L n_l$ is the total number of fermions. Obviously $P^2 = 1$ so that P has only the eigenvalues ± 1 , i.e.

$$P = \begin{cases} +1 & \text{for even } N \\ -1 & \text{for odd } N. \end{cases} \quad (\text{II.2.17})$$

Furthermore P commutes with \mathcal{H}_{xy} , i.e. $[P, \mathcal{H}_{xy}] = 0$. This can most easily be seen from the fact that \mathcal{H}_{xy} changes the particle number by either 0 or 2. Therefore the Hilbert space \mathcal{G} is the direct sum of two subspaces \mathcal{G}_+ and \mathcal{G}_- which contain the states with $P = +1$ and $P = -1$, respectively: $\mathcal{G} = \mathcal{G}_+ \oplus \mathcal{G}_-$. This simplifies the problem since now both cases can be treated separately.

We now can rewrite the boundary term as

$$\sigma_L^x \sigma_1^x = -P(c_L^\dagger - c_L)(c_1^\dagger + c_1). \quad (\text{II.2.18})$$

If we choose antiperiodic boundary conditions ($c_{L+1} = -c_1$, $c_{L+1}^\dagger = -c_1^\dagger$) in the subspace with $P = +1$ and periodic ones ($c_{L+1} = c_1$, $c_{L+1}^\dagger = c_1^\dagger$) for $P = -1$, we can rewrite the fermionic Hamiltonian in both cases as

$$\mathcal{H}_F = -\sum_{j=1}^L \left[(c_j^\dagger c_{j+1} + c_{j+1}^\dagger c_j) + \gamma (c_j^\dagger c_{j+1}^\dagger + c_{j+1} c_j) + 2B c_j^\dagger c_j - B \right]. \quad (\text{II.2.19})$$

The precise relation between \mathcal{H}_{xy} and \mathcal{H}_F is then

$$\mathcal{H}_{xy} = \frac{1+P}{2} \mathcal{H}_F^{(ap)} + \frac{1-P}{2} \mathcal{H}_F^{(per)} \quad (\text{II.2.20})$$

where $\mathcal{H}_F^{(ap)}$ and $\mathcal{H}_F^{(per)}$ denotes the Hamiltonian (II.2.19) with antiperiodic and periodic boundary conditions, respectively. We see that the spectrum of the spin Hamiltonian is composed of half of the spectrum of the fermion Hamiltonian with antiperiodic boundary conditions, and half of the spectrum of \mathcal{H}_F for periodic boundary conditions. The other states appearing in the spectra of the fermion chain have no relevance for the spin problem.

II.2.1 Diagonalization of quadratic forms

In the following we want to discuss a general procedure to diagonalize quadratic forms of fermion operators as given in [8]. For our specific problem of nearest-neighbour interactions there is a simpler alternative which is discussed in Exercise 5. However, since such quadratic forms appear frequently we try to be as general as possible.

We consider the following quadratic form

$$\mathcal{H} = \sum_{i,j=1}^L \left[c_i^\dagger A_{ij} c_j + \frac{1}{2} (c_i^\dagger B_{ij} c_j^\dagger + h.c.) \right] \quad (\text{II.2.21})$$

with fermion operators c_j , c_j^\dagger . “h.c.” denotes the hermitean conjugate of the other term in the brackets. Since \mathcal{H} is an Hamiltonian and thus hermitean, the matrix $\mathbf{A} = (A_{ij})$ is also hermitean and the matrix $\mathbf{B} = (B_{ij})$ is anti-symmetric. In the following we assume \mathbf{A} and \mathbf{B} to be real which is satisfied in most applications.

Our goal is to diagonalize the quadratic form (II.2.21) so that we can easily determine the spectrum. To be more precise we are looking for a transformation (*Bogoliubov transformation*)²

$$\begin{aligned} \eta_k &= \sum_j (g_{kj} c_j + h_{kj} c_j^\dagger), \\ \eta_k^\dagger &= \sum_j (g_{kj} c_j^\dagger + h_{kj} c_j), \end{aligned} \quad (\text{II.2.22})$$

²This transformation mixes creation and annihilation operators and should be familiar from BCS theory.

to new fermion operators η_k, η_k^\dagger , i.e. a canonical transformation, such that the Hamiltonian \mathcal{H} is transformed into

$$\mathcal{H} = \sum_k \Lambda_k \eta_k^\dagger \eta_k + \text{const.} \quad (\text{II.2.23})$$

This new Hamiltonian is a diagonal free-fermion model and we can read off the eigenvalues Λ_k immediately. We now have to show that we can indeed find (real) constants g_{kj} and h_{kj} such that the Bogoliubov transformation (II.2.22) leads to (II.2.23).

First of all we observe that $[\eta_k, \mathcal{H}] = \Lambda_k \eta_k$ which implies explicitly

$$\Lambda_k g_{kj} = \sum_l (g_{kl} A_{lj} - h_{kl} B_{lj}), \quad (\text{II.2.24})$$

$$\Lambda_k h_{kj} = \sum_l (g_{kl} B_{lj} - h_{kl} A_{lj}). \quad (\text{II.2.25})$$

If we define new constants $\phi_{kj} := g_{kj} + h_{kj}$ and $\psi_{kj} := g_{kj} - h_{kj}$ we can rewrite these equations in matrix form:

$$\begin{aligned} \phi_k (\mathbf{A} - \mathbf{B}) &= \Lambda_k \psi_k, \\ \psi_k (\mathbf{A} + \mathbf{B}) &= \Lambda_k \phi_k, \end{aligned} \quad (\text{II.2.26})$$

where we have introduced (row) vectors $\phi = (\phi_{kj})_j$ and $\psi = (\psi_{kj})_j$. Iterating these equations leads to a decoupling

$$\begin{aligned} \phi_k (\mathbf{A} + \mathbf{B})(\mathbf{A} - \mathbf{B}) &= \Lambda_k \phi_k, \\ \psi_k (\mathbf{A} - \mathbf{B})(\mathbf{A} + \mathbf{B}) &= \Lambda_k \psi_k. \end{aligned} \quad (\text{II.2.27})$$

These equations can always be solved. To see this, first observe that

$$(\mathbf{A} + \mathbf{B})^t = \mathbf{A} - \mathbf{B} \quad (\text{II.2.28})$$

and therefore

$$(\mathbf{A} + \mathbf{B})(\mathbf{A} - \mathbf{B}), (\mathbf{A} - \mathbf{B})(\mathbf{A} + \mathbf{B}) \quad \text{symmetric and positive-semidefinit.} \quad (\text{II.2.29})$$

The positivity follows from the fact that e.g. $\mathbf{v}^t (\mathbf{A} + \mathbf{B})(\mathbf{A} - \mathbf{B}) \mathbf{v} \geq 0$ for any vector \mathbf{v} . These properties guarantee that the matrices in (II.2.27) can be diagonalized and that their eigenvalues are non-negative. Therefore the Λ_k are real. Furthermore it is possible to choose ϕ_k, ψ_k as real and orthogonal vectors. This concludes the proof that the desired transformation indeed exists.

In order to determine the transformation explicitly, for $\Lambda_k \neq 0$ one first solves one of the equations in (II.2.27). The other eigenvector can then be obtained from (II.2.26). In the case $\Lambda_k = 0$ it is simpler to solve (II.2.26) directly. For $\Lambda_k \neq 0$, if ϕ_k is normalized, i.e. $\sum_j \phi_{kj} = 1$, then ψ_k will be normalized automatically.

Summarizing, since from the knowledge of ϕ_k and ψ_k we can determine the original parameters g_{kj} and h_{kj} , we have found that

$$\sum_j (g_{kj}g_{k'j} + h_{kj}h_{k'j}) = \delta_{kk'}, \quad (\text{II.2.30})$$

$$\sum_j (g_{kj}h_{k'j} + g_{k'j}h_{kj}) = 0, \quad (\text{II.2.31})$$

are necessary and sufficient conditions that the new operators η_k , η_k^\dagger are Fermi operators that diagonalize the Hamiltonian (II.2.21).

Finally a brief remark about the constant in (II.2.23). It can be determined from the invariance of the trace under the canonical transformation and one finds [8]

$$\mathcal{H} = \sum_k \Lambda_k \eta_k^\dagger \eta_k + E_0 \quad \text{with} \quad E_0 = \frac{1}{2} \left(\sum_j A_{jj} - \sum_k \Lambda_k \right). \quad (\text{II.2.32})$$

II.2.2 Spectrum of the XY model

We are now going back to the XY model and use these results to determine its spectrum. One finds (see also Exercise 5):

$$\Lambda_k = 2\sqrt{(B + \cos k)^2 + \gamma^2 \sin^2 k}. \quad (\text{II.2.33})$$

The allowed wavenumbers for periodic and antiperiodic boundary conditions are obtained from the eigenvalues of the translation operator which implies $e^{ikL} = 1$ and $e^{ikL} = -1$, respectively. Thus we have

$$\text{periodic boundary conditions: } k = \frac{2\pi}{L}n, \quad (\text{II.2.34})$$

$$\text{antiperiodic boundary conditions: } k = \frac{\pi}{L}(2n - 1), \quad (\text{II.2.35})$$

where n takes only integer values. The typical form of this function (of k) is shown in Fig. II.2.1. In the thermodynamic limit $L \rightarrow \infty$ both sets of wavenumbers form a continuous distribution. One also sees that in this limit the differences due to the boundary conditions become unimportant.

Since $\Lambda_k \geq 0$ for all wavenumbers k , the groundstate $|0\rangle$ is characterized by the condition

$$\eta_k |0\rangle = 0 \quad \text{for all } k. \quad (\text{II.2.36})$$

The groundstate energy is then given by the constant

$$E_0 = -\frac{1}{2} \sum_k \Lambda_k \quad (\text{II.2.37})$$

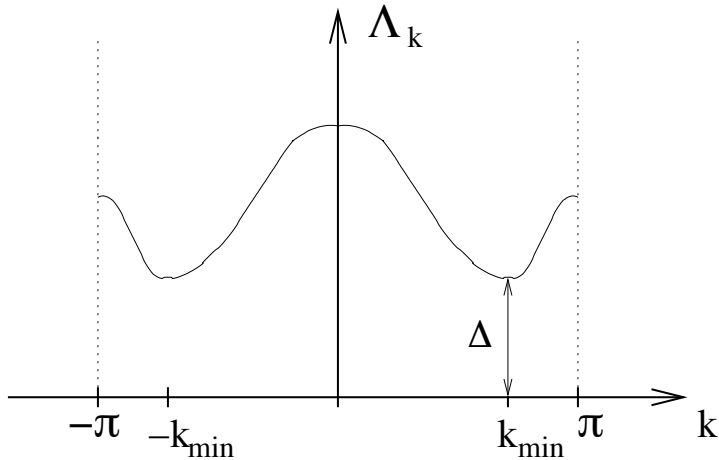


Figure II.2.1: Typical form of the dispersion Λ_k of the XY model.

where one has to choose $A_{jj} = 2B$ in (II.2.32), but this contribution is cancelled by the additional additive constant $-B$ in (II.2.19).

Excitations above this groundstate are generated by η_k^\dagger . One finds that generically an excitation gap $\Delta = \min_k \Lambda_k$ exists:

$$\Delta = \min_k \Lambda_k = \begin{cases} 2\gamma \sqrt{1 - \frac{B^2}{1-\gamma^2}} & \text{for } B < 1 - \gamma^2 \\ 2|B - 1| & \text{for } B \geq 1 - \gamma^2 \end{cases} \quad (\text{II.2.38})$$

where the gap occurs at a wavevector k_{\min} defined by

$$\cos k_{\min} = \begin{cases} -\frac{B}{1-\gamma} & \text{for } B < 1 - \gamma^2 \\ -1 & \text{for } B \geq 1 - \gamma^2 \end{cases} \quad (\text{II.2.39})$$

Both for periodic and antiperiodic boundary conditions the free fermion system has an unique groundstate with 1-, 2-, 3-, ... particle excitations created by η_k^\dagger , $\eta_{k_1}^\dagger \eta_{k_2}^\dagger$ etc. Usually these excitations form continua since different k correspond to different energies. Fig. II.2.2 shows a very schematic illustration of the spectrum for the two boundary conditions.

We now use the above results to determine the spectrum of the XY model. As mentioned before, only those states with the correct value of P contribute (see eq. (II.2.20)). In Fig. II.2.2 we have shown the P -values for the different eigenstates. This is discussed in more detail in Exercise 6 where it is shown that due to the anticommutation of P and η_k^\dagger the n -particle state has the P -value $(-1)^l P_0$ where P_0 is the P -value of the groundstate. The determination of P_0 is nontrivial due to the rather complicated nature of the groundstate of the c -fermion or spin problem. In the case $B = 0$ the latter can be determined in the Ising limit $\gamma = 1$ where one finds the two groundstates $|\pm\rangle = |\uparrow \cdots \uparrow \pm \downarrow \cdots \downarrow\rangle$. Since $P = (-1)^L \prod_{j=1}^L \sigma_j^z$ it is easy to see that $P|\pm\rangle = \pm|\pm\rangle$. If γ is decreased, the discrete quantum number P can only change if the excitation gap closes and some state with different P drops down from the excitation spectrum and becomes the groundstate. This only happens for $\gamma = 0$ (see (II.2.38)). The state $|+\rangle$ transforms into the groundstate of the

fermion problem with antiperiodic boundary conditions and $|-\rangle$ into that of the periodic case. This explains, at least for $B = 0$, the P -values assigned to the spectra in Fig. II.2.2. Since according to (II.2.20) only states with $P = 1$ from the case of antiperiodic and with $P = -1$ from periodic boundary conditions are part of the XY-spectrum, this gives the following picture (see Fig. II.2.3).

- For $B < 1$ both the $2n$ -particle excitations of the periodic and antiperiodic chain have the correct P -values whereas the $(2n + 1)$ -particle excitations do not contribute to the XY-spectrum. Therefore each state of the XY chain is twofold-degenerate, especially the groundstate. Since only excitations with an even number of particles appear, the excitation gap in this case is 2Δ .
- For $B > 1$ the situation changes because now from the periodic chain only the $(2n + 1)$ -particle excitations contribute to the XY-spectrum. Therefore the XY chain has now an unique groundstate (coming from the antiperiodic case) and n -particle excitations with $n = 1, 2, \dots$

Physically a strong magnetic field forces all spins to align parallel to the field. This happens here for $B > 1$ and gives rise to an unique groundstate. For weaker fields, the spins are not aligned in z -direction. However, depending on the asymmetry γ , ordering can occur e.g. along the x -direction such that³ $\langle \sigma^x \rangle \neq 0$ and $\langle \sigma^y \rangle = 0$. Since $\langle \sigma^x \rangle$ can be positive and negative this corresponds to a twofold degenerate groundstate.

II.2.3 Summary

We have shown that we can solve the one-dimensional XY model by mapping it onto a free fermion model. This mapping has been achieved by a *Jordan-Wigner transformation* which allows to express spin operators in terms of fermion operators. The essential advantage was that the fermionic problem was interaction-free and could therefore be solved easily.

Sometimes it is said that in one dimension “statistics is not essential”. What is meant by this — we will see further examples later in this course — is that commutators can be changed into

³This happens in the case $J_x \gg J_y$.

antiperiodic:	periodic ($B < 1$):	periodic ($B > 1$):
$P=-1$ _____	$P=+1$ _____	$P=-1$ _____
$P=+1$ _____ 2-particle	$P=-1$ _____ 2-particle	$P=+1$ _____ 2-particle
$P=-1$ _____ 1-particle	$P=+1$ _____ 1-particle	$P=-1$ _____ 1-particle
$P=+1$ _____ ground state	$P=-1$ _____ ground state	$P=+1$ _____ ground state

Figure II.2.2: Schematic illustration of the free fermion spectrum for antiperiodic and periodic boundary conditions. Also shown are the values of P in the different states.

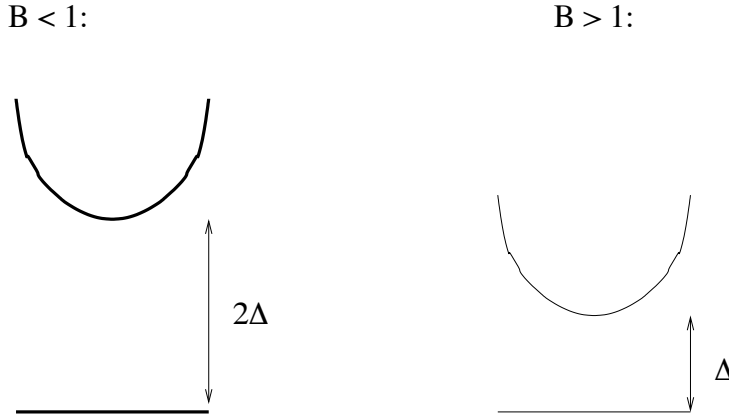


Figure II.2.3: Schematic illustration of the spectrum of the XY model. Thick lines correspond to twofold degenerate states, thin lines to nondegenerate states.

anticommutators etc. However, this is not restricted to one dimension (see Exercise 4 and the review [10]). The essential point is that in one dimension it can lead to a drastic simplification as we have seen in the example above. One has to realize that statistics (fermionic, bosonic) has something to do with the exchange of particles. In two and higher dimensions two particles can be exchanged without ever meeting by moving them “around each other” at a large distance. Thus the interaction between them during this process can be made arbitrarily small. In one dimension, on the other hand, during an exchange the particles have to meet. Therefore their mutual interaction is always important during this exchange process. This makes understandable why in the one-dimensional case the statistics can be built into the interactions which (through compensation) could even lead to interaction-free models, but with particles of a different statistics.

We want to finish with two remarks. First of all, the XY model as discussed here appears as an essential ingredient in the solution of the two-dimensional Ising model. In fact the transfer matrix T_{Ising} of the Ising model can be written in the form

$$T_{\text{Ising}} = \exp(-\beta \mathcal{H}_{XY}) \quad (\text{II.2.40})$$

where β is the inverse temperature. Therefore the transfer matrix commutes with \mathcal{H}_{XY} and both operators share a common eigenbasis.

The second remark concerns a possible extension of the approach to the XXZ case. The Jordan-Wigner transformation for the z -part of the interaction gives

$$\sigma_j^z \sigma_{j+1}^z = (2n_j - 1)(2n_{j+1} - 1) \quad (\text{II.2.41})$$

which is a two-particle interaction. Therefore the corresponding fermion Hamiltonian is not easier to solve than the spin model. It reads

$$\mathcal{H}_{XXZ} \longrightarrow \mathcal{H}_F = -t \sum_j \left(c_j^\dagger c_{j+1} + c_{j+1}^\dagger c_j \right) + U \sum_j n_j n_{j+1} \quad (\text{II.2.42})$$

where we have dropped some constant terms and renamed the interaction constants to emphasize its similarity with the Hubbard model. However, here the fermions are spinless and therefore no doubly-occupied sites are allowed. Therefore the Coulomb interaction U only acts between particles one neighbouring sites.

II.3 Bethe-Ansatz for the XXZ model

Next we want to treat the XXZ model. First we treat the case of vanishing magnetic field, i.e. the Hamiltonian

$$\mathcal{H}_{XXZ} = J \sum_{j=1}^L [\sigma_j^x \sigma_{j+1}^x + \sigma_j^y \sigma_{j+1}^y + \Delta \sigma_j^z \sigma_{j+1}^z] \quad (\text{II.3.1})$$

with periodic boundary conditions.

II.3.1 Symmetries and invariant subspaces

The Hamiltonian (II.3.1) has some symmetries. Obviously it is invariant under a transformation that flips all spins $\sigma_j^z \rightarrow -\sigma_j^z$. Therefore it is sufficient to investigate only $\sigma^z = \sum_{j=1}^L \sigma_j^z \geq 0$. Rotating spins on odd sites by π around the z -axis changes $J \rightarrow -J$ and $\Delta \rightarrow -\Delta$ (see Exercise 3).

The problem of diagonalization can be simplified by observing that \mathcal{H}_{XXZ} commutes with the total spin-component in z -direction:

$$[\mathcal{H}_{XXZ}, S^z] = \left[\mathcal{H}_{XXZ}, \frac{1}{2} \sum_{j=1}^L \sigma_j^z \right] = 0. \quad (\text{II.3.2})$$

This means that the eigenstates can be classified according to their magnetisation S^z , or equivalently, according to the number M of \downarrow -spins. These two quantities are obviously related:

$$S^z = \frac{L}{2} - M. \quad (\text{II.3.3})$$

and the full Hilbert space \mathcal{G} decomposes into invariant subspaces \mathcal{G}_M :

$$\mathcal{G} = \bigoplus_{M=0}^L \mathcal{G}_M. \quad (\text{II.3.4})$$

A simple combinatorical argument⁴ shows that the dimension d_M of \mathcal{G}_M is given by $d_M = \binom{L}{M}$. Indeed $\sum_{M=0}^L d_M = \sum_{M=0}^L \binom{L}{M} = 2^L$ gives the correct dimension of the full Hilbert space since at each of the L sites the spin can be in two different states.

⁴There are $\binom{L}{M}$ different ways of choosing the positions of the M \downarrow -spins.

Although this consideration simplifies the problem somewhat the subspaces are in general extremely large. Especially if we consider antiferromagnetism where we expect that in the ground-state the number of \uparrow - and \downarrow -spins are equal, the subspaces are so huge already for rather small chains that no computer is able to perform this diagonalization task numerically.

To proceed we now choose an appropriate basis in each subspace. A natural choice for \mathcal{G}_M is

$$|x_1, x_2, \dots, x_M\rangle := \sigma_{x_1}^- \sigma_{x_2}^- \cdots \sigma_{x_M}^- |\uparrow\uparrow \dots \uparrow\rangle = |\uparrow\uparrow \dots \underset{x_1}{\uparrow\downarrow} \underset{x_j}{\uparrow} \dots \underset{x_M}{\downarrow} \dots \downarrow\uparrow \dots \uparrow\rangle \quad (\text{II.3.5})$$

i.e. the state $|x_1, x_2, \dots, x_M\rangle$ has \downarrow -spins at sites x_1, x_2, \dots, x_M and \uparrow -spins everywhere else where we always assume $x_1 < x_2 < \dots < x_M$. The state

$$|0\rangle := |\uparrow\uparrow \dots \uparrow\rangle \quad (\text{II.3.6})$$

is called *reference state* or *Bethe-Ansatz vacuum*. It has to be a simple eigenstate of the considered Hamiltonian. In general it will not be the true vacuum state of the system, i.e. the state of lowest energy. However, equation (II.3.5) implies an interpretation of the \downarrow -spins as particles. Using this basis we can now write any eigenstate of the XXZ model in the form

$$|\psi_M\rangle = \sum_{x_1 < x_2 < \dots < x_M} a(x_1, x_2, \dots, x_M) |x_1, x_2, \dots, x_M\rangle \quad (\text{II.3.7})$$

where the amplitudes $a(x_1, x_2, \dots, x_M)$ have still to be determined. This will be achieved by the Bethe-Ansatz.

Before we proceed in order to simplify the following calculations a little bit we will use the Hamiltonian

$$\tilde{\mathcal{H}}_{XXZ} = J \sum_{j=1}^L [\sigma_j^x \sigma_{j+1}^x + \sigma_j^y \sigma_{j+1}^y + \Delta (\sigma_j^z \sigma_{j+1}^z - 1)] \quad (\text{II.3.8})$$

in the following which differs from (II.3.1) just by a constant. We then have

$$\tilde{\mathcal{H}}_{XXZ} |0\rangle = 0, \quad (\text{II.3.9})$$

i.e. it shifts the energy of the reference state to 0. The operator $\sigma_j^z \sigma_{j+1}^z - 1$ has a simple interpretation. It counts the number of antiparallel spin pairs. Note that with equation (II.3.9) we have already solved the problem in the subspace $M = 0$.

II.3.2 The Bethe-Ansatz

We now treat the cases $M = 1, 2, 3$ in more detail. This will allow us to understand the general principles behind the Bethe-Ansatz for the XXZ model.

M = 1

We start with the subspace $M = 1$ corresponding to a magnetization $S^z = \frac{L}{2} - M$. The wavefunctions in \mathcal{G}_1 have the general form

$$|\psi_1\rangle = \sum_{x=1}^L a(x) |x\rangle. \quad (\text{II.3.10})$$

Using the well-known identity

$$\sigma_j^x \sigma_{j+1}^x + \sigma_j^y \sigma_{j+1}^y = 2 (\sigma_j^+ \sigma_{j+1}^- + \sigma_j^- \sigma_{j+1}^+) \quad (\text{II.3.11})$$

which is easily derived from the definition of the ladder operators

$$\sigma_j^x = \sigma_j^+ + \sigma_j^-, \quad \sigma_j^y = \frac{1}{i} (\sigma_j^+ - \sigma_j^-) \quad (\text{II.3.12})$$

we can easily determine how the Hamiltonian acts on the basis states $|x\rangle$. We have already argued that the z -part of the interaction basically counts the number of antiparallel spins. Now we see from (II.3.11) that the xy -part corresponds to the kinetic energy⁵. It describes the motion of a \downarrow -spin to its left or right neighbours. Thus we easily obtain

$$\tilde{\mathcal{H}}_{XXZ}|x\rangle = 2J (|x+1\rangle + |x-1\rangle - 2\Delta|x\rangle) \quad (\text{II.3.13})$$

where the first two terms come from the xy -interaction and the last term from the z -part. Using this result Schrödinger's equation $\tilde{\mathcal{H}}_{XXZ}|\psi_1\rangle = E|\psi_1\rangle$ yields

$$2J[a(x+1) + a(x-1) - 2\Delta a(x)] = Ea(x). \quad (\text{II.3.14})$$

The solution of this equation is a plane wave

$$a(x) = e^{ikx} \quad (\text{II.3.15})$$

with wavenumber k which is also called *quasi-momentum* in the context of the Bethe Ansatz. Due to its similarity with spin waves known from solid-state theory this solution is also called a *magnon*. The corresponding energy is

$$E(k) = 4J(\cos k - \Delta). \quad (\text{II.3.16})$$

As usual the periodic boundary conditions imply a quantization of the allowed k -values:

$$a(x+L) = a(x) \implies e^{ikL} = 1 \quad (\text{II.3.17})$$

and therefore

$$k = \frac{2\pi}{L}n \quad (n = 0, 1, 2, \dots, L-1). \quad (\text{II.3.18})$$

Therefore we have found L independent solutions which is exactly what we need since $d_1 = \binom{L}{1} = L$.

M = 2

We now proceed to the case $M = 2$, i.e. $S^z = \frac{L}{2} - M$. This will lead to something new since now also interactions between the two \downarrow -spins are possible. The general wavefunction in \mathcal{G}_2 is of the form

$$|\psi_2\rangle = \sum_{1 \leq x_1 < x_2 \leq L} a(x_1, x_2) |x_1, x_2\rangle. \quad (\text{II.3.19})$$

⁵This should not come unexpected regarding our experience with the Jordan-Wigner transformation!

For Schrödinger's equation we now have to distinguish two cases.

Case 1: $x_1 \leq x_2 - 2$

This means that the two \downarrow -spins are not on neighbouring sites and thus do not interact. Then we obtain (similar to the case $M = 1$) the equation

$$2J[a(x_1 - 1, x_2) + a(x_1 + 1, x_2) + a(x_1, x_2 - 1) + a(x_1, x_2 + 1) - 4\Delta a(x_1, x_2)] = Ea(x_1, x_2). \quad (\text{II.3.20})$$

This is basically the sum of two equations of the type (II.3.14) reflecting the fact that the \downarrow -spins do not interact.

Case 2: $x_1 = x_2 - 1 =: x$

This means that the \downarrow -spins are on neighbouring sites and thus there interaction has to be taken into account. It follows that two of the four possible hopping processes in (II.3.20) are not possible since this would lead to $x_1 = x_2$ etc. We therefore obtain

$$2J[a(x - 1, x + 1) + a(x, x + 2) - 2\Delta a(x, x + 1)] = Ea(x, x + 1). \quad (\text{II.3.21})$$

Note that also the number of antiparallel pairs is reduced to 2 when the \downarrow -spins are neighbours. The first idea would be to solve the two equations (II.3.20), (II.3.21) by a plane wave $a(x_1, x_2) = \exp(i(k_1 x_1 + k_2 x_2))$. However, it turns out that this does not work because the interaction of the two magnons is not taken into account properly. Bethe suggested to use a superposition of plane wave instead:

$$a(x_1, x_2) = A_{12}e^{i(k_1 x_1 + k_2 x_2)} + A_{21}e^{i(k_2 x_1 + k_1 x_2)}. \quad (\text{II.3.22})$$

This is the famous *Bethe-Ansatz*⁶ for the special case $M = 2$. Note that in both plane waves the same wavenumbers k_1 and k_2 appear, but for different particles.

Using the Bethe-Ansatz (II.3.22) it is immediately clear that the noninteracting equation (II.3.20) is automatically satisfied. We will now show that the second equation (II.3.21) reduces to a condition for the amplitudes. First, we note that formally the Ansatz (II.3.22) satisfies the equation

$$2J[a(x - 1, x + 1) + a(x + 1, x + 1) + a(x, x) + a(x, x + 2) - 4\Delta a(x, x + 1)] = Ea(x, x + 1). \quad (\text{II.3.23})$$

This is just equation (II.3.20) for the case $x_1 = x_2 - 1$. Note that the unphysical amplitudes $a(x, x)$ appear which are not relevant for the wavefunction (II.3.19). Therefore we do not have to choose $a(x, x) = 0$ and can instead use this freedom to find a solution.

Combining (II.3.21) and (II.3.23) we obtain the simpler equation

$$a(x, x) + a(x + 1, x + 1) = 2\Delta a(x, x + 1) \quad (\text{II.3.24})$$

which yields after inserting the Bethe-Ansatz function the condition

⁶Bethe solved the isotropic case $\Delta = 1$ in 1931 [11]. The extension to the XXZ case $\Delta \neq 1$ has been obtained only almost 30 years later [12–14].

$$A_{12} = \frac{\text{magnon 1}}{\text{magnon 2}} \quad \text{magnon 1} \quad \text{magnon 2}$$

$$A_{21} = \frac{\text{magnon 1}}{\text{magnon 2}} \quad \text{magnon 1} \quad \text{magnon 2}$$

Figure II.3.1: Illustration of the Bethe-Ansatz amplitudes. A_{12} describes a situation where magnon 1 has momentum k_1 and magnon 2 a momentum k_2 . For A_{21} this is just reversed.

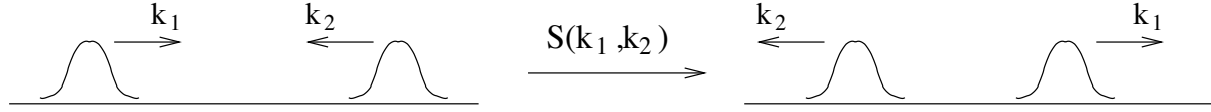


Figure II.3.2: Illustration of the 2-particle scattering amplitude. The left figure shows the situation before the scattering process, the right part the situation after. Note that the set $\{k_1, k_2\}$ of quasi-momenta is conserved.

$$\boxed{\frac{A_{21}}{A_{12}} = -\frac{1 - 2\Delta e^{ik_2} + e^{i(k_1+k_2)}}{1 - 2\Delta e^{ik_1} + e^{i(k_1+k_2)}}. \quad (\text{II.3.25})}$$

Taking $\Delta = 0$, in which case the XXZ model reduces to the symmetric XY model in vanishing field, we get

$$\frac{A_{21}}{A_{12}} = -1 \quad \text{independent of } k_1, k_2 \quad (\text{II.3.26})$$

which implies $a(x_1, x_2) = -a(x_2, x_1)$ as expected for a free fermion system.

What is the physical meaning of the ratio $\frac{A_{21}}{A_{12}}$? It describes the scattering process of an incoming plane wave to an outgoing plane wave illustrated in Fig. II.3.2. The situation is very similar to what one knows from scattering theory. Therefore one defines

$$S(k_1, k_2) = S_{12} = \frac{A_{21}}{A_{12}} = \frac{\text{Amplitude (21)}}{\text{Amplitude (12)}} \quad (\text{II.3.27})$$

with the *2-particle scattering matrix* $S(k_1, k_2)$. It maps the incoming wave onto the outgoing wave. Since in the present case S is a 1×1 -matrix it is also called *scattering amplitude*.

Again the periodic boundary conditions yield further restrictions of the allowed wavenumbers which are now more complicated than in the noninteracting case (see (II.3.18)). Explicitly the periodic boundary conditions imply the condition

$$a(x_1, x_2) = a(x_2, x_1 + L) \quad (\text{II.3.28})$$

where we have used the fact that always $x_1 < x_2$ in the physical amplitudes $a(x_1, x_2)$. This leads to the conditions

$$A_{12} = A_{21}e^{ik_1 L}, \quad A_{21} = A_{12}e^{ik_2 L}. \quad (\text{II.3.29})$$

Furthermore, we can use the translation invariance of the system, i.e. translating the *whole* state by L sites does not change the state. This implies

$$e^{i(k_1+k_2)L} = 1. \quad (\text{II.3.30})$$

We will later see that this implies a quantization of the total momentum P similar to (II.3.18). Before we proceed we want to give a simple interpretation of the result (II.3.29) by clarifying its connection with the uniqueness of the wavefunction. We rewrite the equation in the form

$$\left(\frac{A_{21}}{A_{12}} \right) e^{ik_1 L} = 1. \quad (\text{II.3.31})$$

Imagine now that you take particle 1 with quasi-momentum k_1 and move it once around our lattice. Then one picks up a kinematical phase $k_1 L$. In addition, due to the periodic boundary conditions, in this process it will meet particle 2 and scatter. This creates an additional phase coming from the scattering amplitude. Requiring uniqueness of the wavefunction implies that the sum of these two phase changes is a multiple of 2π . This gives equation (II.3.31).

Combining our previous results we obtain the following equations which determine the quasi-momenta k_1 and k_2 .

$$e^{ik_1 L} = -\frac{1 - 2\Delta e^{ik_1} + e^{i(k_1+k_2)}}{1 - 2\Delta e^{ik_2} + e^{i(k_1+k_2)}}, \quad e^{ik_2 L} = -\frac{1 - 2\Delta e^{ik_2} + e^{i(k_1+k_2)}}{1 - 2\Delta e^{ik_1} + e^{i(k_1+k_2)}}. \quad (\text{II.3.32})$$

These are the famous *Bethe-Ansatz equations* for the case $M = 2$. Solving these equations we can determine the amplitudes⁷ A_{12} and A_{21} which then yield the wavefunction. The energy of the corresponding state is given by

$$E_2 = E(k_1) + E(k_2) = 4J(\cos k_1 - \Delta) + 4J(\cos k_2 - \Delta). \quad (\text{II.3.33})$$

We can rewrite the Bethe-Ansatz equations (II.3.32) in the more compact form

$$\begin{aligned} e^{ik_1 L} &= -e^{-i\theta(k_1, k_2)}, \\ e^{ik_2 L} &= -e^{-i\theta(k_2, k_1)}, \end{aligned} \quad (\text{II.3.34})$$

by introducing the phase factor (phase shift)

$$\theta(k_1, k_2) = 2 \arctan \left(\frac{\Delta \sin \left(\frac{1}{2}(k_1 - k_2) \right)}{\cos \left(\frac{1}{2}(k_1 + k_2) \right) - \Delta \cos \left(\frac{1}{2}(k_1 - k_2) \right)} \right) = -\theta(k_2, k_1) \quad (\text{II.3.35})$$

⁷Note that the amplitudes are only determined up to a normalization factor!

which is basically the phase shift mentioned in the explanation above.

M = 3

Next we will briefly discuss the case $M = 3$ because this is generic for all other cases $M > 2$. We now have \downarrow -spins at the positions $x_1 < x_2 < x_3$. Therefore 4 cases have to be distinguished:

- a) $x_2 \neq x_1 + 1, x_3 \neq x_2 + 1$: This is the case where no two \downarrow -spins are on neighbouring sites. There is no interaction and therefore this case is basically identical to the situation for $M = 1$.
- b) $x_2 = x_1 + 1, x_3 \neq x_2 + 1$: Now \downarrow -spins 1 and 2 are on neighbouring sites and interact. This case is basically identical to $M = 2$.
- c) $x_2 \neq x_1 + 1, x_3 = x_2 + 1$: Here \downarrow -spins 2 and 3 interact, which again can be traced back to the $M = 2$ situation.
- d) $x_2 = x_1 + 1, x_3 = x_2 + 1$: Now all three \downarrow -spins are on neighbouring sites. This situation is new!

The Bethe-Ansatz for the case $M = 3$ is again a superposition of plane waves with fixed wavenumbers k_1, k_2 and k_3 . Taking into account all possible combinations of particles and wavenumbers the Bethe-Ansatz for the amplitudes now reads:

$$\begin{aligned} a(x_1, x_2, x_3) = & A_{123}e^{i(k_1x_1+k_2x_2+k_3x_3)} + A_{132}e^{i(k_1x_1+k_3x_2+k_2x_3)} \\ & + A_{213}e^{i(k_2x_1+k_1x_2+k_3x_3)} + A_{231}e^{i(k_2x_1+k_3x_2+k_1x_3)} \\ & + A_{312}e^{i(k_3x_1+k_1x_2+k_2x_3)} + A_{321}e^{i(k_3x_1+k_2x_2+k_1x_3)}. \end{aligned} \quad (\text{II.3.36})$$

Inserting this into the equations obtained for the four cases lead to constraints on the amplitudes $A_{\alpha\beta\gamma}$. We just give the final results since the calculations are very similar to the previous cases. Case a) is trivially satisfied by the Bethe-Ansatz. In case b) we obtain

$$\frac{A_{123}}{A_{213}} = -e^{-i\theta(k_1, k_2)}, \quad \frac{A_{132}}{A_{312}} = -e^{-i\theta(k_1, k_3)}, \quad \frac{A_{231}}{A_{321}} = -e^{-i\theta(k_2, k_3)} \quad (\text{II.3.37})$$

and case c) gives

$$\frac{A_{123}}{A_{132}} = -e^{-i\theta(k_2, k_3)}, \quad \frac{A_{213}}{A_{231}} = -e^{-i\theta(k_1, k_3)}, \quad \frac{A_{312}}{A_{321}} = -e^{-i\theta(k_1, k_2)} \quad (\text{II.3.38})$$

where we have used the scattering phase (II.3.35). Using these results it can be checked that case d) is also satisfied without imposing further conditions.

The essential point that can be learnt from this case is that all amplitudes can be expressed by A_{123} and the two-particle scattering matrix (amplitude, phase shift), e.g.

$$A_{312} = e^{-i\theta(k_3, k_1)}e^{-i\theta(k_3, k_2)}A_{123} = S_{13}S_{23}A_{123}. \quad (\text{II.3.39})$$

The energy of a Bethe-Ansatz state for $M = 3$ is given by the sum of the single-magnon contributions:

$$E_3 = E(k_1) + E(k_2) + E(k_3). \quad (\text{II.3.40})$$

We now can treat the general case of $M \downarrow$ -spins corresponding to magnetization $S^z = \frac{L}{2} - M$. Note that in principle we could restrict our considerations to the case $M \leq \frac{L}{2}$. The case $M \geq \frac{L}{2}$ can be treated in an analogous fashion by considering the Bethe-Ansatz vacuum $|\bar{0}\rangle = |\downarrow\downarrow \cdots \downarrow\rangle$ instead of $|0\rangle$.

General M

In the general case the wavefunction in \mathcal{G}_M has the form

$$|\psi_M\rangle = \sum_{x_1 < x_2 < \dots < x_M} a(x_1, x_2, \dots, x_M) |x_1, x_2, \dots, x_M\rangle. \quad (\text{II.3.41})$$

The obvious generalization of the Bethe-Ansatz is

$$a(x_1, x_2, \dots, x_M) = \sum_{P \in S_M} A_P e^{i(k_{P_1} x_1 + \dots + k_{P_M} x_M)}. \quad (\text{II.3.42})$$

Here S_M denotes the symmetric group, i.e. the set of all permutations P of $\{1, 2, \dots, M\}$. This implies that (II.3.42) consists of $M!$ terms. We already mention here that no two of the wavenumbers k_1, \dots, k_M can be equal because this would imply the vanishing of the wavefunction⁸. Furthermore the wavenumbers are not necessarily real.

For the cases $M = 0, 1, 2, 3$ the Ansatz (II.3.42) reduces to the previous after a slight change of notation. E.g. for $M = 2$, the symmetric group consists of two elements: the identity I and the transposition τ which exchanges $(12) \longleftrightarrow (21)$. Thus we can identify the amplitudes $A_{12} = A_I$ and $A_{21} = A_\tau$.

The further treatment is now analogous to the case $M = 3$. Again we see that the conditions obtained for the cases of two interacting spins are sufficient to satisfy all possible cases. Furthermore again all amplitudes can be expressed by A_I and the 2-particle scattering matrix in an unique way. The general Bethe-Ansatz equations for the XXZ model then read

$$e^{ik_j L} \prod_{l=1, l \neq j}^M S(k_j, k_l) = 1 \quad (j = 1, 2, \dots, M), \quad (\text{II.3.43})$$

with

$$S(k_j, k_l) = -e^{-i\theta(k_j, k_l)} \quad (\text{II.3.44})$$

where the phase shift $\theta(k_j, k_l)$ is given by (II.3.35). (II.3.43) is a set of highly nonlinear coupled equations. Later we will discuss how these can be solved. The energy of the corresponding state is

⁸This is immediately clear for the case $\Delta = 0$ which corresponds to free fermions.

$$E_M = \sum_{j=1}^M E(k_j) = 4J \sum_{j=1}^M (\cos k_j - \Delta). \quad (\text{II.3.45})$$

Let us summarize the important features of the Bethe-Ansatz.

- The existence of a reference state (Bethe-Ansatz vacuum) is important. This is a simple eigenstate of the Hamiltonian which can be interpreted as a state without particles.
- The Bethe-Ansatz wavefunction is a superposition of plane wave with a fixed set of wavenumbers k_j . The plane waves might be interpreted as magnons.
- All interaction processes can be reduced to 2-particle processes in a unique way using the S -matrix $S(k_1, k_2)$. The uniqueness of this reduction is trivial in the case considered here since the S -matrix is just a phase and the order of the 2-particles processes obviously does not play a role. Later we will see that e.g. for the Hubbard model the S -matrix is a true matrix and then the uniqueness is far from trivial. We want to emphasize that the reduction to 2-particle processes is *the* essential property of Bethe-Ansatz solvable models. This happens only in special cases. The XXZ (or XYZ) model is in this sense an exception since the Bethe-Ansatz works for all values of the interaction parameters. In general, models are not solved by the Bethe-Ansatz or only for special values of the coupling constants.

Finally, we want to conclude with two remarks. First of all, in the above solution we have used the conservation of the magnetization S^z . This is not essential as e.g. the case of the XYZ model shows. Here S^z is not conserved, but nevertheless the model can be solved for any values of the couplings J_x , J_z and J_z . However, this only works for vanishing magnetic field whereas the solution of the XXZ model can be extended to include a magnetic field in z -direction. Here the S^z -conservation is essential.

The second remark concerns the solvability of generalizations of the Heisenberg model, e.g. models with next-nearest neighbour interactions or staggered coupling constants⁹. In general, these modification destroy the exact solvability since obviously 3-particle processes become relevant here.

II.4 Relation between classical and quantum systems

In the previous section we have used the so-called *coordinate Bethe Ansatz* where the wavefunction is constructed explicitly. Similar to the treatment of the harmonic oscillator a more elegant algebraic methods exists, the *algebraic Bethe Ansatz*. This will give also new interesting information, e.g. the creation/annihilation operators for magnons.

Before we present an outline of the algebraic Bethe Ansatz approach we need to discuss the relation of quantum mechanical models with classical models (at finite temperature) in higher dimensions. Quite generally one has the following result:

⁹E.g. Δ could alternate: $\Delta = \Delta_1$ for bonds $(j, j+1)$ with j even and $\Delta = \Delta_2$ for j odd.

d – dimensional quantum model \Updownarrow $(d+1)$ – dimensional classical model (at finite temperature)	(II.4.1)
--	---

In the following we will only consider the case $d = 1$, but most results presented hold in arbitrary dimension d .

As we have already seen in the treatment of the XY model it is sometimes convenient to have two equivalent languages. It might turn out that a problem is simpler in one of them, e.g. as the XY model in fermion language. In fact we will see that the above equivalence might be used for analytical as well numerical problems. In the latter case it is often advantageous to treat a classical problem on a computer since one does not have to take care of noncommuting variables. This is essential e.g. for so-called *Quantum Monte-Carlo simulations (QMC)*.

Before we use the equivalence explicitly, we give a brief overview of the various classes of classical models.

II.4.1 Spin models

The most natural ones are the so-called (*classical*) *spin systems*, with the Ising model being the most famous example.

Fig. II.4.1 shows a typical spin model on a square lattice of $N = L \cdot \tilde{L}$ sites. Each lattice site l carries a classical variable (“spin”) σ_l which in the simplest case can take two values $\sigma_l = \pm 1$. This spin interacts with the spins on its (four) nearest neighbour sites where the interaction is characterized by a coupling constant J_{ij} . Usually $J_{ij} = J_1$ (J_2) for horizontal (vertical) neighbours. The interaction defines an energy function $E(\sigma_1, \dots, \sigma_N)$, e.g. for the Ising model

$$E(\sigma_1, \dots, \sigma_N) = - \sum_{\langle ij \rangle} J_{ij} \sigma_i \sigma_j - H \sum_{j=1}^N \sigma_j \quad (\text{II.4.2})$$

where H is a magnetic field and $\langle ij \rangle$ denotes nearest neighbours. The Ising model is exactly solvable for vanishing magnetic field [15], even for anisotropic interactions ($J_1 \neq J_2$) between nearest neighbour spins. Here “exact solvability” means that the partition function

$$Z_N = \sum_{\sigma} e^{-\beta E_N(\sigma)} = \sum_{\{\sigma_1, \dots, \sigma_N\}} \exp \left[\sum_{\langle ij \rangle} K_{ij} \sigma_i \sigma_j + h \sum_{j=1}^N \sigma_j \right] \quad (\text{II.4.3})$$

with $\beta = 1/(k_B T)$, can be calculated without any approximations. Here we have introduced the abbreviations $K_{ij} = \beta J_{ij}$ and $h = \beta H$ which are usually used as independent variables instead of the couplings and temperature. As usual, we define the *free energy* F and the *free energy density* f by

$$F = -k_B T \ln Z_N, \quad f = -k_B T \lim_{N \rightarrow \infty} \frac{\ln Z_N}{N} \quad (\text{II.4.4})$$

which then gives the thermodynamic properties.

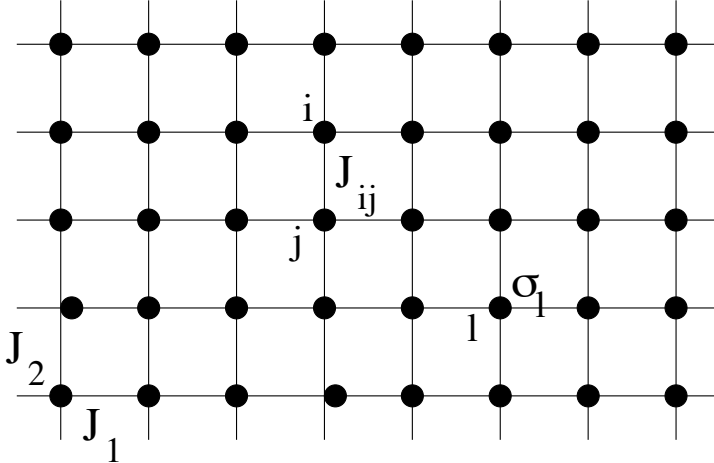


Figure II.4.1: A typical spin model with nearest-neighbour interactions J_{ij} . Each site l of the lattice carries a classical variable σ_l . For interactions along horizontal bonds $\langle ij \rangle$ one sets $J_{ij} = J_1$ whereas $J_{ij} = J_2$ along vertical bonds.

One possible generalization of the Ising model is the so-called (*q -state*) *Potts model*. Here the classical variables are allowed to take q different states $\sigma_j = 1, 2, \dots, q$. The energy function of the Potts model is defined by

$$E(\sigma_1, \dots, \sigma_N) = - \sum_{\langle ij \rangle} J_{ij} \delta_{\sigma_i, \sigma_j}, \quad (\text{II.4.5})$$

where δ_{ab} denotes the Kronecker delta. The energy of a bond can therefore only take two values, depending on whether the spins are in the same state or not. For $q = 2$ the Potts model is equivalent to the Ising model up to a shift of the energy. However, the case of general q is only exactly solvable in special cases. To be precise a solution is possible for couplings that satisfy the relation

$$(e^{K_1} - 1)(e^{K_2} - 1) = q \quad (\text{II.4.6})$$

which is known as “self-dual line”.

The main feature of (classical) spin models is the fact that the dynamical variables live on the lattice sites. The interaction energy then belongs to the bonds between these sites. This is not the only possibility.

II.4.2 Vertex models

In so-called *vertex models* the situation is just reversed. Here the dynamical variables are situated on the bonds¹⁰. The energy is then assigned to the lattice sites depending on the configuration of

¹⁰We just mention for completeness that a third class of models exist, the so-called *IRF models*. IRF means “interaction round faces”. Here a Boltzmann weight is assigned to each plaquette of the lattice, depending on the state of the four spins forming the plaquette.

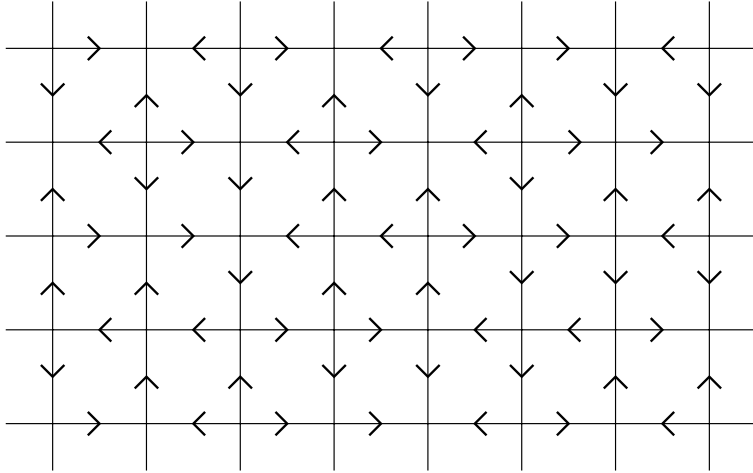


Figure II.4.2: A typical vertex model. In contrast to spin models the dynamical variables live now on the bonds.

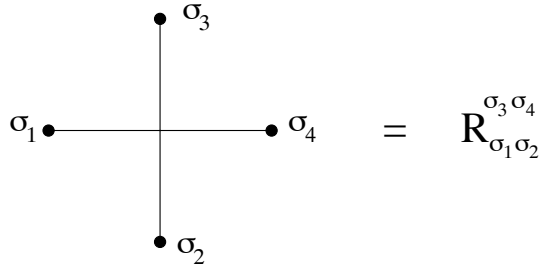


Figure II.4.3: To each vertex of the lattice a corresponding vertex weight is assigned.

the variables around it (see Fig. II.4.2). In the simplest case of a 2-state variable one conventionally uses arrows to denote the state of the bond. Each lattice site together with its surrounding four bonds and arrows is called a *vertex* (see Fig. II.4.3). To each vertex we assign a vertex weight $R_{\sigma_1 \sigma_2}^{\sigma_3 \sigma_4}$ which is interpreted as local Boltzmann weight. We could also interpret it as the energy of the local vertex configuration via the identification $R_{\sigma_1 \sigma_2}^{\sigma_3 \sigma_4} = \exp(-\beta E(\sigma_1 \sigma_2, \sigma_3 \sigma_4))$, however, this is rarely done. Note that sometimes it is more convenient to use spin variables $\sigma_j = \pm 1$ instead of arrows, especially for calculations. Then a value $\sigma = +1$ is assigned to each right- or up-pointing arrow and a value $\sigma = -1$ to each left- or down-pointing arrow.

The partition function of a vertex model is now defined as the sum over all possible arrow configurations of each lattice where for each configuration the contribution is obtained as the product of the occurring vertex weights.

Historically vertex models have been introduced in order to understand a practical physical problem, namely the residual entropy of ice. In ice the oxygen atoms form a (three-dimensional)¹¹ lattice with coordination number 4. On each bond between two neighbouring O-atoms a H-atom is located. This H-atom feels a double-well potential so that it can be located in two different

¹¹In the following we will use a two-dimensional lattice instead, which does not change the essentials.

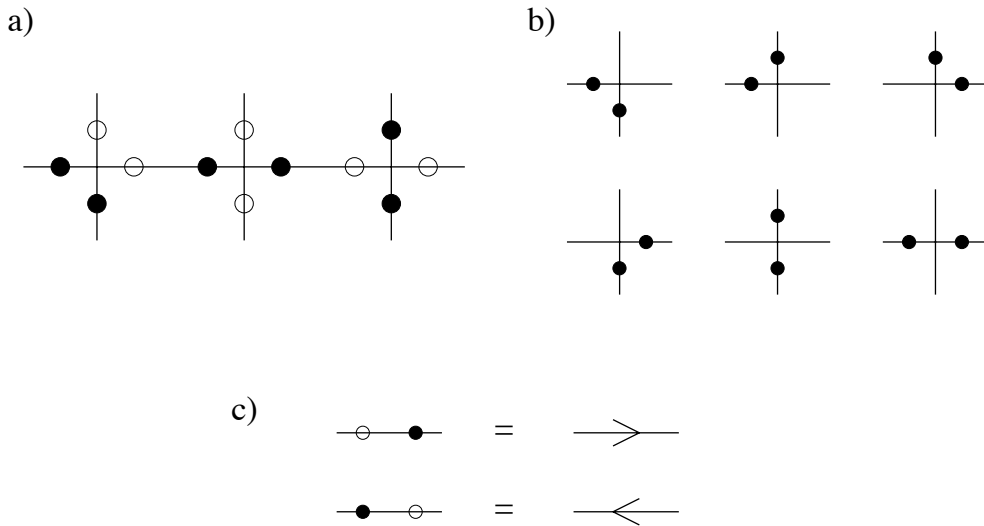


Figure II.4.4: Simple model for ice. a) Each lattice site corresponds to the position of an O -atom. On each bond there are two equivalent positions for an H -atom, denoted by circles (for unoccupied positions) and dots (for occupied positions). Around each O -atom, two positions are empty and two are occupied (ice rule). b) Due to the ice rule only six local configurations are possible. c) Identification of the bond configurations with an arrow denoting the direction of displacement of the H -atom. An analogous identification holds for vertical bonds.

positions (see Fig. II.4.4(a)). Since locally the system should be electrically neutral, each O -atom has exactly two H -atom close to it. This is the so-called *ice rule*. This leaves six different configurations for each O -position (Fig. II.4.4(b)). Each bond configuration can equivalently be specified by an arrow that denotes the direction of displacement of the H -atom from the symmetric position (Fig. II.4.4(c)).

This simple model allows now to understand the residual entropy S_0 of ice. It has been observed that $S(T \rightarrow 0) = S_0 \neq 0$. From the third law of thermodynamics one would expect $S_0 = 0$. However, this only holds if the groundstate is not highly degenerate. This is not satisfied here as there are a macroscopic number of allowed configurations. Using the model described above this number, and thus S_0 , can be estimated. Without constraints one would expect $S_0 = Nk_B \ln 4$. For the two-dimensional ice model this is reduced to $S_0 = Nk_B \ln 1.5396\dots$.

The model as defined so far, describes only the case $T = 0$. Generalizations have been introduced and applied e.g. for ferroelectric materials. Since every bond can be in two states, there are in principle sixteen different vertex configurations. However, usually certain symmetries exist implying that some vertices are not allowed or have the same Boltzmann weight. Most relevant models are special cases of the so-called *8-vertex model*. The allowed vertices, i.e. those with a

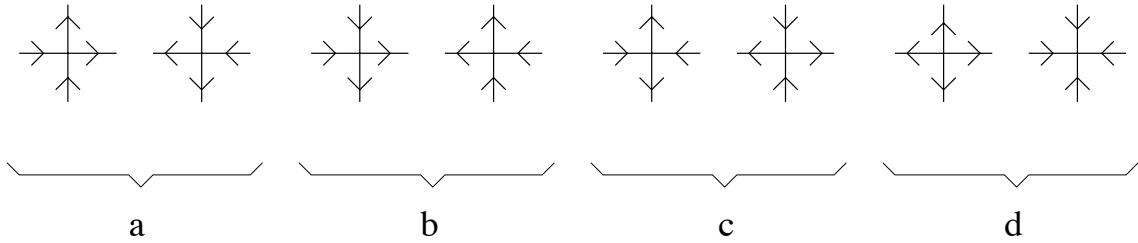


Figure II.4.5: Allowed vertices (type 1, ..., type 8) of the 8-vertex model and the corresponding Boltzmann weights. In the 6-vertex model the vertices of type 7 and 8 are forbidden corresponding to $d = 0$.

non-vanishing Boltzmann weight $R_{\sigma_1 \sigma_2}^{\sigma_3 \sigma_4}$, are depicted in Fig. II.4.5. Explicitly one has

$$R = \begin{pmatrix} a & 0 & 0 & d \\ 0 & c & b & 0 \\ 0 & b & c & 0 \\ d & 0 & 0 & a \end{pmatrix} \quad (\text{II.4.7})$$

where the following identification of indices has been used: $(\sigma_1 = +, \sigma_2 = +) \rightarrow 1$, $(+, -) \rightarrow 2$, $(-, +) \rightarrow 3$, $(-, -) \rightarrow 4$, and similar for (σ_3, σ_4) . Note that all allowed vertices weights are invariant under changes of the direction of all arrows. Therefore this model is also called zero-field 8-vertex model. It is worth mentioning that for periodic boundary conditions in any allowed configuration there has to be an equal number of the two vertices with weight d . The reason is that the left one is a source and the right one a sink of arrows. Assuming that these two have different weights d_1 and d_2 the partition function would only depend on $d_1 d_2$ since these vertices appear only pairwise. Therefore it is no restriction to assume that $d_1 = d_2$. In fact, a similar argument applies to the vertices with weight c that are sources/sinks of horizontal arrows [6].

An important special case is $d = 0$. Then only six vertices are allowed and the resulting model is called *6-vertex model*. This is the model that we investigate in the following. Note that all vertices in the 6-vertex model satisfy the ice rule since there are no local sources or sinks. It is therefore a generalization of the ice model to finite temperatures.

II.4.3 Partition function and transfer matrix

The partition function of the eight vertex model can be written as

$$Z = \sum a^{n_a} b^{n_b} c^{n_c} d^{n_d} \quad (\text{II.4.8})$$

where the sum is over all allowed configurations. n_α denotes the number of vertices of type α , i.e. $n_a + n_b + n_c + n_d = N$. Although this looks rather simple it is no real simplification of the problem. For a practical calculation of the partition function it is useful to introduce a *transfer matrix*. This is basically the partition function of one row (or column) in the lattice (Fig. II.4.6).

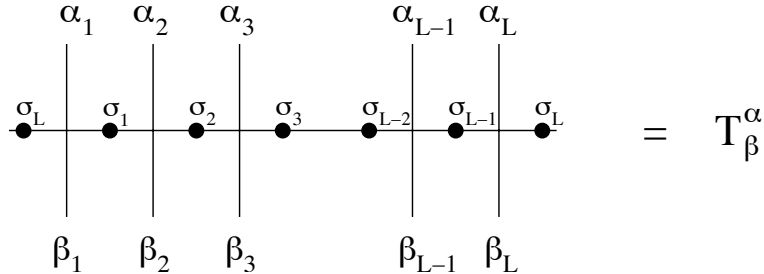


Figure II.4.6: Definition of the transfer matrix. The configurations α and β of the vertical arrows are fixed whereas one has to sum over all states of the horizontal arrows denoted by \bullet . Note that periodic boundary conditions are used.

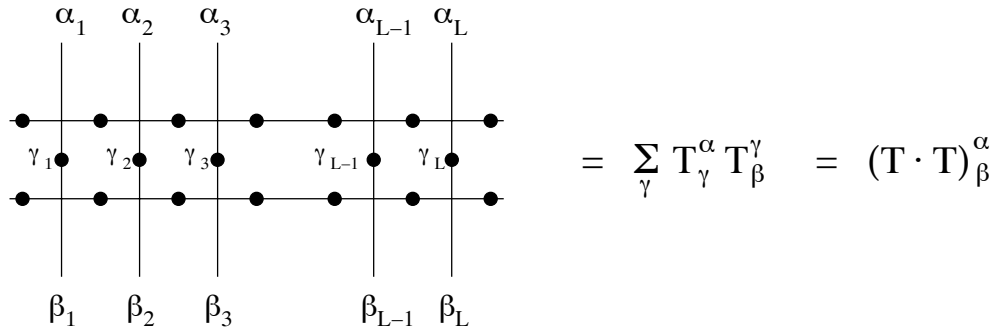


Figure II.4.7: Graphical representation of the product of two transfer matrices. One has to sum over all arrows indicated by \bullet .

For fixed configurations α and β of the vertical arrows one has to sum over all horizontal arrows where periodic boundary conditions are used. The resulting sums are the elements T_β^α of the transfer matrix \mathbf{T} . Thus \mathbf{T} is a $2^L \times 2^L$ matrix. This means that it grows rapidly with the size of the lattice. This is different from the one-dimensional case. For the one-dimensional Ising model the transfer matrix is always 2×2 independent of the lattice size.

Explicitly the transfer matrix reads when expressed by the Boltzmann weights

$$T_\beta^\alpha = \sum_{\sigma} R_{\sigma_L \beta_1}^{\alpha_1 \sigma_1} R_{\sigma_1 \beta_2}^{\alpha_2 \sigma_2} \cdots R_{\sigma_{L-1} \beta_L}^{\alpha_L \sigma_L}. \quad (\text{II.4.9})$$

What is the big advantage of introducing a transfer matrix? Fig. II.4.7 shows a graphical representation of the product of two transfer matrices. One sees that it corresponds to the partition function of *two* rows of the lattice. Iterating this observation one obtains

$$Z = \text{Tr } \mathbf{T}^{\tilde{L}} \quad (\text{II.4.10})$$

where the trace is used if periodic boundary conditions are also imposed on vertical direction. Usually one is interested in the thermodynamic limit where the size of the lattice becomes infinite, i.e. $L, \tilde{L} \rightarrow \infty$. Assuming now that we can diagonalize the transfer matrix and find its

eigenvalues λ_j where we assume $|\lambda_1| > |\lambda_2| \geq \dots$. Then we can write the partition function as

$$Z = \sum_j \lambda_j^{\tilde{L}} = \lambda_1^{\tilde{L}} \left(1 + \left(\frac{\lambda_2}{\lambda_1} \right)^{\tilde{L}} + \dots \right) \stackrel{\tilde{L} \gg 1}{\approx} \lambda_1^{\tilde{L}}. \quad (\text{II.4.11})$$

Therefore in the thermodynamic limit we need only to determine the largest eigenvalue of the transfer matrix if we want to calculate the partition function¹². The next-leading eigenvalues also contain interesting information. We will come back to this later.

Note that the transfer matrix already indicates that we are moving towards quantum models. We started out with a classical model where everything commutes. Now we are dealing with matrices which are a non-commuting objects. In fact, in general the transfer matrices belonging to two different sets of Boltzmann weights do not commute. However, the key to the exact solvability of a classical model is to identify families of commuting transfer matrices.

II.4.4 Commuting transfer matrices

In the following we discuss as an example the 6-vertex model. The partition function can be written in a form analogous¹³ to equation (II.4.8). This shows that it depends non-trivially only on two ratios, e.g. $\frac{a}{c}$ and $\frac{b}{c}$, such that $Z = c^N \sum \left(\frac{a}{c} \right)^{n_a} \left(\frac{b}{c} \right)^{n_b}$. Therefore the parameter space is basically two-dimensional as illustrated in Fig. II.4.8. If a subset parametrized by a parameter u exist such that all transfer matrices within this set commute, one has a family of commuting transfer matrices. Usually many such subsets exist which allows to introduce another parameter λ to distinguish these sets.

Especially for the 6-vertex model it can be shown (see later) that

$$[\mathbf{T}(a, b, c), \mathbf{T}(a', b', c')] = 0 \iff \Delta = \Delta' \quad \text{where } \Delta := \frac{a^2 + b^2 - c^2}{2ab}. \quad (\text{II.4.12})$$

So if we have two different models specified by the weights (a, b, c) and (a', b', c') , respectively, their corresponding transfer matrices will commute provided that $\Delta = \Delta'$. As a side remark we just mention here, that this parameter is not called Δ by coincidence, but it will turn out to determine the anisotropy in the associated XXZ model¹⁴.

The form of Δ indicates that a parametrisation in terms of trigonometric or hyperbolic functions is possible (see Appendix B.1). Indeed, for the case $\Delta > 1$ we set

$$a = \rho \sinh(\lambda + u), \quad b = \rho \sinh(u) \quad c = \rho \sinh(\lambda) \quad (\text{II.4.13})$$

where ρ is just some normalization and $u, \lambda > 0$ to guarantee the positivity of the Boltzmann weights, which then implies from the definition of Δ

$$\Delta = \cosh \lambda. \quad (\text{II.4.14})$$

¹²If the largest eigenvalue is degenerate a little more care has to be taken.

¹³Only the factor d^{n_d} has to be dropped.

¹⁴In fact, with our conventions, we will find $\Delta_{XXZ} = -\Delta_{6VM}$.

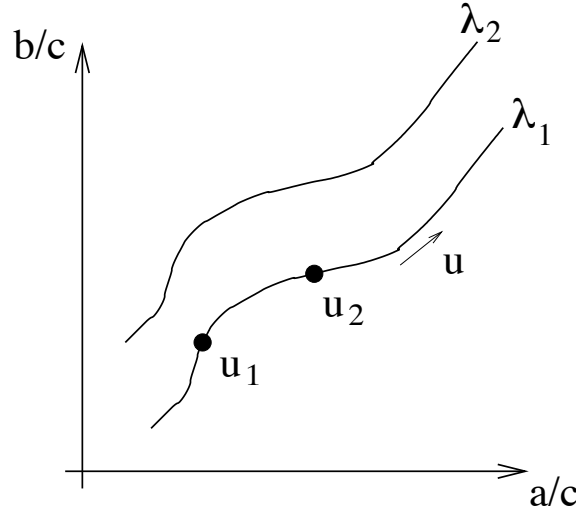


Figure II.4.8: Illustration of the existence of families of commuting transfer matrices. The different families are specified by a parameter λ . For fixed λ all members of the family, parametrized by the spectral parameter u , commute.

Now we can regard the transfer matrix $\mathbf{T}(a,b,c)$ as a function of ρ , λ and u . For fixed λ , all transfer matrices (with different u) commute. This corresponds to the situation depicted in Fig. II.4.8. The parameter u is usually called *spectral parameter* for reasons that should become clear soon. λ is called *crossing parameter*.

Now let us assume that we have found a family of commuting transfer matrices $\mathbf{T}(u)$. What conclusions can we draw from this?

First of all, the mutual commutation implies that a common eigenbasis $|\xi_n\rangle$ of all $\mathbf{T}(u)$ exist which therefore should be independent of the spectral parameter u . Next we can conclude that the eigenvalue functions

$$\Lambda_n(u) := \frac{\langle \xi_n | \mathbf{T}(u) | \xi_n \rangle}{\langle \xi_n | \xi_n \rangle} \quad (\text{II.4.15})$$

are analytical functions of u . Of course this only holds if all matrix elements of the transfer matrix itself are analytical functions of u . Usually one chooses a parametrization which satisfies this, as seen in the example given above.

II.4.5 Transfer matrix and conserved quantities

We now consider the following operators defined as logarithmic derivatives of the transfer matrix at some point u_0 , i.e.

$$I_n := \frac{1}{n!} \frac{d^n}{du^n} \ln \mathbf{T}(u) \Big|_{u=u_0} \quad (\text{II.4.16})$$

$$T(u_0) = \begin{array}{c} | \\ u_0 \end{array} \quad \begin{array}{c} | \\ u_0 \end{array} = \begin{array}{c} \alpha_1 \\ \beta_1 \end{array} \quad \begin{array}{c} \alpha_2 \\ \beta_2 \end{array} \quad \begin{array}{c} \alpha_3 \\ \vdots \end{array} \quad \begin{array}{c} \alpha_{L-1} \alpha_L \\ \beta_{L-1} \beta_L \end{array}$$

Figure II.4.9: Illustration of the shift operator. The bold lines indicate the states which have to be equal in order to give a non-vanishing matrix element.

$$R(u_0) = \begin{array}{c} \nearrow \\ \searrow \end{array}$$

Figure II.4.10: For the six-vertex model, at $u = 0$ the matrix R of vertex weights reduces to a local shift operator.

which is equivalent to the expansion

$$\ln T(u) = \sum_{n=0}^{\infty} I_n (u - u_0)^n. \quad (\text{II.4.17})$$

All these operators I_n commute mutually since they have been generated from a commuting family of operators. This holds for arbitrary points u_0 . Thus we have found an infinite set of (independent) conserved quantities. In analogy with the terminology used in classical mechanics, a system that possesses an infinite number of conservation laws is called *integrable*. Often the two notions *integrability* and *exact solvability* are used synonymously.

However, usually there are special values of u_0 which imply that the operators I_n contain only local interactions (between a few neighbour sites). This happens when u_0 is chosen such that $T(u_0)$ is a *translation operator*, sometimes also called *shift operator*. Such an operator has the property

$$(T(u_0))_{\beta}^{\alpha} = C \delta_{\alpha_2, \beta_1} \delta_{\alpha_3, \beta_2} \cdots \delta_{\alpha_L, \beta_{L-1}} \delta_{\alpha_1, \beta_L} \quad (\text{II.4.18})$$

where the constant C is independent of α and β . This means that only those elements of the transfer matrix are nonzero which satisfy $\alpha_{j+1} = \beta_j$ for all j , i.e. the arrow configuration β is just shifted by one site to the right (see Fig. II.4.9).

In our example for the 6-vertex model given above we have $u_0 = 0$. At this point

$$\begin{aligned} a_0 &= a(u_0 = 0) = \rho \sinh \lambda, & b_0 &= b(u_0 = 0) = 0, \\ c_0 &= c(u_0 = 0) = \rho \sinh \lambda = a_0. \end{aligned} \quad (\text{II.4.19})$$

This implies (see Fig. II.4.5) that only vertices of the structure shown in Fig. II.4.10 survive.

The inverse of the shift operator to the right is obviously the shift operator to left. This is demonstrated graphically in Fig. II.4.11 to show how the graphical representation can be used in calculations.

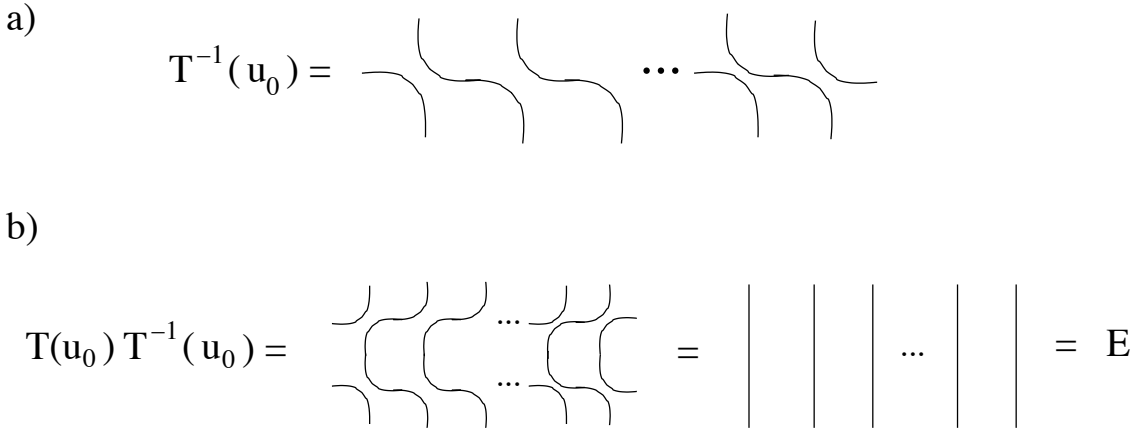


Figure II.4.11: a) Graphical representation of the the inverse shift operator; b) Graphical proof that the two opposite shift operators are inverse.

We are now able to give an interpretation of the conserved quantities I_0 and I_1 . For $n = 0$ we have seen that $T(u_0)$ is the translation operator. That implies that we can write

$$T(u_0) = e^{iP} \quad (\text{II.4.20})$$

and interpret P as the momentum operator. Thus we have $I_0 = iP$. Note that P is the sum of operators acting only at a single site.

For $n = 1$ we have to calculate

$$\frac{d}{du} \ln T(u) \Big|_{u=u_0} = T^{-1}(u_0) T'(u_0) \quad (\text{II.4.21})$$

where T' denotes the derivative of the transfer matrix with respect to the spectral parameter. Now the graphical calculation in Fig. II.4.12 shows that this derivative can be written as

$$T'(u_0) = -T^{-1}(u_0) \sum_{j=1}^L h_{jj+1} \quad (\text{II.4.22})$$

where the $h_{jj+1} = -R'_{j,j+1}(u_0)$ are matrices that act nontrivially only at the (neighbouring) sites j and $j + 1$. It is defined in terms of the derivative of the matrix R of Boltzmann weights. Therefore we might interpret

$$I_1 = - \sum_{j=1}^L h_{jj+1} = -\mathcal{H} \quad (\text{II.4.23})$$

as Hamiltonian of a spin chain with nearest neighbour interactions. Here $I_1 = -\mathcal{H}$ is chosen instead of $I_1 = +\mathcal{H}$ so that the thermodynamics is determined by the low-lying spectrum of \mathcal{H} . Similar calculations for $n > 1$ lead to operators the couple $n + 1$ neighbouring sites. Since these operators commute with the Hamiltonian they are sometimes called *higher conservation laws*.

$$\begin{aligned}
 T'(u_0) &= \sum_{j=1}^L \text{Diagram } 1 \\
 &= \sum_{j=1}^L \text{Diagram } 2 \\
 &= \sum_{j=1}^L \text{Diagram } 3 \\
 &\equiv -T(u_0) \sum_{j=1}^L h_{j,j+1}
 \end{aligned}$$

site j

Figure II.4.12: Graphical calculation of the derivative of the transfer matrix \mathbf{T} at $u = u_0$. Since $\mathbf{T}(u)$ is a product of local Boltzmann weights the derivative is a sum of terms where one of the local factors, indicated by a prime, is differentiated. In the third step, this factor has been reinterpreted as product of the shift operator $T(u_0)$ with a matrix $-h_{j,j+1}$, that acts only at the vertices j and $j + 1$.

Summarizing these results we have

$$\ln \mathbf{T}(u) = iP - \mathcal{H}(u - u_0) + \sum_{n=2}^{\infty} I_n(u - u_0)^n. \quad (\text{II.4.24})$$

If we use the transfer matrix of the 6-vertex model then we find that $\mathcal{H} = -\mathcal{H}_{XXZ}$.¹⁵ E.g. for $\Delta > 1$ we have from (II.4.7) using the parametrisation (II.4.13) with $\rho = 2J$:

$$R'_{j,j+1}(u=0) = 2J \begin{pmatrix} \Delta & 0 & 0 & 0 \\ 0 & 0 & 1 & 0 \\ 0 & 1 & 0 & 0 \\ 0 & 0 & 0 & \Delta \end{pmatrix} = -\langle \tilde{\sigma}_1 \tilde{\sigma}_2 | h_{j,j+1} | \sigma_1 \sigma_2 \rangle \quad (\text{II.4.25})$$

with $h_{j,j+1} = -J(\sigma_j^x \sigma_{j+1}^x + \sigma_j^y \sigma_{j+1}^y + \Delta \sigma_j^z \sigma_{j+1}^z + \Delta)$ (see also Exercise 9). Thus the investigation of the 6-vertex model tells us something about the physics of the XXZ chain.

Let us recapitulate our findings. We have seen that we can generate an infinite set of commuting operators by taking the logarithmic derivatives of the transfer matrix at some point u_0 . If we can choose u_0 such that $\mathbf{T}(u_0)$ becomes a translation operator then the momentum operator and an operator with only nearest-neighbour interactions belong to the set. The latter might be interpreted as Hamiltonian of a spin chain. So this special choice of u_0 guarantees that we have a conserved momentum operator and a Hamiltonian with finite-interaction range. Of course this procedure is not unique. In principle we could use any other I_n as a Hamiltonian.

Before we discuss the important questions how one can find families of commuting transfer matrices we want to say a few words about the consequences of integrability. It has become clear that integrability is the exception, not the rule. This implies the question how generic the behaviour of integrable model actually is. As a rule of thumb one can say that the spectral properties, structure of excited state etc. are generic for a large class of systems. On the other hand, transport properties (e.g. electrical or thermal conductivities) are rather special. Here the infinite number of conservation laws becomes important e.g. by suppressing certain dissipation mechanisms.

II.4.6 The Yang-Baxter equation

We have seen that from a set of commuting transfer matrices we can generate a Hamiltonian and its conservation laws. An important question is how one can find families of commuting transfer matrices. Since the transfer matrix is built from simple local elements, the R -matrix, a purely local criterion should exist which involves only the vertex weights itself and not the full transfer matrix. Such a criterion indeed exists.

Consider three sets R , R' , R'' of vertex weights, e.g. for a 6-vertex model we would have $R = R(a, b, c)$, $R' = R(a', b', c')$ and $R'' = R(a'', b'', c'')$. The existence of a family of commuting transfer matrices is then guaranteed if for all $\sigma_1, \dots, \sigma_6$ the following conditions are satisfied:

¹⁵Equivalently we have $\mathcal{H} = \mathcal{H}_{XXZ}(-\Delta)$ which explains why in our conventions $\Delta_{XXZ} = -\Delta_{6VM}$.

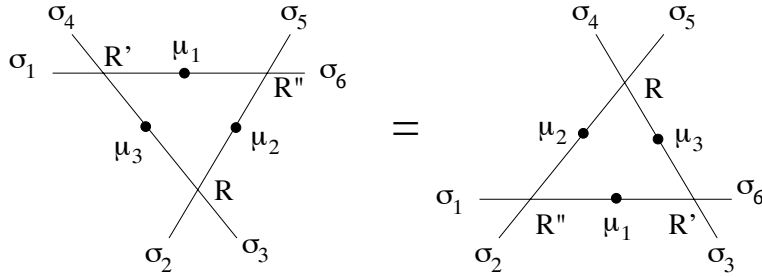


Figure II.4.13: Graphical representation of the Yang-Baxter equation. The outer arrows σ_j are fixed and one has to sum over the internal arrows μ_l . The different set of weights of the vertices are denoted by R , R' and R'' .

$$\sum_{\mu_1, \mu_2, \mu_3} R_{\sigma_2 \sigma_3}^{\mu_3 \mu_2} R_{\sigma_1 \mu_3}^{\sigma_4 \mu_1} R_{\mu_1 \mu_2}^{\sigma_5 \sigma_6} = \sum_{\mu_1, \mu_2, \mu_3} R_{\sigma_1 \sigma_2}^{\mu_2 \mu_1} R_{\mu_1 \sigma_3}^{\mu_3 \sigma_6} R_{\mu_2 \mu_3}^{\sigma_4 \sigma_5}. \quad (\text{II.4.26})$$

These are the famous *Yang-Baxter equations*. Fig. II.4.13 shows a graphical representation of this set of equations ¹⁶.

If we regard the horizontal direction as time and the vertical direction as space, Fig. II.4.13 has a nice interpretation. It is a space-time diagram for a 3-particle scattering process. In the left diagram, first the particles 1 and 2 collide, then 2 and 3, and finally 1 and 3. On the right hand side, the first collision happens between 1 and 3, then 2 and 3, and finally 1 and 2. The Yang-Baxter equation then states that the result of this 3-particle process does not depend on the order of the 2-particle processes. Note that the similarity with the argument given in the derivation of the Bethe-Ansatz equations is no coincidence. We will come back to this later in more detail.

Another interesting remark concerns the relation of the Yang-Baxter equation with knot theory. Knot theory tries to classify knots, especially those that are equivalent to the trivial (unknotted) case. Then the graphical representation shown in Fig. II.4.13 describes an elementary move that transforms a knot into an equivalent one. For an elementary introduction, see [16]. A more technical treatment can be found in [17].

We now can derive the result (II.4.12) about the commutation of 6-vertex model transfer matrices. For the 6-vertex model the Yang-Baxter equations (II.4.26) are a set of $2^6 = 64$ coupled equations. However, due to the ice rule, all equation with $\sigma_1 + \sigma_2 + \sigma_3 \neq \sigma_4 + \sigma_5 + \sigma_6$ are trivially satisfied. This leaves us with 20 equations. If we use the symmetries of the vertex weights, these can further be reduced to just 3 equations. One of these is obtained by the choice¹⁷ $\sigma_1 = \sigma_4 = -$ and $\sigma_2 = \sigma_3 = \sigma_5 = \sigma_6 = +$. For this configuration the Yang-Baxter equation (II.4.26) translates into $ac'a'' = ca'a'' + bc'b''$. Similarly the two other independent equations can be derived. Regarding these as equations which determine the weights R'' for given R and R' one easily finds that a nontrivial solution only exists iff

$$\frac{a^2 + b^2 - c^2}{2ab} = \frac{a'^2 + b'^2 - c'^2}{2a'b'}. \quad (\text{II.4.27})$$

¹⁶In the context of classical spin models similar relations exist and are known as *star-triangle equations*.

¹⁷Remember, that '+' denotes a right- or upward-pointing arrow and '-' a left- or downward-pointing one.

$$\begin{aligned}
 T' \cdot T &= \text{Diagram 1} \\
 &= \text{Diagram 2} \\
 &= \text{Diagram 3} = T \cdot T'
 \end{aligned}$$

The diagrams show a sequence of vertical lines representing lattice sites. Horizontal lines connect adjacent sites. A central vertex at site 3 has weight R'' . It is connected to site 2 by a horizontal line and to site 4 by another horizontal line. The Yang-Baxter equation is used to move this vertex through the lattice. In Diagram 1, the vertex is moved from site 3 to site 4. In Diagram 2, it is moved from site 3 to site 2. In Diagram 3, it is moved from site 2 to site 4. The final result is $T \cdot T'$.

Figure II.4.14: Graphical proof that two transfer matrices T and T' commute if their weights R and R' satisfy the Yang-Baxter equation.

It should be emphasized that the Yang-Baxter equations are a strongly constrained system of equations. For a q -state vertex model, which has q^4 local Boltzmann-weights, there are q^6 equations. Therefore it is not surprising that solutions exist only in very special cases.

Finally we want to prove that the Yang-Baxter equations indeed imply the commutation of the transfer matrices. This is again done graphically in Fig. II.4.14. Somewhere in the chain, an identity matrix in the form $R''(R'')^{-1}$ is inserted. Using the Yang-Baxter equation the vertex with weight R'' is moved through the lattice thereby exchanging the weights R and R' in each step. Due to the periodic boundary conditions it finally meets $(R'')^{-1}$ from the “other side” and vanishes.

II.4.7 Trotter-Suzuki decomposition

We have seen how to generate an interesting quantum Hamiltonian in one dimension from a solvable classical model in two dimensions. Is it possible to invert this procedure? In principle yes, but usually it is not practical. Starting from a quantum Hamiltonian we could try to determine all conserved quantities I_n and then use (II.4.24) to define the transfer matrix of a classical model. Normally it is not possible to obtain all I_n explicitly. If only a subset is used, the resulting classical model might have a complicated structure. Therefore other methods are needed. Since there is no unique relation between the transfer matrix and an associated Hamiltonian, several methods exist.

In the following we show how the thermodynamics of a d -dimensional quantum Hamiltonian $\mathcal{H} = \sum_j h_{jj+1}$ can be mapped onto that of a classical system in $d + 1$ dimensions. The big problem for the quantum systems come from the factor $\exp(\beta\mathcal{H})$ appearing in the partition function. Since the local interactions usually do not commute with each other the exponential can not be decomposed into local factors $\exp(-\beta h_{jj+1})$ easily. Note that in general for two noncommuting operators \mathcal{A} and \mathcal{B} one has the identity

$$e^{\Delta\tau(\mathcal{A}+\mathcal{B})} = e^{\Delta\tau\mathcal{A}}e^{\Delta\tau\mathcal{B}} + [\mathcal{A}, \mathcal{B}] O((\Delta\tau)^2) \quad (\text{II.4.28})$$

where $O((\Delta\tau)^2)$ denotes corrections of the order $(\Delta\tau)^2$.

A mathematical result due to Trotter (1959) allows to solve this problem. Trotter has shown that

$$e^{-\beta(\mathcal{A}+\mathcal{B})} = \lim_{m \rightarrow \infty} \left(e^{-\frac{\beta}{m}\mathcal{A}} e^{-\frac{\beta}{m}\mathcal{B}} \right)^m. \quad (\text{II.4.29})$$

This result, which has been used in a physics context first by Suzuki, is known as *Trotter-Suzuki decomposition*. It can be applied to the Hamiltonian in the following way. First, we split the interaction in two parts acting on even and odd bonds only:

$$\mathcal{H} = \sum_{j \text{ even}} h_{jj+1} + \sum_{j \text{ odd}} h_{jj+1} =: \mathcal{H}_1 + \mathcal{H}_2. \quad (\text{II.4.30})$$

This has the advantage, the all local interactions contained in H_α commute. However, the partial Hamiltonians itself do not commute: $[\mathcal{H}_1, \mathcal{H}_2] \neq 0$. Here we apply the decomposition (II.4.29). Then we can rewrite the partition function of the quantum system in the following way:

$$\begin{aligned} Z &= \text{Tr } e^{-\beta\mathcal{H}} \cong \text{Tr} \left(\underbrace{e^{-\Delta\tau\mathcal{H}_1} e^{-\Delta\tau\mathcal{H}_2} e^{-\Delta\tau\mathcal{H}_1} e^{-\Delta\tau\mathcal{H}_2} \dots}_{2m \text{ factors}} \right) \\ &= \sum_{\{|\psi_1\rangle, \dots, |\psi_{2m}\rangle\}} \langle \psi_1 | e^{-\Delta\tau\mathcal{H}_1} | \psi_2 \rangle \langle \psi_2 | e^{-\Delta\tau\mathcal{H}_2} | \psi_3 \rangle \dots \langle \psi_{2m-1} | e^{-\Delta\tau\mathcal{H}_1} | \psi_{2m} \rangle \langle \psi_{2m} | e^{-\Delta\tau\mathcal{H}_2} | \psi_1 \rangle, \end{aligned} \quad (\text{II.4.31})$$

where the $\{|\psi_j\rangle\}$ are copies of a basis of the Hilbert space and m is supposed to be large. The last expression corresponds to the partition function of a classical model defined by the Boltzmann weights $\langle \psi | e^{-\Delta\tau\mathcal{H}_1} | \tilde{\psi} \rangle$ and $\langle \psi | e^{-\Delta\tau\mathcal{H}_2} | \tilde{\psi} \rangle$. Thus the weights have an alternating structure and the classical model has a checkerboard structure as shown in Fig. II.4.15. Thus the Trotter-Suzuki decomposition has introduced a second space dimension which is called *Trotter direction*. The other direction corresponding to the space dimension of the quantum model is called *quantum direction*.

The Trotter-Suzuki decomposition is starting point for one of the most important numerical approaches for studying quantum systems, the so-called *quantum Monte Carlo method* (QMC). It uses the above mapping and then studies the resulting classical system using Monte Carlo simulations, i.e. defining a random dynamics that converge to the equilibrium state.

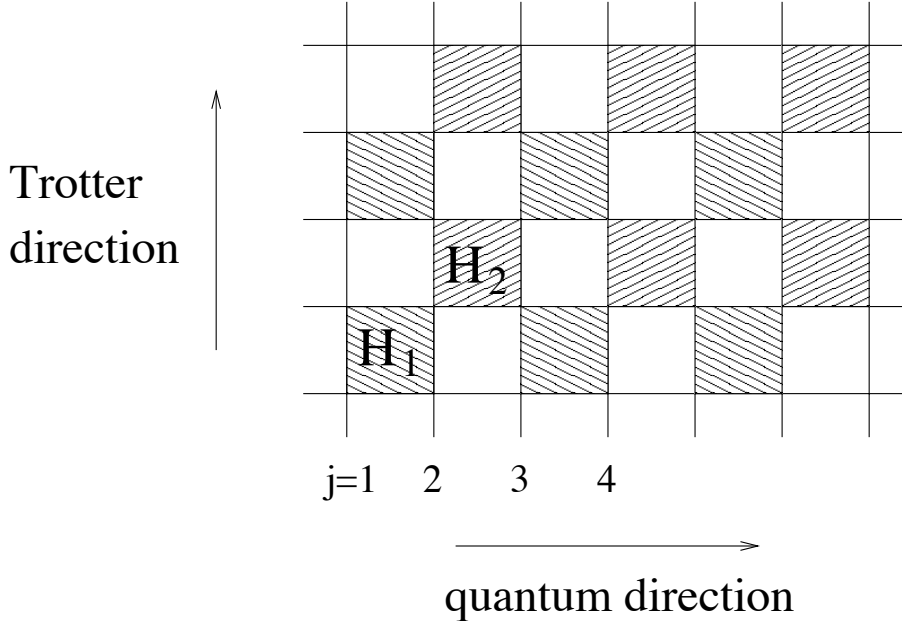


Figure II.4.15: Checkerboard lattice of the classical system obtained from a quantum chain by Trotter-Suzuki decomposition.

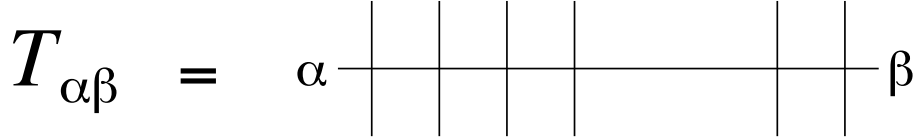
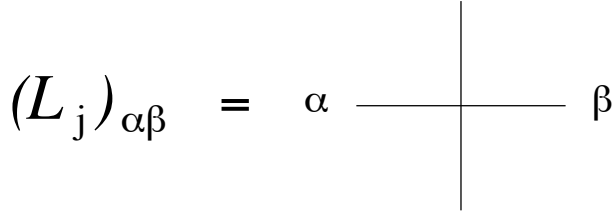
II.5 Algebraic Bethe Ansatz

In Sec. II.3 we have described the so-called *coordinate Bethe Ansatz* where the wavefunction is constructed explicitly. However, similar to the harmonic oscillator, it is also possible to derive the Bethe Ansatz algebraically by defining appropriate creation operators. This is the *algebraic Bethe Ansatz* which is also known as *quantum inverse scattering method* because it is inspired by ideas used in the (classical) inverse scattering method where one tries to determine the form of a potential from the results of scattering processes. The algebraic Bethe Ansatz has been developed by Faddeev and coworkers around 1980. An extensive overview can be found in [18]. Starting point for the algebraic Bethe Ansatz is a classical model, e.g. a vertex model, with a transfer matrix that generates a quantum Hamiltonian as described in the previous section. Furthermore the model should satisfy the Yang-Baxter equation. In the following we will usually take the 6-vertex model as an example and will later show that the associated Hamiltonian is the XXZ chain.

First, one defines the so-called *monodromy matrix* T . It is basically a transfer matrix that is not periodically closed in horizontal direction. Fig. II.5.1 shows a graphical representation. The matrix elements correspond to the allowed configurations of the arrows at the left and the right hand. Usually the monodromy matrix is written as a 2×2 matrix in an *auxiliary space* as

$$\mathcal{T} = \begin{pmatrix} \mathcal{T}_{++} & \mathcal{T}_{+-} \\ \mathcal{T}_{-+} & \mathcal{T}_{--} \end{pmatrix} = \begin{pmatrix} A & B \\ C & D \end{pmatrix}. \quad (\text{II.5.1})$$

Note that each entry $\mathcal{T}_{\alpha\beta}$ is itself a matrix defined similar to equation (II.4.9), but without periodical boundary conditions. The latter mean identification and summation over the boundary

Figure II.5.1: Definition of the monodromy matrix T .Figure II.5.2: Definition of the L -operators.

variables $\alpha = \beta$, i.e. the transfer matrix is obtained as

$$\mathbf{T} = \text{Tr } \mathcal{T} = A + D, \quad (\text{II.5.2})$$

where the trace has to be taken only over the auxiliary space. Later we will see, that the other two elements B and C of the monodromy matrix can be interpreted as creation and annihilation operators of spin waves.

Since we the monodromy matrix is defined in an auxiliary space it is useful to reinterpret the matrix R containing the Boltzmann weights taking into account this additional structure. This leads to the local L -operators defined in Fig. II.5.2. This operator is identical to the R -matrix, just the elements are rearranged. For the 6-vertex model we can write the operator in terms of Pauli-matrices as

$$\mathcal{L}_j = \begin{pmatrix} \frac{a+b}{2} + \frac{a-b}{2}\sigma_j^z & c\sigma_j^- \\ c\sigma_j^+ & \frac{a+b}{2} - \frac{a-b}{2}\sigma_j^z \end{pmatrix}. \quad (\text{II.5.3})$$

Inserting the explicit expressions of the Pauli matrices, the R -matrix (II.4.7) is recovered up to a permutation:

$$\mathcal{L} = \begin{pmatrix} a & 0 & 0 & 0 \\ 0 & b & c & 0 \\ 0 & c & b & 0 \\ 0 & 0 & 0 & a \end{pmatrix} = \begin{pmatrix} 1 & 0 & 0 & 0 \\ 0 & 0 & 1 & 0 \\ 0 & 1 & 0 & 0 \\ 0 & 0 & 0 & 1 \end{pmatrix} R. \quad (\text{II.5.4})$$

The monodromy matrix can now be written as

$$\mathcal{T} = \mathcal{L}_1 \mathcal{L}_2 \cdots \mathcal{L}_L. \quad (\text{II.5.5})$$

Note that here we can already see an indication that the operators B and C of the monodromy matrix can be interpreted as creation and annihilation operators due to the appearance of the ladder operators σ_j^\pm in the off-diagonal elements in (II.5.3).

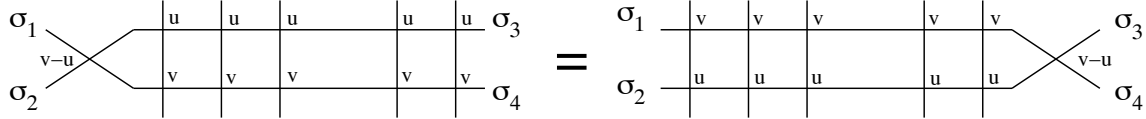


Figure II.5.3: Yang-Baxter equation for the monodromy matrix. The arrows σ_j at the ends are fixed.

As in the coordinate Bethe Ansatz we need a simple *reference state* or *pseudo-vacuum* $|0\rangle$. In the case of the 6-vertex model the standard choice is $|0\rangle = |++\dots+\rangle$. Application of the operator \mathcal{L}_j that acts only at site j gives according to (II.5.3)

$$\mathcal{L}_j|+\rangle_j = \begin{pmatrix} a|+\rangle_j & c|- \rangle_j \\ 0 & b|+\rangle_j \end{pmatrix}. \quad (\text{II.5.6})$$

Therefore we have

$$\mathcal{T}|0\rangle = \overbrace{\prod_j}^{\curvearrowleft} \mathcal{L}_j|+\rangle_j = \begin{pmatrix} a^L|0\rangle_j & * \\ 0 & b^L|+\rangle_j \end{pmatrix} \quad (\text{II.5.7})$$

where the arrow over the product sign indicates in which order the product has to be taken. In the final result the asterics indicates a complicated expression which is not explicitly needed in the following. The important result is that $\mathcal{T}|0\rangle$ is upper triangular matrix. Therefore we have

$$\mathbf{T}|0\rangle = (\text{Tr } \mathcal{T})|0\rangle = (a^L + b^L)|0\rangle. \quad (\text{II.5.8})$$

The strategy will now be the following: The operator B will be used as creation operator for excitations above the reference state $|0\rangle$. This is partly motivated by the raising operator appearing in the $(1, 2)$ -element of the \mathcal{L} -operator (II.5.3). The Yang-Baxter equation can be extended to the monodromy matrix and will give an operator algebra for the operators A, B, C and D .

First, we derive the Yang-Baxter equation for the monodromy matrix \mathcal{T} . For the transfer matrix the local Yang-Baxter relations (II.4.26) lead to commuting of the transfer matrices. In the derivation, the periodic boundary conditions played an essential role. Since \mathcal{T} has open ends, the Yang-Baxter equation will not lead to the commutation of two monodromy matrices, but rather some nontrivial relations between their elements.

We look at the R -matrices $R = R(u)$, $R' = R(v)$ and $R'' = R(v - u)$ at three different values of the spectral parameter such that the (local) Yang-Baxter equations (II.4.26) are satisfied. Then we have

$$R(v - u)\mathcal{T}(u)\mathcal{T}(v) = \mathcal{T}(v)\mathcal{T}(u)R(v - u). \quad (\text{II.5.9})$$

This is the Yang-Baxter equation for the monodromy matrix. A graphical proof is given in Fig. (II.5.3). It is almost identical to the Fig. II.4.14, but without periodical boundary conditions.

If we regard (II.5.9) as an equation in auxiliary space, it corresponds to 16 equations relating the operators A, B, C and D . For instance choosing $\sigma_1 = \sigma_2 = +$ and $\sigma_3 = \sigma_4 = -$, one obtains the relation

$$R_{++}^{++}(v - u)B(u)B(v) = B(v)B(u)R_{--}^{--}(v - u) \quad (\text{II.5.10})$$

which reduces to

$$[B(u), B(v)] = 0 \quad (\text{II.5.11})$$

since $R_{++}^{++}(v - u) = R_{--}^{--}(v - u) = a(v - u)$. Thus we see that two B -operators for different spectral parameters commute. Similarly one can prove that also the other three operators commute at different spectral parameters. In the following construction of the eigenstates of the transfer matrix we will need two further relations explicitly. These are obtained for the choices $\sigma_1 = \sigma_2 = +, \sigma_3 = -, \sigma_4 = +$ and $\sigma_1 = -, \sigma_2 = +, \sigma_3 = \sigma_4 = -$ after a minor rearrangement:

$$A(u)B(v) = \frac{a(v - u)}{b(v - u)} B(v)A(u) - \frac{c(v - u)}{b(v - u)} B(u)A(v), \quad (\text{II.5.12})$$

$$D(u)B(v) = \frac{a(u - v)}{b(u - v)} B(v)D(u) - \frac{c(u - v)}{b(u - v)} B(u)D(v). \quad (\text{II.5.13})$$

The other commutation relations of the algebra formed by A, B, C and D are not needed in the following. They can be found e.g. in [18].

We now state the central result of this section:

$$|v_1, \dots, v_M\rangle := \prod_{j=1}^M B(v_j)|0\rangle \quad (\text{II.5.14})$$

is an eigenstate of $\mathbf{T}(u) = \text{Tr } \mathcal{T}(u) = A(u) + D(u)$ with eigenvalue

$$\Lambda(u) = a^L(u) \prod_{j=1}^M \frac{a(v_j - u)}{b(v_j - u)} + b^L(u) \prod_{j=1}^M \frac{a(u - v_j)}{b(u - v_j)} \quad (\text{II.5.15})$$

if the Bethe-Ansatz equations

$$\frac{a^L(v_j)}{b^L(v_j)} = \prod_{l=1, l \neq j}^M \frac{a(v_j - v_l)}{a(v_l - v_j)} \quad (j = 1, \dots, M) \quad (\text{II.5.16})$$

are satisfied.

(II.5.14) shows explicitly that the B -operators create magnon excitations. Note that due to (II.5.11) the ordering of the B -operators is not important.

In the following we sketch the derivation of this central result without giving all the details (see also Exercise 14). First we investigate how $A(u)$ acts on the states $|v_1, \dots, v_M\rangle$ to determine $A(u)B(v_1) \cdots B(v_M)|0\rangle$. Since we know from (II.5.8) how it acts on the reference state, we will try to commute $A(u)$ to the right. Using (II.5.12) M times, we generate $M+1$ terms of the form $B \cdots BA|0\rangle$. One term is proportional to $B(v_1) \cdots B(v_M)A(u)|0\rangle$, whereas in the others one of the arguments v_l is exchanged with u . Explicitly one obtains (see Exercise 14)

$$\begin{aligned} A(u)|v_1, \dots, v_M\rangle &= a^L(u) \prod_{l=1}^M \frac{a(v_l - u)}{b(v_l - u)} \underbrace{B(v_1) \cdots B(v_M)|0\rangle}_{=|v_1, \dots, v_M\rangle} \\ &\quad + \sum_{j=1}^M \left[-\frac{c(v_j - u)}{b(v_j - u)} \prod_{l=1, l \neq j}^M \frac{a(v_l - v_j)}{b(v_l - v_j)} \right] a^L(v_j)B(u) \prod_{l=1, l \neq j}^M B(v_l)|0\rangle \end{aligned} \quad (\text{II.5.17})$$

where the factors a^L come from the $A|0\rangle$. Similarly one obtains for the application of $D(u)$

$$\begin{aligned} D(u)|v_1, \dots, v_M\rangle &= a^L(u) \prod_{l=1}^M \frac{a(u - v_l)}{b(u - v_l)} |v_1, \dots, v_M\rangle \\ &\quad + \sum_{j=1}^M \left[-\frac{c(u - v_j)}{b(u - v_j)} \prod_{l=1, l \neq j}^M \frac{a(v_j - v_l)}{b(v_j - v_l)} \right] b^L(v_j) B(u) \prod_{l=1, l \neq j}^M B(v_l) |0\rangle. \end{aligned} \quad (\text{II.5.18})$$

We now can determine the way the transfer matrix $\mathbf{T}(u)$ acts on the states (II.5.14):

$$\begin{aligned} \mathbf{T}(u)|v_1, \dots, v_M\rangle &= (A(u) + D(u))|v_1, \dots, v_M\rangle \\ &= \Lambda(u)|v_1, \dots, v_M\rangle + \sum_{j=1}^M \tilde{\Lambda}_j(u; \{v_l\}) B(u) \prod_{l=1, l \neq j}^M B(v_l) |0\rangle \end{aligned} \quad (\text{II.5.19})$$

where $\Lambda(u)$ is given by (II.5.15). The form of the $\tilde{\Lambda}_j(u; \{v_l\})$ can be obtained from (II.5.17) and (II.5.18). Inspection shows that $|v_1, \dots, v_M\rangle$ is indeed an eigenstate of $\mathbf{T}(u)$ if the terms proportional to $B(u) \prod_{l=1, l \neq j}^M B(v_l) |0\rangle$ vanish. These are therefore called *unwanted terms*. In fact they can be made to vanish by imposing conditions on the $\tilde{\Lambda}_j(u; \{v_l\})$. It is not hard to see that these conditions are exactly the Bethe-Ansatz equations (II.5.16), i.e. the unwanted terms can only be made to vanish for certain choices of the parameters v_j . It then remains to be seen whether this still allows to generate enough eigenstates of the transfer matrix that form a complete set.

We finish we some remarks:

1. The Bethe-Ansatz equations can be derived directly from the functional form (II.5.15) of the eigenvalues $\Lambda(u)$ since, as we have explained earlier, these functions have to be analytic. Clearly the denominator of $\Lambda(u)$ vanishes for $u = v_j$ since¹⁸ $b(0) = 0$. In order for $\Lambda(u)$ to be analytic this zero must be compensated by a corresponding zero of the numerator. It is easy to check that this leads to the Bethe-Ansatz equations (II.5.16).
2. It can be shown by explicit calculation that

$$S^z|v_1, \dots, v_M\rangle = \left(\frac{L}{2} - M \right) |v_1, \dots, v_M\rangle \quad (\text{II.5.20})$$

since each B -operator is a product of σ_i^z -operators with exactly one σ_j^- (corresponding to a plane wave of a flip spin). In the isotropic case $|\Delta| = 1$ the Hamiltonian has a $SU(2)$ -symmetry. In this case all Bethe-Ansatz states have total spin $S = S^z$, i.e. they are highest weight states of the spin multiplets. The other states of the multiplet can then be obtained by application of $(S^-)^l$ on the Bethe-state.

¹⁸This is a rather general property that follows from the fact that $\mathbf{T}(u = 0)$ is the shift operator.

3. A careful analysis reveals that a maximal allowed values M_{\max} of flipped spins exists for the algebraic Bethe-Ansatz to work, namely $M_{\max} = \frac{L}{2}$, corresponding to $S^z = 0$. The states with $S^z < 0$ can be obtained by using the spin flip symmetry of the Hamiltonian or starting the Bethe-Ansatz with reference state $|\downarrow \cdots \downarrow\rangle$.
4. Using the parametrisation (II.4.13) for $\Delta > 1$ one can show that the eigenvalue $\Lambda(u)$ can be rewritten in the form

$$\Lambda(u) = \rho^L \frac{\sinh^L(u + \lambda)q(u - \lambda) + \sinh^L(u)q(u + \lambda)}{q(u)} \quad (\text{II.5.21})$$

where we have introduced the function

$$q(u) := \prod_{j=1}^M \sinh(u - v_j). \quad (\text{II.5.22})$$

For small u one then has, since $\sinh^L(u) = O(u^L)$,

$$\Lambda(u) \approx \rho^L \frac{\sinh^L(u + \lambda)q(u - \lambda)}{q(u)} \quad (\text{II.5.23})$$

and, after shifting the argument by λ ,

$$\begin{aligned} \Lambda(u - \lambda) &= \rho^L \frac{\sinh^L(u)q(u - 2\lambda) + \sinh^L(u - \lambda)q(u)}{q(u - \lambda)} \\ &\approx \rho^L \frac{\sinh^L(u - \lambda)q(u)}{q(u - \lambda)}. \end{aligned} \quad (\text{II.5.24})$$

Multiplying these two equations gives

$$\Lambda(u)\Lambda(u - \lambda) = \rho^{2L} (\sinh(u + \lambda)\sinh(u - \lambda))^L (1 + O(e^{-CL})). \quad (\text{II.5.25})$$

This result is called *inversion relation* since it implies that for the transfer matrix a relation of the type

$$\mathbf{T}(u)\mathbf{T}(u - \lambda) = \rho^{2L} (\sinh(u + \lambda)\sinh(u - \lambda))^L (\mathbf{1} + O(e^{-CL})). \quad (\text{II.5.26})$$

holds where $\mathbf{1}$ is the unit matrix. Therefore the transfer matrices at spectral parameters u and $u - \lambda$ are ‘almost’ inverse to each other.

The investigation of such inversion relations, that also can be derived for the case $\Delta \leq 1$ not covered by the parametrisation (II.4.13), provides an elegant alternative method to the solution of the Bethe-Ansatz equations. One then has to solve the functional equation taking into account the analytic properties of the eigenvalue function $\Lambda(u)$.

II.6 Spectrum and structure of excitations in the XXZ model

In the following we will show how the Bethe-Ansatz equations are solved and how the ground-state energy and the low-lying excitations can be obtained in the thermodynamic limit. The structure of the corresponding eigenstates is extremely involved and therefore they are hardly ever used explicitly. Instead we will see that a lot about the excitations can be learnt by just considering the solutions of the Bethe-Ansatz equations alone.

We will first discuss the isotropic Heisenberg model with $\Delta = 1$ and consider the ferromagnetic and antiferromagnetic case separately [19]. Finally a brief overview over the results for the anisotropic cases is given.

II.6.1 Isotropic ferromagnet

We start with the case¹⁹ $\Delta = 1$ and $J = -|J| < 0$. For classical spin variables, a parallel orientation would be favoured. In order to see what happens in the quantum case we first rewrite the Hamiltonian in the form (see Exercise 13)

$$\begin{aligned}\mathcal{H}_{XXX} &= -|J| \sum_{j=1}^L (\sigma_j \cdot \sigma_{j+1} - 1) \\ &= 4|J| \sum_{j=1}^L (\sigma_j \cdot \sigma_{j+1} - 1)^2.\end{aligned}\tag{II.6.1}$$

The last form explicitly shows that \mathcal{H}_{XXX} is a positive-semidefinit operator. Since we already know that for the reference state $\mathcal{H}_{XXX}|0\rangle = 0$, the state $|\Omega\rangle := |0\rangle = |\uparrow \cdots \uparrow\rangle$ is a groundstate in the ferromagnetic case.

This groundstate is highly degenerate since it belongs to a multiplet with $2S^z + 1 = 2\frac{L}{2} + 1 = L + 1$ states

$$|\Omega_l\rangle := (\sigma^-)^l |\Omega\rangle \quad (l = 0, 1, \dots, L - 1)\tag{II.6.2}$$

where $\sigma^- = \sum_{j=1}^L \sigma_j^-$. This is a consequence of the $SU(2)$ -symmetry in the isotropic case which implies

$$[\mathcal{H}_{XXX}, \sigma_j^\pm] = 0.\tag{II.6.3}$$

Especially for $l = L$ we obtain the spin-flipped state $|\Omega_L\rangle = |\downarrow \cdots \downarrow\rangle$. As mentioned earlier, using the formalism of the algebraic Bethe-Ansatz one can show that for any Bethe-Ansatz state²⁰

$$\sigma^+ |\text{BA-state}\rangle = 0.\tag{II.6.4}$$

Therefore the Bethe-Ansatz only gives the states of highest weight in a multiplet, i.e. those with $S^z = S$ where S is the total spin.

¹⁹According to Exercise 3 this is equivalent to $\Delta = -1$ and $J > 0$.

²⁰with finite spectral parameters

It can be shown that all other states different from the $|\Omega_l\rangle$ have positive energies. They have to be determined from the solutions of the Bethe-Ansatz equations. Here it is useful to rewrite the Bethe-Ansatz equations (II.3.43) by using the parametrisation

$$k_j = 2 \operatorname{arccot}(2\lambda_j) = \frac{1}{i} \ln \frac{2\lambda_j + i}{2\lambda_j - i} \quad (\text{II.6.5})$$

in terms of new variables λ_j . These are basically the spectral parameters appearing in (II.5.14)²¹. This gives the standard form

$$\left(\frac{\lambda_j + i/2}{\lambda_j - i/2} \right)^L = - \prod_{l=1}^M \frac{\lambda_j - \lambda_l + i}{\lambda_j - \lambda_l - i} \quad (\text{II.6.6})$$

of the Bethe-Ansatz equations (see Exercise 12). The parameters λ_j are sometimes called *Bethe-Ansatz roots*. The corresponding eigenstates are given by $|\lambda_1, \dots, \lambda_M\rangle = B(\lambda_1) \cdots B(\lambda_M)|\Omega\rangle$. Energy and momentum are given by (see Exercise 12)

$$E = 4|J| \sum_{j=1}^M (1 - \cos k_j) = 2|J| \sum_{j=1}^M \frac{1}{\lambda_j^2 + 1/4}, \quad (\text{II.6.7})$$

$$P = \sum_{j=1}^M k_j = 2 \sum_{j=1}^M \operatorname{arccot}(2\lambda_j). \quad (\text{II.6.8})$$

Thus the parameters λ_j parametrise energy and momentum. Therefore they are sometimes called *rapidities* to emphasize the similarity with the rapidity parameter θ used in relativistic theories as a parametrisation: $E = m \cosh \theta$ and $P = m \sinh \theta$. Thus the relativistic dispersion $p^2 + m^2 = E^2$ is satisfied for all values of θ .

After we have already found the groundstate we now discuss the low-lying excitations. It is reasonable that they deviate not too strongly from the groundstate, i.e. can be found in the subspaces for small M . This can also be seen from (II.6.7). Each λ_j gives a positive contribution $\frac{1}{\lambda_j^2 + 1/4} > 0$ to the energy. Therefore one should look for the cases where there are only a few λ 's to minimize the energy.

First we discuss the case $M = 1$. Here we only have one λ or equivalently one wavenumber k that is determined by the Bethe-Ansatz equation

$$\left(\frac{\lambda_j + i/2}{\lambda_j - i/2} \right)^L = 1 = e^{ikL}. \quad (\text{II.6.9})$$

In the thermodynamic limit $L \rightarrow \infty$, the allowed wavenumbers k fill the whole interval $[0, 2\pi[$. The corresponding numbers take all values on the real axis. The dispersion of these 1-magnon states is therefore given by

²¹Therefore it would be better to call these parameters v_j to avoid possible confusion with the crossing parameter. However, we will follow the usual conventions here.

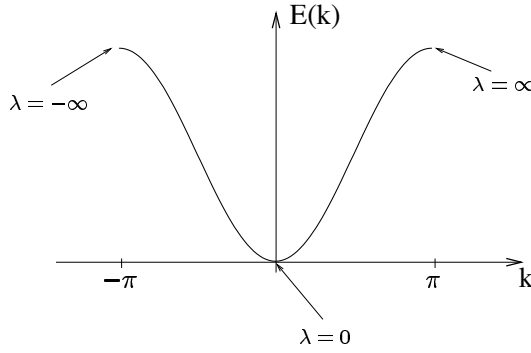


Figure II.6.1: Dispersion of 1-magnon excitations over the ferromagnetic groundstate of the isotropic Heisenberg model. Indicated are also the corresponding values of the Bethe-Ansatz parameters λ .

$$E_1(P) = 4|J|(1 - \cos P) \quad (\text{II.6.10})$$

since the momentum is just $P = k$. Obviously $E_1(P) \geq 0$, but excitations of arbitrarily small energies exist, i.e. there is no gap to the excited states in the case of the isotropic ferromagnet. Relative to the groundstate this excited state has $S^z = 1$, since we have flipped one spin. The highest weight property of the Bethe-Ansatz states then tells us that a magnon, the elementary excitation above the ferromagnetic state, has (total) spin 1.

We now investigate 2-magnon states. In this case the Bethe-Ansatz equations read

$$\left(\frac{\lambda_1 + i/2}{\lambda_1 - i/2} \right)^L = \frac{\lambda_1 - \lambda_2 + i}{\lambda_1 - \lambda_2 - i}, \quad \left(\frac{\lambda_2 + i/2}{\lambda_2 - i/2} \right)^L = \frac{\lambda_2 - \lambda_1 + i}{\lambda_2 - \lambda_1 - i}. \quad (\text{II.6.11})$$

First we search for solutions with λ_j real. In this case, after taking the L -th root of the equations, one obtains

$$\begin{aligned} \frac{\lambda_1 + i/2}{\lambda_1 - i/2} &= \xi_1 e^{\frac{i}{L}\phi(\lambda_1 - \lambda_2)} \xrightarrow{L \rightarrow \infty} \xi_1, \\ \frac{\lambda_2 + i/2}{\lambda_2 - i/2} &= \xi_2 e^{\frac{i}{L}\phi(\lambda_2 - \lambda_1)} \xrightarrow{L \rightarrow \infty} \xi_2, \end{aligned} \quad (\text{II.6.12})$$

where ξ_j are arbitrary roots of unity and ϕ is some phase function. Therefore in the thermodynamic limit the two Bethe-equations decouple and we are left with two equations of the 1-magnon type. These correspond to *scattering states* of the two magnons since the energy is additive:

$$E_2^{(s)}(k_1, k_2) = 4|J|(2 - \cos k_1 - \cos k_2) = 8|J| \left(1 - \cos \frac{k_1 + k_2}{2} \cos \frac{k_1 - k_2}{2} \right). \quad (\text{II.6.13})$$

These scattering states form a continuum. The lowest energy for fixed total momentum $P = k_1 + k_2$ is reached for $k_1 = k_2 = \frac{P}{2}$. The highest energy corresponds to the choice $k_1 = \frac{P}{2} + \pi$ and $k_1 = \frac{P}{2} - \pi$. Therefore the lower and upper limiting curves of the 2-magnon scattering states are

$$E_l(P) = 8|J| \left(1 - \cos \left(\frac{P}{2} \right) \right), \quad E_u(P) = 8|J| \left(1 + \cos \left(\frac{P}{2} \right) \right). \quad (\text{II.6.14})$$

However, the Bethe-Ansatz equations also allow complex solutions. Therefore we assume that $\lambda_{1/2} = x_{1/2} + iy_{1/2}$. Taking the modulus of the Bethe equations (II.6.11) one obtains

$$\left(\frac{x_1^2 + (y_1 + 1/2)^2}{x_1^2 + (y_1 - 1/2)^2} \right)^L = \frac{(x_1 - x_2)^2 + (y_1 - y_2 + 1)^2}{(x_1 - x_2)^2 + (y_1 - y_2 - 1)^2}. \quad (\text{II.6.15})$$

Now assume that $y_1 > 0$ ²². Then the fraction on the left hand side is larger than 1 and thus the left side grows exponentially with L . Therefore the right hand side must also grow exponentially. This leads to

$$x_1 = x_2, \quad y_1 - y_2 = 1 + O(e^{-L}) \quad (\text{II.6.16})$$

which leads to a denominator of order e^{-L} . Next we consider the product of the two Bethe equations:

$$\begin{aligned} 1 &= \left(\frac{x_1 + i(y_1 + 1/2)}{x_1 + i(y_1 - 1/2)} \cdot \frac{x_2 + i(y_2 + 1/2)}{x_2 + i(y_2 - 1/2)} \right)^L \\ &= \left(\frac{x_1 + i(y_1 + 1/2)}{x_1 + i(y_1 - 1/2)} \cdot \frac{x_1 + i(y_1 - 1/2)}{x_1 + i(y_1 - 3/2)} \right)^L = \left(\frac{x_1 + i(y_1 + 1/2)}{x_1 + i(y_1 - 3/2)} \right)^L \end{aligned} \quad (\text{II.6.17})$$

where we have used the result (II.6.16). This equality than requires that $y_1 = \frac{1}{2}$ so that the modulus of the last fraction becomes 1.

Thus in the thermodynamic limit the Bethe-Ansatz equations do not only have real solutions, but also complex ones in the form of *2-strings*

$$\lambda_{1/2} = x \pm \frac{i}{2} \quad (\text{II.6.18})$$

with $x \in \mathbb{R}$. Here x , which is also called *position* or *center of the string*, parametrises the momentum:

$$e^{iP(\lambda_1, \lambda_2)} = e^{i(k_1 + k_2)} = e^{2i \operatorname{arccot}(2\lambda_1)} e^{2i \operatorname{arccot}(2\lambda_2)} = \frac{x - i}{x + i}. \quad (\text{II.6.19})$$

The energy of the 2-string state is given by

$$E_2^{(b)}(\lambda_1, \lambda_2) = \frac{2|J|}{(x + i/2)^2 + 1/4} + \frac{2|J|}{(x - i/2)^2 + 1/4} \quad (\text{II.6.20})$$

or

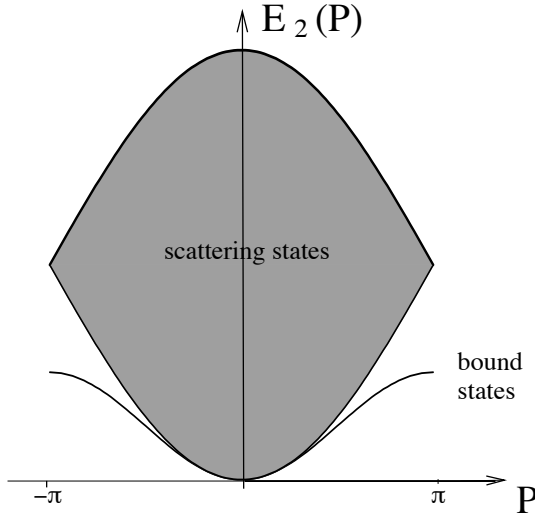


Figure II.6.2: Spectrum of the 2-magnon excitations of the isotropic ferromagnet. It consists of a continuum of scattering states described by real solutions of the Bethe-Ansatz equations and a branch of bound states corresponding to 2-string solutions.

$$E_2^{(b)}(P) = 2|J|(1 - \cos P). \quad (\text{II.6.21})$$

The energy of such states is lower than that of any 2-particle scattering state. Therefore they are called *bound states*. Fig. II.6.2 shows the complete spectrum of 2-magnon states.

The l -particle Bethe states can be treated in a similar fashion as the case $l = 2$, at least as long as l is finite. Again one finds solutions with real λ 's that describe l independent magnons. In addition, solutions with complex λ exist that group in strings of length m (see Fig. II.6.3):

$$\lambda_m = x + i\mu \quad \text{with} \quad \mu = \frac{-m+1}{2}, \frac{-m+3}{2}, \dots, \frac{m-3}{2}, \frac{m-1}{2}. \quad (\text{II.6.22})$$

These solutions are called *m -strings*. Magnons itself might then be considered as 1-string solutions. The roots of an m -string have distance 1 in imaginary direction and are symmetric with respect to the real axis. This ensures that the total momentum is real. For odd m the center root of the string is real.

In general the l roots λ_j will form q strings of different lengths. Let ν_m be the number of m -strings ($m = 1, 2, \dots$) and $\lambda_j^{(m)}$ ($j = 1, \dots, \nu_m$) their real parts (or centers). Then we have

$$l = \sum_{m \in \mathbb{N}} m\nu_m, \quad q = \sum_{m \in \mathbb{N}} \nu_m \quad (\text{II.6.23})$$

The set $\{l, q, \{\nu_m\}\}$ determines the Bethe states up to the positions $\lambda_j^{(m)}$ that have to be calculated from the Bethe-Ansatz equations. These can be reduced to equations that only contain the real

²²In the case $y_1 < 0$ the reciprocal of (II.6.15) should be considered.

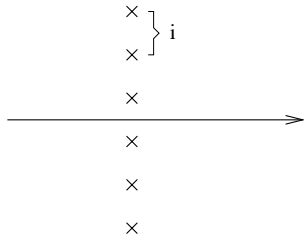


Figure II.6.3: An m -string for $m = 6$. The roots are symmetric with respect to the real axis and have distance i . For m odd the center root is real.

parts $\lambda_j^{(m)}$ (see Appendix B.2). Energy and momentum of such a configuration can also be expressed solely by the real parts.

Usually when solving the Bethe-Ansatz equations the so-called *string hypothesis* is made. It states that any solution consists only of strings. However, it is known that this assumption is usually problematic although the physical properties seem to be rather robust. We refer to Appendix B.2 for a more detailed discussion of the string picture.

II.6.2 Isotropic antiferromagnet

Next we consider the case of isotropic antiferromagnetic interaction corresponding to $\Delta = 1$ and $J > 0$ in (II.3.8). The spectrum in this case is just the inverse of the ferromagnetic case since we have the obvious symmetry $E(J) = -E(-J)$. However, for the ferromagnetic interactions we have only determined the lowest eigenstates. We will now do the same for the antiferromagnetic case [20].

Classically one expects that antiparallel spins are energetically favoured. However, the *Néel state* $|\uparrow\downarrow\uparrow\downarrow\dots\rangle$ is not an eigenstate of the Heisenberg model! Nevertheless we expect the groundstate to be located in the subspace with $M = \frac{L}{2}$. A further indication comes from the 1-magnon energies (II.6.10) that are negative for $J > 0$: $E_1(P) = 4J(\cos P - 1) \leq 0$. Therefore the reference state is unstable against the creation of magnons. A candidate for the true antiferromagnetic groundstate is then one where $L/2$ magnons have been created in the reference state. Since we are then dealing with a macroscopic number of magnons we can expect a different physics from the ferromagnetic case.

First we have to solve the question how to deal with a macroscopic number of Bethe-Ansatz equations. These can be handled easier in a logarithmic form. Using the identity

$$e^{2i \arctan(z)} = \frac{1 + iz}{1 - iz} \quad (\text{II.6.24})$$

we can rewrite the left hand side of the Bethe-Ansatz equations (II.6.6) in the form

$$\left(\frac{\lambda_j + i/2}{\lambda_j - i/2} \right)^L = (-1)^L \left(\frac{1 - 2i\lambda_j}{1 + 2i\lambda_j} \right)^L = (-1)^L e^{-2Li \arctan(2\lambda_j)}. \quad (\text{II.6.25})$$

Similarly each factor on the right hand side can be expressed through the arctan:

$$\frac{\lambda_j - \lambda_l + i}{\lambda_j - \lambda_l - i} = -\frac{1 - i(\lambda_j - \lambda_l)}{1 + i(\lambda_j - \lambda_l)} = -e^{-2i \arctan(\lambda_j - \lambda_l)}. \quad (\text{II.6.26})$$

In the following we assume that the chain length L is even. We then have

$$e^{-2Li \arctan(2\lambda_j)} = (-1)^{M+1} e^{\sum_{l=1}^M 2i \arctan(\lambda_j - \lambda_l)} \quad (\text{II.6.27})$$

or, after taking the logarithm,

$$2Li \arctan(2\lambda_j) = 2\pi \tilde{I}_j i + (M+1)\pi i + \sum_{l=1}^M 2i \arctan(\lambda_j - \lambda_l). \quad (\text{II.6.28})$$

Here \tilde{I}_j are integers related to the different branches of the logarithm. This can be written in more compact form as

$$2 \arctan(2\lambda_j) = \frac{2\pi}{L} I_j + \frac{1}{L} \sum_{l=1}^M 2 \arctan(\lambda_j - \lambda_l) \quad (\text{II.6.29})$$

Now the parameters I_j , called *Bethe-Ansatz quantum numbers*, can be integers or half-odd integers depending on the parity of M :

$$I_j \in \begin{cases} \mathbb{Z} & \text{for } M \text{ odd} \\ \mathbb{Z} + \frac{1}{2} & \text{for } M \text{ even.} \end{cases} \quad (\text{II.6.30})$$

We can also rewrite the expression for the momentum:

$$P = \sum_{j=1}^M k_j = \sum_{j=1}^M \operatorname{arccot}(2\lambda_j) = \sum_{j=1}^M (\pi - 2 \arctan(2\lambda_j)) = M\pi - \frac{2\pi}{L} \sum_{j=1}^M I_j \quad \text{mod } 2\pi. \quad (\text{II.6.31})$$

Here the relation between arccot and arctan has been used. In the last step the sum over the arctan has been obtained by summing over the Bethe-Ansatz equations (II.6.29) where the double sum vanishes since arctan is an odd function. Summarizing, energy and momentum are determined by

$$E = -2J \sum_{j=1}^M \frac{1}{\lambda_j^2 + 1/4} \quad (\text{II.6.32})$$

$$P = M\pi - \frac{2\pi}{L} \sum_{j=1}^M I_j \quad \text{mod } 2\pi. \quad (\text{II.6.33})$$

The strategy is now to characterize states using a set of Bethe quantum numbers $\{I_j\}$ and then determine the corresponding λ 's by solving (II.6.29). The Bethe quantum numbers have to be pairwise distinct since the λ_j have to be. Sometimes the mapping between these two sets is made more explicit by introducing the so-called *counting function*

$$z(\lambda) := \frac{1}{2\pi} \left(2 \arctan(2\lambda) - \frac{1}{L} \sum_{l=1}^M 2 \arctan(\lambda - \lambda_l) \right) \quad (\text{II.6.34})$$

such that the Bethe-Ansatz equations read

$$z(\lambda_j) = \frac{I_j}{L}. \quad (\text{II.6.35})$$

This implies a monotonous relation between the I_j and the λ_j . Note that the counting function is not explicitly known until the parameters λ_j have been determined by solving the Bethe-Ansatz equations. Nevertheless it is a useful quantity. E.g. we can use it to determine the range of the allowed Bethe quantum numbers I_j . The maximal allowed value I_{\max} satisfies the condition²³

$$z(\lambda = \infty) = \frac{1}{L}(I_{\max} + 1) \quad (\text{II.6.36})$$

since $\lambda_j < \infty$. This can be easily evaluate. We have²⁴ $z(\infty) = \frac{1}{2\pi}(\pi - \frac{M-1}{L}\pi)$ and therefore

$$I_{\max} = \frac{L - M - 1}{2}. \quad (\text{II.6.37})$$

Therefore, for $M \downarrow$ -spins there are $2I_{\max} + 1 = L - M$ allowed I_j -values (if all λ_j are real). We now determine the solution for the case of $M = \frac{L}{2}$ real λ 's. In this case $I_{\max} = \frac{L/2-1}{2}$ and there are $L - M = \frac{L}{2}$ possible I_j values which is exactly the same as the number of λ -parameters. Therefore we have no freedom in choosing the Bethe quantum numbers:

$$I_j = -\frac{L/2-1}{2}, -\frac{L/2-1}{2} + 1, \dots, \frac{L/2-1}{2} \quad (\text{II.6.38})$$

In the thermodynamic limit the corresponding λ 's lie dense in the interval $]-\infty, \infty[$. Thus we can introduce their density

$$\rho(\lambda_j) := \lim_{L \rightarrow \infty} \frac{1}{L(\lambda_{j+1} - \lambda_j)} \quad (\text{II.6.39})$$

where we have already anticipated that their difference is of order $1/L$. This is to be expected from the noninteracting case (see e.g. (II.3.18)). An alternative definition is

$$\rho(\lambda) := \frac{dz(\lambda)}{d\lambda}. \quad (\text{II.6.40})$$

²³Here we assume that all λ_j are real.

²⁴Note that the term corresponding to $\lambda_l = \lambda$ does not contribute.

The strategy will now be the following. First we will rewrite the (logarithmic) Bethe equations (II.6.29) as a linear integral equation for the density $\rho(\lambda)$. Solving this equation we then can calculate the energy of the corresponding state.

Taking the difference of the equations (II.6.29) for $j+1$ and j , we obtain

$$2 \arctan(2\lambda_{j+1}) - 2 \arctan(2\lambda_j) = \frac{2\pi}{L} (I_{j+1} - I_j) + \frac{2}{L} \sum_{l=1}^{L/2} [\arctan(\lambda_{j+1} - \lambda_l) - \arctan(\lambda_j - \lambda_l)]. \quad (\text{II.6.41})$$

Since $\lambda_{j+1} - \lambda_j$ is small we can use a Taylor expansion:

$$\begin{aligned} 2 \arctan(2\lambda_{j+1}) - 2 \arctan(2\lambda_j) &= 2 \arctan'(2\lambda_j) \cdot 2(\lambda_{j+1} - \lambda_j) \\ &= \frac{2}{1 + (2\lambda_j)^2} \cdot \frac{1}{L\rho_0(\lambda_j)} \end{aligned} \quad (\text{II.6.42})$$

where we also made use of (II.6.39) and the prime indicates the derivative. The sum in (II.6.41) can be treated analogously resulting in

$$\frac{4}{1 + (2\lambda_j)^2} \cdot \frac{1}{L\rho_0(\lambda_j)} = \frac{2\pi}{L} + \frac{2}{L} \sum_{l=1}^{L/2} \frac{1}{1 + (\lambda_j - \lambda_l)^2} \cdot \frac{1}{L\rho_0(\lambda_j)} \quad (\text{II.6.43})$$

where we have used that $I_{j+1} - I_j = 1$ in the groundstate. This is equivalent to

$$\frac{1}{1 + \lambda_j^2/4} = 2\pi\rho_0(\lambda_j) + 2 \sum_{l=1}^{L/2} \frac{1}{1 + (\lambda_j - \lambda_l)^2} \rho_0(\lambda_l)(\lambda_{l+1} - \lambda_l) \quad (\text{II.6.44})$$

where the identity $\rho_0(\lambda_l)(\lambda_{l+1} - \lambda_l) = \frac{1}{L}$ has been used in the sum. For $L \rightarrow \infty$ the sum becomes an integral and we obtain the integral equation

$$\frac{1}{1 + \lambda^2/4} = 2\pi\rho_0(\lambda) + 2 \int_{-\infty}^{\infty} \frac{\rho_0(\tilde{\lambda})}{(\lambda - \tilde{\lambda})^2 + 1} d\tilde{\lambda} \quad (\text{II.6.45})$$

that determines the density $\rho_0(\lambda)$ of Bethe roots in the groundstate.

Analogous calculations allow to express the corresponding energy (II.6.32) through the density

$$E = -2LJ \int_{-\infty}^{\infty} \frac{\rho_0(\lambda)}{\lambda^2 + 1/4} d\lambda. \quad (\text{II.6.46})$$

The integral equation can be solved through Fourier transformation since it is linear and has a difference kernel $K(\lambda, \tilde{\lambda}) = K(\lambda - \tilde{\lambda}) = \frac{1}{(\lambda - \tilde{\lambda})^2 + 1}$. Therefore we can make use of the convolution theorem that states that the Fourier transform of a convolution $f * g(x) = \int_{-\infty}^{\infty} f(x-y)g(y)dy$ is just the product of the Fourier transforms of the functions f and g :

$$FT(f * g) = FT \left(\int_{-\infty}^{\infty} f(x-y)g(y)dy \right) = FT(f) \cdot FT(g). \quad (\text{II.6.47})$$

Defining the Fourier transform by

$$\tilde{\rho}_0(\omega) := \int_{-\infty}^{\infty} \rho_0(\lambda) e^{i\omega\lambda} d\lambda \quad (\text{II.6.48})$$

we obtain from (II.6.45)

$$e^{-|\omega|/2} = 2\pi\tilde{\rho}_0(\omega) + 2\pi\tilde{\rho}_0(\omega)e^{-|\omega|} \quad (\text{II.6.49})$$

where we have used that the Fourier transform of $\frac{1}{\lambda^2+a^2}$ is given by $\frac{\pi}{a}e^{-a|\omega|}$. Thus we have

$$\tilde{\rho}_0(\omega) = \frac{e^{-|\omega|/2}}{1+e^{-|\omega|}} \quad (\text{II.6.50})$$

and therefore

$$\rho(\lambda) = \frac{1}{2\pi} \int_{-\infty}^{\infty} \tilde{\rho}_0(\omega) e^{-i\omega\lambda} d\omega = \frac{1}{2\cosh \pi\lambda}. \quad (\text{II.6.51})$$

Using this result the groundstate energy can be calculated

$$E_0 = -2LJ \int_{-\infty}^{\infty} \frac{\rho_0(\lambda)}{\lambda^2 + 1/4} d\lambda = -2LJ \int_{-\infty}^{\infty} \frac{e^{-|\omega|}}{1+e^{-|\omega|}} d\omega. \quad (\text{II.6.52})$$

In the last step we have used the convolution theorem to simplify the calculation. The integral can be evaluated explicitly and we obtain for the groundstate

$$E_0 = -4LJ \ln 2, \quad (\text{II.6.53})$$

$$P_0 = \frac{L\pi}{2} \mod 2\pi \quad (\text{II.6.54})$$

where we have used (II.6.33) to determine the momentum.

By construction the groundstate has vanishing magnetization $S^z = 0$. Due to the general properties of Bethe states it has also spin $S = 0$ and thus is a singlet. Furthermore we have seen that we have no freedom in choosing the Bethe quantum numbers. Therefore the groundstate is also non-degenerate. Note that the groundstate has an extremely complicated structure, i.e. it is *highly correlated*. It should also be emphasized that it is rather different from the classical Néel states.

Next we try to find the lowest excited states. We expect them to be described by ‘small’ deviations from the groundstate configuration. There are two simple possibilities.

(i): The first possible deviation is to flip one spin, i.e. to consider $M = \frac{L}{2} - 1$ and look for the lowest state in this subspace. We anticipate that is also described by real λ only. In this case we have $I_{\max} = \frac{L}{4}$ and therefore $2I_{\max} + 1 = \frac{L}{2} + 1 = M + 2$ possible I_j -values. This means that the choice is no longer unique, since we have M different I_j -parameters, but $M + 2$ possible positions. Therefore we have two free parameters that are given by those possible I_j -values that are not occupied. These positions are denoted by I_j^h and are usually called *holes*. The situation is depicted graphically in Fig. II.6.4.

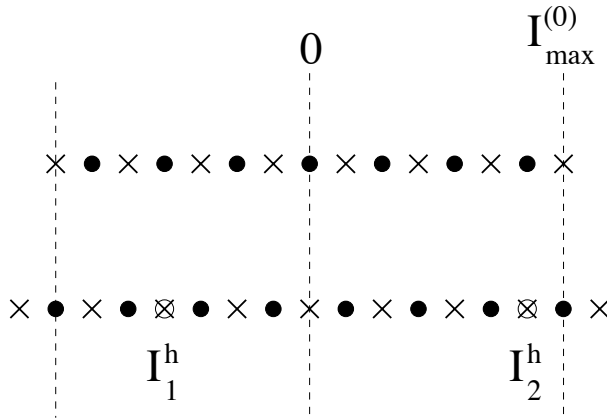


Figure II.6.4: Distribution of the Bethe quantum numbers in the groundstate (top) and an excited state with only real λ . The allowed values of I_j are indicated by a cross, the forbidden values by a dot. In the excited state the allowed values change parity since M does. Furthermore the allowed range becomes larger. Therefore there are more positions than quantum numbers and any excited state has two ‘holes’ I_j^h ($j = 1, 2$).

(ii): The second possible excitation does not involve spin flips. Therefore we stay in the subspace $M = \frac{L}{2}$. We have already seen that here no other state with only real λ_j exist. Therefore we must consider states with complex λ_j . The simplest possibility is one 2-string $\lambda_{\pm} = x \pm \frac{i}{2}$ and $M - 2 = \frac{L}{2} - 2$ real λ . Such a state can be constructed from the groundstate by leaving two I_j -positions open and adding the 2-string. The two open positions correspond to holes I_j^h just as in case (i). In addition we have the center x of the 2-string as parameter. However, analysing the Bethe-Ansatz equations shows that it is determined uniquely by the position of the holes. Therefore also in this case (ii) we have two free parameters.

We now determine the excitation energies corresponding to these two cases. We start with case (i) that is characterized by two holes I_1^h and I_2^h . The corresponding λ -values that are missing compared to the groundstate are λ_1^h and λ_2^h . As in the case of the groundstate we can transform the Bethe-Ansatz equations in the thermodynamic limit into an integral equation for the density $\rho(\lambda)$ and obtain

$$2\pi\rho_t(\lambda) + 2 \int_{-\infty}^{\infty} \frac{\rho_t(\tilde{\lambda})}{(\lambda - \tilde{\lambda})^2 + 1} d\tilde{\lambda} = \frac{1}{1 + \lambda^2/4} - \frac{2\pi}{L} (\delta(\lambda - \lambda_1^h) + \delta(\lambda - \lambda_2^h)). \quad (\text{II.6.55})$$

The last term takes into account that two possible positions are not occupied. This gives rise to the δ -functions. Note that this is not the only effect of the holes. In addition it leads to a redistribution of the other λ 's compared to groundstate. This is sometimes called *backflow*. Both corrections are of order $1/L$. It is therefore useful to define a correction density $\sigma(\lambda)$ by

$$\rho_t(\lambda) = \rho_0(\lambda) + \frac{1}{L} (\sigma(\lambda - \lambda_1^h) + \sigma(\lambda - \lambda_2^h)) \quad (\text{II.6.56})$$

where $\rho_0(\lambda)$ is the groundstate density (II.6.51). This density then satisfies the integral equation

$$2\pi\sigma(\lambda) + 2 \int_{-\infty}^{\infty} \frac{\sigma(\tilde{\lambda})}{(\lambda - \tilde{\lambda})^2 + 1} d\tilde{\lambda} = -2\pi\delta(\lambda). \quad (\text{II.6.57})$$

Again this equation can be solved easily by Fourier transform which yields

$$\sigma(\lambda) = \frac{1}{2\pi} \int_{-\infty}^{\infty} \tilde{\sigma}(\omega) e^{-i\omega\lambda} d\omega \quad \text{with} \quad \tilde{\sigma}(\omega) = -\frac{1}{1 + e^{-|\omega|}}. \quad (\text{II.6.58})$$

The excitation energy $\epsilon = E - E_0$ can now be calculated easily:

$$\epsilon_t(\lambda_1^h, \lambda_2^h) = -2JL \int_{-\infty}^{\infty} \frac{\rho_t(\lambda) - \rho_0(\lambda)}{\lambda^2 + 1/4} d\lambda = \epsilon(\lambda_1^h) + \epsilon(\lambda_2^h) \quad (\text{II.6.59})$$

with

$$\epsilon(\lambda) = -2J \int_{-\infty}^{\infty} \frac{\sigma(\lambda)}{\lambda^2 + 1/4} d\lambda = \frac{2\pi J}{\cosh \pi\lambda}. \quad (\text{II.6.60})$$

The corresponding momentum $P_t(\lambda_1^h, \lambda_2^h)$ can also be calculated explicitly. The excitation energy (II.6.60) corresponds to the following dispersion:

$$\epsilon(k) = 2\pi J |\sin k| \quad \text{with} \quad k \in [0, \pi]. \quad (\text{II.6.61})$$

The spin for excitations of type (i) is $S = 1$ since we are in the subspace $S^z = 1$ and the highest-weight property. Therefore the states of type (i) are *triplet excitations*.

Next we analyze the 2-string state in a similar way. Again we have two holes λ_1^h and λ_2^h compared to the groundstate. But now in addition we have two complex roots $\lambda_{\pm} = x \pm \frac{i}{2}$ that also have to fulfill the Bethe-Ansatz equations. A detailed investigation shows that the position x of the string is completely determined by the holes:

$$x = \frac{\lambda_1^h + \lambda_2^h}{2}. \quad (\text{II.6.62})$$

We leave out the details of the calculation of the energy of this state which is rather similar to the case (i). In the end one obtains

$$\epsilon_s(\lambda_1^h, \lambda_2^h) = \epsilon(\lambda_1^h) + \epsilon(\lambda_2^h) \quad (\text{II.6.63})$$

with the same dispersion (II.6.61) as in the triplet case (i). The excitation (ii) has $S^z = 0$ and therefore also $S = 0$. Thus it constitutes a *singlet excitation*.

There has been a longstanding controversy about the nature of the excitations. The deeper reason behind this was the fact that the excitations are 2-parametric was not recognized. In fact, the triplet dispersion has first been calculated by des Cloiseaux and Pearson [21] in 1962. They found the result (II.6.61). The singlet excitations were studied by Ovchinnikov [22] in 1969. He found the dispersion

$$\epsilon_{Ov}(P) = 4\pi J \left| \sin \frac{P}{2} \right|. \quad (\text{II.6.64})$$

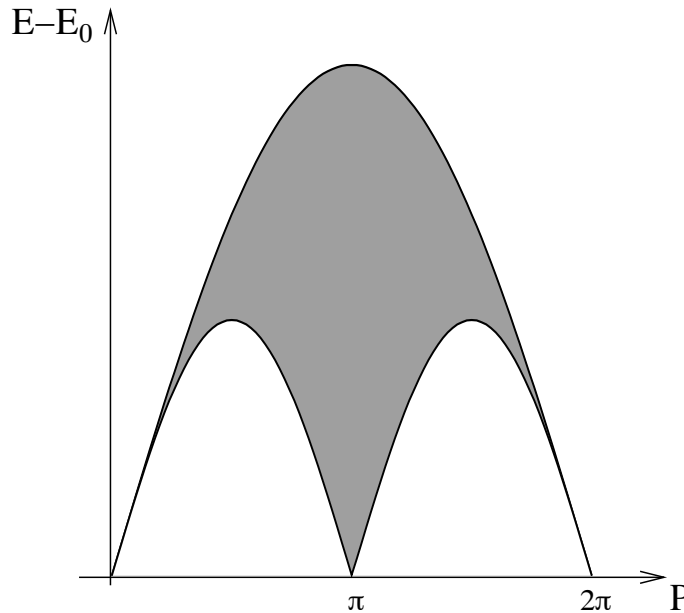


Figure II.6.5: Excitation spectrum of the antiferromagnetic Heisenberg chain.

Both results appeared to depend on just one parameter since in the calculations the position of one hole has implicitly been fixed. Thus it was not clear what the elementary dispersion of the antiferromagnetic excitations is. This was only understood later in 1981 in a work by Faddeev and Takhtajan [23]. The title of this paper emphasizes the problem: “What is the spin of a spin wave?”. Faddeev and Takhtajan recognized that there are no 1-particle excitations in the antiferromagnetic Heisenberg model. In fact the lowest excitations depend on two parameters [24]. This was somehow disguised in previous works where one parameter has been fixed implicitly. In [23] it is argued that the elementary excitation in the antiferromagnetic Heisenberg chain has the dispersion

$$\epsilon_s(k) = 2\pi J \sin k \quad \text{with} \quad k \in [0, \pi]. \quad (\text{II.6.65})$$

This is now called a *spinon* after P.W. Anderson [25] pointed out its possible relevance for the understanding of high-temperature superconductors.

The important point is that spinons can only be excited in pairs. This explains the two-parametric nature of the low-lying spectrum. The spinons of a pair can then form either a triplet or a singlet leading to the excitations of type (i) and (ii), respectively. Therefore spinons (or ‘antiferromagnetic magnons’) should be regarded as spin-1/2 particles! This is very different from the (ferromagnetic) magnons that have spin 1 as we have seen in Sec. II.6.1.

Fig. II.6.5 shows the 2-particle continuum of excitations. The result of des Cloiseaux and Pearson corresponds to one half of the lower bound, whereas the Ovchinnikov dispersion corresponds to the upper bound of the continuum.

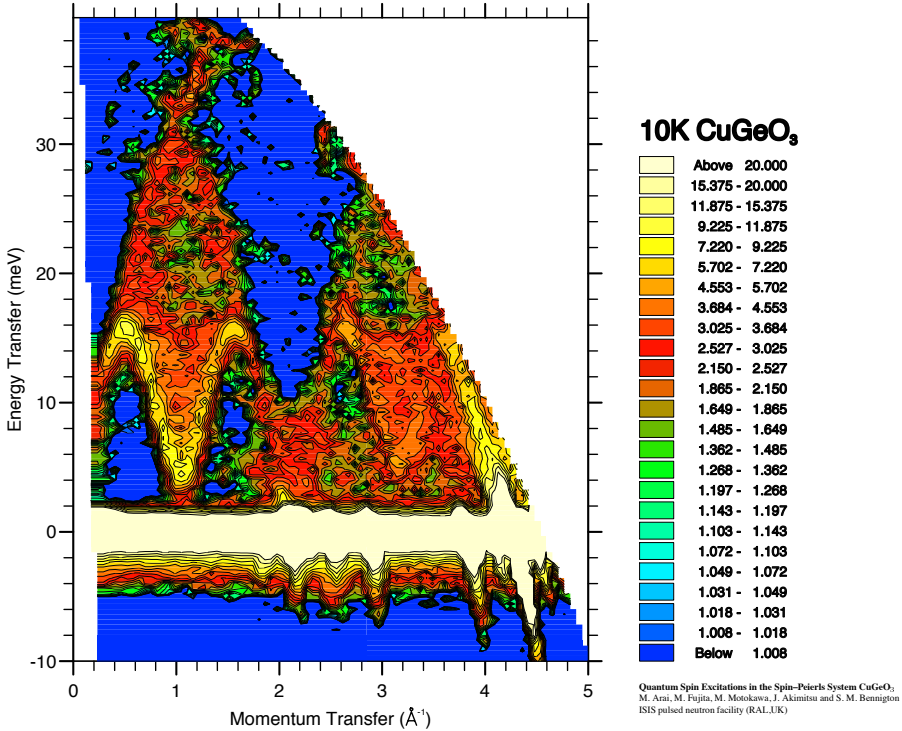


Figure II.6.6: Excitation spectrum obtained using inelastic neutron scattering on CuGeO₃ [26]. The figure shows the dynamical structure factor at temperature 10 K. The colours indicate the intensity.

Fig. II.6.6 shows an experimental result obtained using inelastic neutron scattering. We clearly see the similarity to Fig. II.6.5. One should emphasize that CuGeO₃ is not well described by a simple Heisenberg model of the type (II.3.8). Instead interactions between next nearest neighbouring spins at sites j and $j+2$ are also important. Nevertheless the agreement is surprisingly good. This already points to a certain universality of the results obtained from the exact solution. This aspect will be discussed further in the next Chapter.

How can this different nature of the elementary excitations be understood in a simple way? Obviously one should not interpret a spinon as spin-wave of a flipped spin as the usual magnon. Instead it is more natural to interpret it as a *kink* or *domain wall*. This is depicted in Fig. II.6.7 for a Néel-state. Flipping one spin creates two ‘defects’, i.e. parallel spins. These form a ‘kink’ or a domain-wall between two perfectly Néel-ordered regimes.

Finally we mention that a system with an odd number L of spins is much more difficult to describe. In fact it has no true groundstate for periodic boundary conditions because a kink is always present.

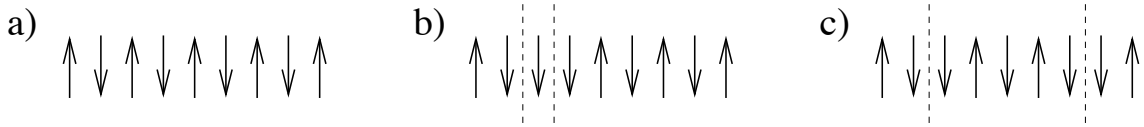


Figure II.6.7: Interpretation of a spinon as a domain wall or kink in an otherwise perfectly ordered Néel state (a). Flipping one spin always creates two kinks (spinons), indicated by broken lines in (b), that can move through the system (c).

II.6.3 Anisotropic XXZ model

We have already seen in Exercise 9 that for the 2-site XXZ chain ($L = 2$) one has to distinguish three regimes, namely $\Delta < -1$, $-1 < \Delta < 1$ and $\Delta > 1$. This remains true for arbitrary chain length L . In the following we will assume $J > 0$ and vary the anisotropy Δ . The results can be translated to the case $J < 0$ by using the symmetry

$$E(J, \Delta) = E(-J, -\Delta) \quad (\text{II.6.66})$$

of the spectrum. The isotropic ferromagnet of Sec. II.6.1 then corresponds to $\Delta = -1$. We will now discuss the three regimes separately. Since the derivation and solution of the Bethe-Ansatz is rather similar (up to certain subtleties) to the isotropic cases discussed previously, only the main results will be given.

$$\Delta < -1$$

In this case the Hamiltonian can be written as $\mathcal{H}_{XXZ} = \mathcal{H}_{XXZ}(\Delta = -1) + J(\Delta + 1) \sum_{j=1}^L \sigma_j^z \sigma_{j+1}^z$ where $\mathcal{H}_{XXZ}(\Delta = -1)$ is the isotropic ferromagnet. For this Hamiltonian we have already shown the existence of a ferromagnetic groundstate. Due to $J(\Delta + 1) < 0$, the additional term indicates an even stronger tendency towards ferromagnetism in the anisotropic case. Therefore for $\Delta < -1$, the reference state $|\uparrow\uparrow \dots \uparrow\rangle$ is still a groundstate. However, the degeneracy is much smaller due to the absence of a $SU(2)$ -symmetry. Therefore the groundstate is just twofold degenerate, the other state being the spin-flipped ferromagnetic state $|\downarrow\downarrow \dots \downarrow\rangle$.

We parametrize the anisotropy Δ by a parameter γ through

$$\Delta = -\cosh \gamma \quad (\gamma > 0). \quad (\text{II.6.67})$$

If we introduce spectral parameters λ_j through

$$k_j = 2 \arctan \left(\coth \left(\frac{\gamma}{2} \right) \tan \lambda_j \right) \quad (\text{II.6.68})$$

we can rewrite the Bethe-Ansatz equations (II.3.43) in the form

$$\left(\frac{\sin(\lambda_j + i\gamma/2)}{\sin(\lambda_j - i\gamma/2)} \right)^L = - \prod_{l=1}^M \frac{\sin(\lambda_j - \lambda_l + i\gamma)}{\sin(\lambda_j - \lambda_l - i\gamma)} \quad (\text{II.6.69})$$

The groundstate energy is obviously given by

$$E_0 = 0 \quad (\text{II.6.70})$$

since the groundstate is just our reference state. In general the energy of a Bethe-Ansatz state is given by (II.3.45) which reads in terms of the new variables λ_j and γ

$$E = -4J \sum_{j=1}^M \frac{\sinh^2 \gamma}{\cosh \gamma - \cos(2\lambda_j)} \quad (\text{II.6.71})$$

As in the isotropic ferromagnet, bound states exist. These are the excitations with the lowest energy. Their dispersion is given by

$$E_m(P) = 4J(\cosh(m\gamma) - \cos P) \frac{\sinh \gamma}{\sinh(m\gamma)}. \quad (\text{II.6.72})$$

In the limit $\gamma \rightarrow 0$ this reduces to the result of Exercise 15 for the isotropic case. Note that for $\Delta < -1$ ($\gamma > 0$) the bound states have a finite energy gap

$$\Delta E_m = E_m(P=0) = 4J(\cosh(m\gamma) - 1) \frac{\sinh \gamma}{\sinh(m\gamma)} > 0. \quad (\text{II.6.73})$$

$$-1 < \Delta < 1$$

In this case we parametrize the anisotropy by

$$\Delta = \cos \gamma \quad (0 < \gamma < \pi) \quad (\text{II.6.74})$$

and the Bethe quasi-momenta by

$$k_j = 2 \operatorname{arccot} \left(\cot \left(\frac{\gamma}{2} \right) \tanh \lambda_j \right). \quad (\text{II.6.75})$$

The Bethe-Ansatz equations read

$$\left(\frac{\sinh(\lambda_j + i\gamma/2)}{\sinh(\lambda_j - i\gamma/2)} \right)^L = - \prod_{l=1}^M \frac{\sinh(\lambda_j - \lambda_l + i\gamma)}{\sinh(\lambda_j - \lambda_l - i\gamma)} \quad (\text{II.6.76})$$

with the energy

$$E = 4J \sum_{j=1}^M \frac{\sin^2 \gamma}{\cosh(2\lambda_j) + \cos \gamma} = -4J \sum_{j=1}^M \frac{\sin^2 \gamma}{\cosh(2\lambda_j) - \cos \gamma} \quad (\text{II.6.77})$$

where the last identity is derived from the symmetry (II.6.66). Formally this follows from the case $\Delta = -1$ (and L even) by substituting $\gamma \rightarrow i\gamma - i\pi$ and $\lambda_j \rightarrow \frac{\pi}{2} - i\lambda_j$.

The groundstate energy is

$$E_0 = -4LJ \sin^2 \gamma \int_{-\infty}^{\infty} \frac{d\lambda}{\cosh(\pi\lambda) (\cosh(2\gamma\lambda) - \cos\gamma)}. \quad (\text{II.6.78})$$

The excitation spectrum above the groundstate is gapless for all $\Delta \in [-1, 1]$. However, the structure of excitations is different for $0 < \Delta < 1$ and $-1 < \Delta < 0$. These cases are called repulsive and attractive, respectively, because after a Jordan-Wigner transformation they are translated into a fermionic model (II.2.42) with repulsive or attractive interactions $U = J\Delta$.

In the repulsive case $0 < \Delta < 1$ the excited states are superpositions of elementary spin- $\frac{1}{2}$ excitations, similar to the isotropic antiferromagnet $\Delta = 1$. Energy and momentum of the excitations are given by

$$E - E_0 = \sum_n \epsilon(\lambda_n^{(h)}) = \sum_n \frac{2\pi J \sin \gamma}{\gamma \cosh\left(\frac{\pi \lambda_n^{(h)}}{\gamma}\right)}, \quad (\text{II.6.79})$$

$$P - P_0 = \sum_n p(\lambda_n^{(h)}) = \sum_n 2 \arctan e^{\lambda_n^{(h)} \pi / \gamma}. \quad (\text{II.6.80})$$

The dispersion of the elementary excitations is therefore given by

$$\epsilon(p) = \frac{2\pi J \sin \gamma}{\gamma} \sin p. \quad (\text{II.6.81})$$

An important quantity is the Fermi velocity $v_F = \frac{\partial \epsilon}{\partial P}(P=0) = \left| \frac{\partial \epsilon}{\partial P}(P=\pi) \right|$ which is given by

$$v_F = \frac{2\pi J \sin \gamma}{\gamma}. \quad (\text{II.6.82})$$

For the isotropic antiferromagnet this reduces to $v_F = 2\pi J$. These excitations can be shown to correspond to $S^z = 0$. However, it should be mentioned that the points where the anisotropy $\frac{\gamma}{\pi}$ is rational are somewhat special. Here states with $S^z \neq 0$ are possible.

In the attractive regime $-1 < \Delta < 0$ two kinds of excited states exist. The first is a superposition of elementary spin-1/2 excitations as in the repulsive case. Again there dispersion is given by (II.6.81). The second type are bound states with dispersion

$$E_m(P) = \frac{4\pi J}{\gamma} \frac{\sin \gamma}{\sin\left(\frac{\pi}{2\gamma}m(\pi - \gamma)\right)} \sqrt{1 - \cos^2\left(\frac{\pi}{2\gamma}m(\pi - \gamma)\right) \cos^2\left(\frac{P}{2}\right)} \sin\left(\frac{P}{2}\right) \quad (\text{II.6.83})$$

and $S^z = 0$.

Note that the point $\Delta = 0$ corresponds to the symmetric XY model (II.2.1). Here we recover the results derived in Sec. II.2 by mapping onto a system of free fermions.

$$\Delta > 1$$

This case is rather similar to $\Delta < -1$. In fact the standard parametrization can be obtained by substituting $\gamma \rightarrow \gamma - i\pi$ and $\lambda_j \rightarrow \frac{\pi}{2} - \lambda_j$ in the formulas for $\Delta < -1$. Then the anisotropy is parametrized by

$$\Delta = \cosh \gamma \quad (\gamma > 0) \quad (\text{II.6.84})$$

The wave numbers are rewritten in terms of the rapidities and the Bethe-Ansatz equations read

$$\left(\frac{\sin(\lambda_j + i\gamma/2)}{\sin(\lambda_j - i\gamma/2)} \right)^L = - \prod_{l=1}^M \frac{\sin(\lambda_j - \lambda_l + i\gamma)}{\sin(\lambda_j - \lambda_l - i\gamma)} \quad (\text{II.6.85})$$

with the energy

$$E = 4J \sum_{j=1}^M \frac{\sinh^2 \gamma}{\cosh \gamma + \cos(2\lambda_j)} \quad (\text{II.6.86})$$

The groundstate energy is

$$E_0 = -4JL \sinh \gamma \left[\frac{1}{2} + 2 \sum_{n=1}^{\infty} \frac{1}{1 + e^{2n\gamma}} \right]. \quad (\text{II.6.87})$$

In the thermodynamic limit the groundstate is twofold degenerate. The two groundstates show a Néel-type order, i.e. have a finite sublattice magnetization $M_s = \langle (-1)^j S_j^z \rangle$ given by

$$M_s = \frac{1}{2} \prod_{n=1}^{\infty} \left(\frac{1 - e^{-2n\gamma}}{1 + e^{-2n\gamma}} \right)^2. \quad (\text{II.6.88})$$

For $\Delta \rightarrow \infty$, where the XXZ model reduces to the classical one-dimensional antiferromagnetic Ising model, the groundstates become the classical Néel states $|\uparrow\downarrow\uparrow\downarrow\cdots\rangle$ and $|\downarrow\uparrow\downarrow\uparrow\cdots\rangle$. In this limit ($\gamma \rightarrow \infty$) the sublattice magnetisation becomes $M_s = \frac{1}{2}$. For $\Delta \searrow 1$ the sublattice magnetization vanishes like

$$M_s \cong \frac{\pi}{\sqrt{2(\Delta - 1)}} e^{-\frac{\pi^2}{4\sqrt{2(\Delta - 1)}}}. \quad (\text{II.6.89})$$

Note that in a finite system $L < \infty$ the two groundstates are not exactly degenerate, but have an energy difference of order $O(e^{-L})$. Both of these finite groundstates have no sublattice magnetization that appears only in the thermodynamic limit or if some small staggered or boundary magnetic fields are applied. For large Δ the two groundstates in the finite system are basically given by $|\uparrow\downarrow\cdots\uparrow\downarrow\rangle \pm |\downarrow\uparrow\cdots\downarrow\uparrow\rangle$.

The excitation spectrum has a finite gap. The elementary excitations, which can only appear in pairs as in the isotropic case, have a dispersion given by

$$\epsilon(P) = 4J \frac{K}{\pi} \sinh \gamma \cdot \sqrt{1 - \bar{k}^2 \cos^2 P} \quad (-\pi < P \leq 0). \quad (\text{II.6.90})$$

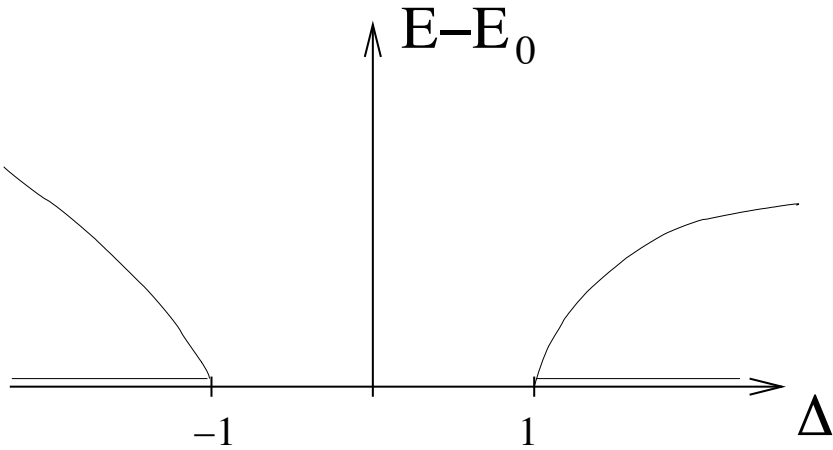


Figure II.6.8: Phase diagram of the XXZ model.

K is the complete elliptic integral of the first kind with modulus $\bar{k} = 4e^{-\gamma/2} \prod_{n=1}^{\infty} \left(\frac{1+e^{-2n\gamma}}{1+e^{-(2n-1)\gamma}} \right)^4$. The energy gap is then given by

$$\Delta E = 4J \frac{K}{\pi} \sqrt{1 - \bar{k}^2} \sinh \gamma. \quad (\text{II.6.91})$$

For $\Delta \searrow 1$ the gap vanishes like

$$\Delta E \cong 16J e^{-\frac{\pi^2}{2\sqrt{2(\Delta-1)}}}. \quad (\text{II.6.92})$$

Phase diagram

Fig. II.6.8 summarizes the results. It shows the groundstate degeneracy and the energy gap as function of the anisotropy Δ . For $|\Delta| > 1$ which is usually called *easy-axis anisotropy* the XXZ model has a twofold degenerate groundstate with a finite excitation gap. For $|\Delta| < 1$ which is called *easy-plane anisotropy* the groundstate is unique and there is no gap to the excited states. At the isotropic points $|\Delta| = 1$ the model has a SU(2)-symmetry. Therefore the groundstate degeneracy is L in the ferromagnetic case $\Delta = -1$. For the antiferromagnetic case $\Delta = 1$ the groundstate is a singlet and thus nondegenerate. Note that for $\Delta < 0$ bound states exist.

The physics for the cases $|\Delta| > 1$ interpolates between the isotropic cases discussed in Sec. II.6.1 and II.6.2, respectively, and the (classical) Ising limits $\Delta \rightarrow \pm\infty$. Thinking of the ferro- or antiferromagnetic Ising model with quantum fluctuations therefore gives a good account of the behaviour for easy-axis anisotropy.

II.6.4 Magnetic field effects

So far we have only treated the zero-field case $B = 0$. However, the Zeman energy $-B \sum_{j=1}^N \sigma_j$ commutes with the Hamiltonian $\tilde{\mathcal{H}}_{XXZ}$ of the anisotropic Heisenberg model. Therefore the

Bethe-Ansatz states are also eigenstates of

$$\tilde{\mathcal{H}}_{XXZ} = J \sum_{j=1}^L [\sigma_j^x \sigma_{j+1}^x + \sigma_j^y \sigma_{j+1}^y + \Delta (\sigma_j^z \sigma_{j+1}^z - 1)] - B \sum_{j=1}^N \sigma_j. \quad (\text{II.6.93})$$

Especially the Bethe-Ansatz equations are not changed. However, for finite fields $B \neq 0$ the groundstate and its energy may change. Starting e.g. in the antiferromagnetic region, switching on the magnetic field in general leads to a groundstate that has a finite magnetization

$$S^z = \frac{1}{2} \sum_{j=1}^L \langle \sigma_j^z \rangle. \quad (\text{II.6.94})$$

Up to now we have only encountered states with $\lim_{L \rightarrow \infty} \frac{1}{L} S^z = 0, \frac{1}{2}$ corresponding to $M \approx L/2$ or $M \approx 0$ overturned spins. In these cases the Bethe-Ansatz equations could be solved in closed form.

In general, we will have an arbitrary number M of flipped spins given rise to a state with magnetization $S^z = \frac{1}{2}(L - M)$. In this case the Bethe-Ansatz equations can be treated in a way very similar to the antiferromagnetic case. However, the λ 's are no longer distributed on the whole real axis, but only in a finite interval $[-\lambda_0, \lambda_0]$. E.g. in the isotropic case of Sec. II.6.2 we would obtain an integral equation as in (II.6.45), but now the integration is over the finite interval instead over $]-\infty, \infty[$:

$$\frac{1}{1 + \lambda^2/4} = 2\pi\rho(\lambda) + 2 \int_{-\lambda_0}^{\lambda_0} \frac{\rho(\tilde{\lambda})}{(\lambda - \tilde{\lambda})^2 + 1} d\tilde{\lambda}. \quad (\text{II.6.95})$$

Therefore the convolution theorem can no longer be applied and we have to solve the integral equation numerically. The magnetization $m = \frac{1}{L} S^z$ per site corresponding to a given λ_0 is then given by

$$m = \frac{1}{L} S^z = \frac{1}{2L} (L - M) = \frac{1}{2} \left(1 - \frac{1}{L} \sum_{j=1}^M 1 \right) = \frac{1}{2} \left(1 - \int_{-\lambda_0}^{\lambda_0} \rho(\lambda) d\lambda \right). \quad (\text{II.6.96})$$

The groundstate energy per site is

$$\begin{aligned} \frac{1}{L} E_0(B) &= -2J \int_{-\lambda_0}^{\lambda_0} \frac{\rho(\lambda)}{\lambda^2 + 1/4} d\lambda - B \left(1 - \int_{-\lambda_0}^{\lambda_0} \rho(\lambda) d\lambda \right) \\ &= - \int_{-\lambda_0}^{\lambda_0} \left[\frac{2J}{\lambda^2 + 1/4} - B \right] \rho(\lambda) d\lambda - B. \end{aligned} \quad (\text{II.6.97})$$

The anisotropic case can be treated analogously.

An important quantity is the (zero-field) susceptibility

$$\chi = \left. \frac{\partial m}{\partial B} \right|_{B=0} \quad (\text{II.6.98})$$

which can be calculated exactly. For $B \ll 1$ one has $\lambda_0 \gg 1$. In this limit the integral equation (II.6.95) (or its anisotropic analogon) can be solved asymptotically using the Wiener-Hopf method. This is sufficient to determine χ . In the regime $-1 < \Delta \leq 1$ without excitation gap one finds²⁵

$$\chi = \frac{\gamma}{\pi J(\pi - \gamma) \sin \gamma} \quad (\text{II.6.99})$$

where $\Delta = \cos \gamma$. For the isotropic antiferromagnet this reduces to $\chi = \frac{1}{\pi^2 J}$.

Another interesting quantity is the critical magnetic field B_c . For all fields $B \geq B_c$ the ground-state is the ferromagnet $|\uparrow\uparrow \dots \uparrow\rangle$. It is given by

$$B_c = 2(1 + \Delta)J. \quad (\text{II.6.100})$$

Obviously $B_c \rightarrow 0$ for $\Delta \rightarrow -1$, where the ferromagnetic region starts.

For the gapped phases a second critical field B_0 exists. Here a field corresponding to an energy less than the value of the excitation gap has no effect. For the antiferromagnet therefore a finite field $B \geq B_0$ is required to enforce a non-vanishing magnetization in the groundstate.

²⁵ χ changes by a factor 2 if one uses the Hamiltonian (II.6.93) with all Pauli matrices replaced by spin-1/2 operators because the magnetic field has then to be rescaled by a factor of 2.

Appendix A

Exercises

1. Spin operators

Show that the operators

$$\mathbf{S}_j = \frac{1}{2} \sum_{\alpha, \beta} c_{j\alpha}^\dagger \tau_{\alpha\beta} c_{j\beta}$$

defined in (I.2.12) satisfy the commutation relations of angular momentum operators.

2. Spin exchange

Show that the operator P_{ij} that exchanges two spins i and j (with spin 1/2) can be expressed through spin operators \mathbf{S}_j by

$$P_{ij} = 2\mathbf{S}_i \cdot \mathbf{S}_j + \frac{1}{2}.$$

3. XXZ model

Show that the relative sign of the anisotropy $\Delta = J_z/J_{xy}$ of the XXZ model

$$\mathcal{H} = \sum_{j=1}^L [J_{xy} (S_j^x S_{j+1}^x + S_j^y S_{j+1}^y) + J_z S_j^z S_{j+1}^z]$$

can be changed through a canonical transformation ($\Delta \rightarrow -\Delta$).

4. Jordan-Wigner transformation

- a) Show, that σ_j^+ etc. defined in (II.2.8) satisfy the spin commutation relations provided that c_j^\dagger etc. are Fermi operators.
- b) Determine the “inverse” Jordan-Wigner transformation!
- c) Discuss the applicability of Jordan-Wigner transformations in dimensions $d > 1$.

5. XY model and free fermions

In Sec II.2 we have sketched a general method for the diagonalisation of fermionic bilinear-forms. For the XY model it is simpler to perform the Fourier transformation first and then

apply the Bogoliubov transformation. Use this approach to diagonalise the Hamiltonian

$$\mathcal{H} = - \sum_{j=1}^L \left[(c_j^\dagger c_{j+1} + c_{j+1}^\dagger c_j) + \gamma (c_j^\dagger c_{j+1}^\dagger + c_{j+1} c_j) + 2B c_j^\dagger c_j \right].$$

(with periodic boundary conditions).

6. Excitations of free fermions

Show that the quantum number P defined by $P = \exp\left(i\pi \sum_{l=1}^L c_l^\dagger c_l\right)$ for an n -particle state of the free fermion Hamiltonian $\mathcal{H}_F = \sum_k \Lambda_k \eta_k^\dagger \eta_k + E_0$ is given by $(-1)^n P_0$ where P_0 is the P -quantum number of the groundstate. Remind that η_k and c_j are related by a Bogoliubov transformation.

7. Particle-hole transformation

Show that the transformation $c_j \rightarrow d_j := c_j^\dagger$, $c_j^\dagger \rightarrow d_j^\dagger := c_j$ is canonical and discuss its relevance for the spectrum of free fermions.

8. Limiting cases of the XY model

Discuss the excitation spectrum of the XY model for the cases

- $\gamma = 0$ (symmetric XY model = XX model)
- $\gamma = 1$ (Ising model in transversal field)
- $B = 0$ (zero-field XY model).

Investigate the excitation gap Δ and the behaviour for small momenta.

9. XXZ model for $L = 2$

Diagonalize the Hamiltonian $\tilde{\mathcal{H}}_{XXZ}$ of the XXZ model explicitly for the case $L = 2$ of two sites (without using the Bethe-Ansatz). Discuss the groundstate and excitations as a function of the anisotropy Δ .

10. Completeness of the Bethe-Ansatz for $M = 2$

Discuss the number of solutions of the Bethe-Ansatz equations in the subspace $M = 2$. Does a sufficient number of solutions exist to guarantee completeness?

Hint: Consider the variables $z_j = e^{ik_j}$!

11. Bethe-Ansatz wavefunction

Investigate the Bethe-Ansatz wavefunction for the case that two quasi-momenta are equal, e.g. $k_1 = k_2$. Consider first the subspaces $M = 2, 3$.

12. Standard form of the Bethe-Ansatz equations

Derive the standard form (II.6.6) of the Bethe-Ansatz equations in the isotropic case $\Delta = 1$ by using the variable transformation $k_j = 2 \operatorname{arccot}(2\lambda_j) = \frac{1}{i} \ln \frac{2\lambda_j + i}{2\lambda_j - i}$. Express the energy through the new variables.

13. *Isotropic Heisenberg model*

Show that the Hamiltonian of the isotropic ferromagnetic Heisenberg model can be written in the form

$$\tilde{\mathcal{H}}_{XXX} = 4|J| \sum_{j=1}^L (\vec{\sigma}_j \cdot \vec{\sigma}_{j+1} - 1)^2.$$

Discuss the consequences of this identity.

14. *Algebraic Bethe-Ansatz*

Show explicitly for $M = 2$ and $M = 3$ that the states $|v_1, \dots, v_M\rangle := B(v_1) \cdots B(v_M)|0\rangle$ are eigenstates of the transfer matrix, provided the Bethe-Ansatz equations are satisfied. Follow the sketch given in Sec. II.5 for the general case.

15. *Bound states*

Show that the dispersion of an m -string is given by

$$E_m(P_m) = \frac{4|J|}{m}(1 - \cos P_m).$$

Compare with the energy of a state consisting of a m_1 - and a m_2 -string with $m_1 + m_2 = m$ at the same momentum ($P_m = P_{m_1} + P_{m_2}$).

Appendix B

Supplementary material

B.1 Phase diagram of the 6-vertex model

We have seen in Sec. II.4.4 that 6-vertex models with the same parameter $\Delta = \frac{a^2+b^2-c^2}{2ab}$ have commuting transfer matrices. This has been proved in Sec. II.4.6 using the Yang-Baxter relation. Depending on the value of Δ the following parametrisations in terms of a spectral parameter u are used:

$$\begin{aligned} \Delta < -1 : \quad a &= \rho \sinh(\lambda - u), & b &= \rho \sinh u, & c &= \rho \sinh \lambda, \\ &\Delta = -\cosh \lambda && (0 < u < \lambda) \end{aligned} \tag{B.1.1}$$

$$\begin{aligned} -1 < \Delta < 1 : \quad a &= \rho \sin(\lambda - u), & b &= \rho \sin u, & c &= \rho \sin \lambda, \\ &\Delta = -\cos \lambda && (0 < u < \lambda, 0 < \lambda < \pi) \end{aligned} \tag{B.1.2}$$

$$\begin{aligned} \Delta > 1 : \quad a &= \rho \sinh(\lambda + u), & b &= \rho \sinh u, & c &= \rho \sinh \lambda, \\ &\Delta = \cosh \lambda && (u, \lambda > 0) \end{aligned} \tag{B.1.3}$$

where we have also specified the parameter range that leads to positive Boltzmann weights. We can associate energies ϵ_a, ϵ_b and ϵ_c with each vertex through $a = \exp(-\beta\epsilon_a)$ etc. With the above parametrisations the Yang-Baxter equations (II.4.26) are satisfied with $R = R(u)$, $R' = R(u')$ and $R'' = R(u' - u)$.

The eigenvalues and -vectors can be determined using the Bethe-Ansatz. From (II.4.10) the thermodynamic properties can then be derived. One finds four different phases (see Fig. B.1.1).

I. Ferroelectric phase ($a > b + c$)

In this case $\Delta > 1$ and $\epsilon_a < \epsilon_b, \epsilon_c$. The lowest energy state is one where all vertices are either of type 1, or all of type 2 (see Fig. II.4.5). Thus all arrows point up or to the right, or all arrows point down or to the left. At very low temperatures the system is ferromagnetically ordered, i.e. all dipoles tend to point into the same direction (compare Fig. II.4.4). The free energy is equal to ϵ_a and the excited states have a negligible contribution to the partition function. Throughout region I the system is frozen in one of the two possible groundstates corresponding to complete ferromagnetic order.

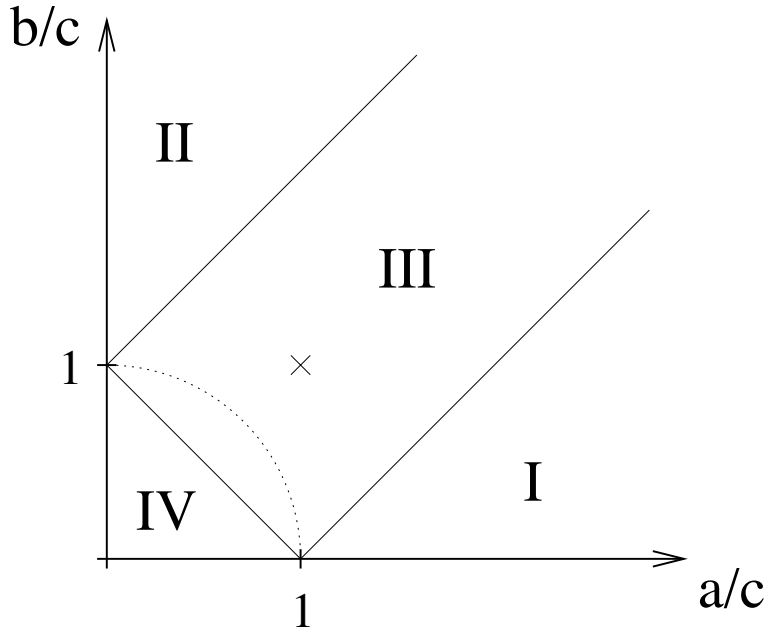


Figure B.1.1: Phase diagram of the 6-vertex model. The cross denotes the point corresponding to temperature $T = \infty$. The dotted line marks $\Delta = 0$ where the model is equivalent to free fermions.

II. Ferroelectric phase ($b > a + c$)

This case is very similar to region I, except that now vertices of type 3 or type 4 are dominant. Effectively all arrows either point up and to the left or down and to the right.

III. Disordered phase ($a, b, c < \frac{1}{2}(a + b + c)$)

In this case $-1 < \Delta < 1$. This region contains the infinite temperature case $\beta = 0$ with $a = b = c = 1$. Therefore one expects it to be disordered. This is indeed true in the sense that all correlations decay to zero with increasing distance r . However, for $a^2 = b^2 = c^2$ (such that $a, b, c < \frac{1}{2}(a + b + c)$) we have $\Delta = 0$. The model is then equivalent to free fermions and can be solved e.g. using Pfaffians. Correlations decay as inverse power law in r , rather than exponential. The correlation length is therefore infinite. The system is not disordered in the usual sense, but is critical. In fact in this region III, the 6-vertex model corresponds to the critical limit of the 8-vertex model. There is no spontaneous order, but the correlation length is infinite. Thus the 6-vertex model has the rather unusual property of being critical for the whole region III.

IV. Antiferroelectric phase ($c > a + b$)

In this case $\Delta < -1$ and $\epsilon_c < \epsilon_a, \epsilon_b$. The lowest energy is the one where all neighbouring arrows in the direction of the main axis point in opposite directions. This gives two possible lowest energy states. At sufficiently low temperatures we therefore expect the system to be in an ordered state with antiferroelectric order.

The four phases are separated by phase transitions. Between II. and III. and between I. and III.

these transitions are of first order. However, the transition between the phases IV. and III. shows only a very weak singularity. All derivatives exist and are equal on both sides of the transition point. Therefore this transition is of infinite order. The singular part of the free energy behaves as $f_{\text{sing}} \propto e^{-\text{const}/\sqrt{-t}}$ with $t = \frac{a+b-c}{c}$.

Note that the logarithmic derivative of the 6-vertex model transfer matrix generates $-\mathcal{H}_{XXZ}$. Therefore Δ_{XXZ} corresponds to $-\Delta_{6VM}$.

B.2 More on strings

As already pointed out in Sec. II.6.1 in the solution of Bethe-Ansatz equations frequently the so-called *string hypothesis* is made. One then assumes that *all* solutions of the Bethe equations consist only of strings of different length. An m -string consists of the roots

$$\lambda_j^{(m)} - \frac{i}{2}(m-1), \lambda_j^{(m)} - \frac{i}{2}(m-3), \dots, \lambda_j^{(m)} + \frac{i}{2}(m-3), \lambda_j^{(m)} + \frac{i}{2}(m-1). \quad (\text{B.2.1})$$

Then the set $\{M, q, \{\nu_m\}\}$ determines the Bethe states up to the positions $\lambda_j^{(m)}$. Here M is the number of \downarrow -spins, q the total number of strings and ν_m the number of m -strings ($m = 1, 2, \dots$). Therefore we have $M = \sum_{m \in \mathbb{N}} m\nu_m$ and $q = \sum_{m \in \mathbb{N}} \nu_m$ (see Sec. B.2).

Some of the Bethe equations to derive the form of the strings and therefore are already satisfied. Therefore it is possible to reduce the number of equations. In fact one can reduce it to a set of equations that only involve the positions $\lambda_j^{(m)}$ of the strings. For the isotropic case these equations for the center of a m_1 -string read:

$$\left[V_1 \left(\frac{2\lambda_j^{(m_1)}}{m_1} \right) \right]^L = \prod_{m_2} \prod_{l=1, (l, m_2) \neq (j, m_1)}^{\nu_{m_2}} V_{m_1, m_2}(\lambda_j^{(m_1)} - \lambda_l^{(m_2)}). \quad (\text{B.2.2})$$

Here we have defined the functions

$$V_1(\lambda) := \frac{\lambda + i}{\lambda - i}, \quad (\text{B.2.3})$$

$$V_m(\lambda) := V_1 \left(\frac{2\lambda}{m+1} \right) V_1 \left(\frac{2\lambda}{m-1} \right), \quad (\text{B.2.4})$$

$$V_{m_1, m_2}(\lambda) := V_{m_1+m_2-1}(\lambda) V_{m_1+m_2-3}(\lambda) \cdots V_{|m_1-m_2|+1}(\lambda). \quad (\text{B.2.5})$$

Energy and momentum are then given by

$$E = 2J \sum_{m=1}^{\nu_m} \sum_{j=1}^{\nu_m} \frac{m}{\left(\lambda_j^{(m)} \right)^2 + m^2/4}, \quad (\text{B.2.6})$$

$$P = \frac{1}{i} \sum_{m=1}^{\nu_m} \sum_{j=1}^{\nu_m} \ln \frac{\lambda_j^{(m)} + im/2}{\lambda_j^{(m)} - im/2}. \quad (\text{B.2.7})$$

A big advantage of the string hypothesis is its simplicity. It has been used e.g. for the investigation of the thermodynamics [27]. In order to calculate the partition function one needs the full eigenspectrum. Using the string hypothesis in principle all eigenvalues and their degeneracies can be determined. Note, however, that one proceeds as in Sec. II.6.2 and then obtains an infinite set of coupled integral equations from (B.2.2). Therefore in practice one has to make approximations.

The big disadvantage of the string hypothesis is that — strictly speaking — it is wrong. Considering our derivation it might not be surprising that it fails for finite chain lengths L [28, 29]. Here non-ideal string configurations appear. E.g. for roots λ_j with large real part such that $\text{Re}(\lambda_j) \ll \sqrt{L}$ is not satisfied, the strings are “deformed” significantly [28]. Even the number of complex roots predicted by the string hypothesis can be wrong [29]. Additional real solutions appear that compensate for missing strings.

It has been shown [30–32] that the elementary solutions — besides real roots — of the Bethe Ansatz equations for the isotropic antiferromagnet can be classified as follows:

- 2-strings: $\lambda_j = \lambda_j^{(2)} \pm \frac{i}{2}$
- wide pairs: $\lambda_j = \lambda_j^{(w)} \pm iw$ with $w \geq 1$
- quartets: $\lambda_j = \lambda_j^{(q)} \pm i\eta, \lambda_j^{(q)} \pm i(\pi - \eta)$.

Quartets can be interpreted as two independent bound states [33]. Larger strings can appear accidentally as superposition of these elementary solutions.

Surprisingly many physical quantities are rather robust, i.e. although the string hypothesis is incorrect calculations based on it often yield correct results. An alternative approach to the calculation of thermodynamic properties without using the string hypothesis has been developed in [34]. It is based on a Trotter-Suzuki mapping and the use of inversion relations (see App. B.3). Finally we mention a problem that is not directly related to the string conjecture. It concerns the so-called *singular Bethe states*. E.g. it can be checked directly that the state

$$|\psi\rangle = \sum_{j=1}^L (-1)^j \sigma_j^- \sigma_{j+1}^- |0\rangle \quad (\text{B.2.8})$$

is an eigenstate of the isotropic Heisenberg model. At first sight it appears that this state can not be obtained by the Bethe Ansatz [11, 29, 35]. However, a detailed analysis shows that it is described by diverging wavenumbers $k_j \rightarrow \pm i\infty$. The variables λ_j , in terms of which we have rewritten the Bethe Ansatz equations, are well-behaved, but the coefficients of the Bethe wavefunction are singular. After a suitable rescaling also the state (B.2.8) can be obtained.

B.3 Inversion relations

We have already mentioned in Sec. II.5 the existence of an elegant method for the solution of the Bethe-Ansatz equation that is based on the use of functional equations. The *inversion relation*

method has the big advantage of not being based on the string assumption. Instead it only depends on a finite number of parameters that will turn out to be the rapidities parametrizing the excitation spectrum. In the following we will discuss the approach for the isotropic antiferromagnet. We introduce the functions

$$q(\lambda) := \prod_{l=1}^M (\lambda - \lambda_l), \quad \phi(\lambda) := \lambda^L. \quad (\text{B.3.1})$$

The Bethe-Ansatz equations (II.6.6) can than be interpreted as conditions guaranteeing the analyticity of the function

$$\Lambda(\lambda) := \frac{\phi(\lambda + i/2)q(\lambda - i) + \phi(\lambda - i/2)q(\lambda + i)}{q(\lambda)}. \quad (\text{B.3.2})$$

The denominator has the zeroes λ_j that have to be cancelled by zeroes of the numerator, i.e.

$$\frac{\phi(\lambda_j + i/2)}{\phi(\lambda_j - i/2)} = -\frac{q(\lambda_j + i)}{q(\lambda_j - i)} \quad (\text{B.3.3})$$

which are just the Bethe-Ansatz equations (II.6.6). As already mentioned in Sec. II.5, the equation (B.3.2) can be derived directly from the 6-vertex model where $\Lambda(\lambda)$ turns out to be an eigenvalue of the transfer matrix.

For $\lambda \in U_\delta :=]-\frac{i}{2} - \delta, -\frac{i}{2} + \delta[$, obviously $\phi(\lambda + i/2) = O(\delta^L)$ and therefore

$$\Lambda(\lambda) = \frac{\phi(\lambda - i/2)q(\lambda + i)}{q(\lambda)} + O(\delta^L). \quad (\text{B.3.4})$$

Similarly, after substituting $\lambda \rightarrow \lambda + i$ in (B.3.2) one obtains

$$\Lambda(\lambda + i) = \frac{\phi(\lambda + \frac{3i}{2})q(\lambda)}{q(\lambda + i)} + O(\delta^L). \quad (\text{B.3.5})$$

Multiplying these two equations gives

$$\Lambda(\lambda)\Lambda(\lambda + i) = \phi(\lambda - i/2)\phi(\lambda + \frac{3i}{2}) + O(\delta^L) \quad (\text{B.3.6})$$

for $\lambda \in U_\delta$. Note this relation does no longer contain the Bethe-Ansatz roots λ_j explicitly that only enter via the function $q(\lambda)$. The functional equation (B.3.6) is called *inversion relation* because it implies that the transfer matrices $\mathbf{T}(\lambda)$ and $\mathbf{T}(\lambda + i)$ are basically inverse to each other (see below). It allows to determine the spectrum when some additional information about the analytic properties of the function $\Lambda(\lambda)$ are known.

The inversion relation can also be derived directly from the underlying vertex model. There it is based on the identity shown in Fig. B.3.1 for two vertices with spectral parameters λ and $\lambda + i$. From this local identity one can derive the following relation for the transfer matrix [36–38]:

$$\mathbf{T}(\lambda)\mathbf{T}(\lambda + i) = \phi(\lambda - i/2)\phi(\lambda + \frac{3i}{2}) \left(1 + O((\lambda + i/2)^L)\right) \quad (\text{B.3.7})$$

$$\text{Diagram: A vertical line with points } \alpha, \gamma, \eta, \beta. \text{ A curved path starts at } \lambda \text{ on the line, goes up and to the right, then turns back to the left, ending at } \lambda + i. \text{ To the right of the diagram is an equals sign followed by the expression } f(\lambda) \delta_{\alpha\beta} \delta_{\gamma\eta}.$$

Figure B.3.1: Local identity that leads to the inversion relation for the transfer matrix.

which is just the operator version of (B.3.6).

In order to determine the spectrum from the inversion relation, we need further information about $\Lambda(\lambda)$, especially about its zeroes. It can be shown¹ that the groundstate function $\Lambda_0(\lambda)$ is analytic and has no zeroes in the strip $-1 < \text{Im}(\lambda) < 1$. Note that here qualitatively information about the λ_j enters. Furthermore from the definition (B.3.2) we can determine its asymptotics: $\Lambda(\lambda) \sim \lambda^L$ for $|\lambda| \rightarrow \infty$. These properties together with the inversion relation (B.3.6) determine the function $\Lambda_0(\lambda)$ uniquely (up to a sign):

$$\Lambda_0(\lambda) = z^L(\lambda) \quad (\text{B.3.8})$$

with

$$z(\lambda) = (\lambda - \frac{i}{2})\varphi(\lambda + \frac{i}{2}), \quad \varphi(\lambda) = i \frac{\Gamma(1 + \frac{i\lambda}{2})\Gamma(\frac{1}{2} - \frac{i\lambda}{2})}{\Gamma(1 - \frac{i\lambda}{2})\Gamma(\frac{1}{2} + \frac{i\lambda}{2})} \quad (\text{B.3.9})$$

with the Gamma-function Γ . This result can be derived by taking the logarithm of the inversion relation (which is allowed to the absence of zeroes) and the expanding all functions. However, from the property $\Gamma(z+1) = z\Gamma(z)$ it is easily checked that $z(\lambda)z(\lambda+i) = (\lambda - i/2)(\lambda + \frac{3i}{2})$. The derivative of the transfer matrix at $\lambda = i/2$ yields the Hamiltonian of the quantum chain, up to an additional constant. This can also be seen from (B.3.5) from which after comparing with (II.6.32) we obtain

$$E = 2J \left(i \frac{\partial}{\partial \lambda} \ln \Lambda(\lambda) \Big|_{\lambda=i/2} - L \right). \quad (\text{B.3.10})$$

for the energy of the state described by the eigenvalue $\Lambda(\lambda)$.

The groundstate energy of the Heisenberg antiferromagnet is given by

$$\begin{aligned} E_0 &= 2J \left(i \frac{\partial}{\partial \lambda} \ln \Lambda_0(\lambda) \Big|_{\lambda=i/2} - L \right) = 2JL \left(i \frac{\partial}{\partial \lambda} \ln(\lambda - \frac{i}{2})\varphi(\lambda + \frac{i}{2}) \Big|_{\lambda=i/2} - 1 \right) \\ &= 2JL(1 - 2 \ln 2 - 1) = -4JL \ln 2. \end{aligned} \quad (\text{B.3.11})$$

¹The proof uses methods from complex analysis, e.g. $\frac{1}{2\pi i} \int_c \frac{\Lambda'(\lambda)}{\Lambda(\lambda)} d\lambda = N_z - N_p$ where N_z and N_p are the number of zeroes and poles in the region bounded by the closed path c .

Excitations are correspond to Λ -functions that have zeroes $\theta_1, \dots, \theta_\nu$ in the strip $-1 < \text{Im}(\lambda) < 1$. The excitation function

$$l(\lambda) := \frac{\Lambda(\lambda)}{\Lambda_0(\lambda)} \quad (\text{B.3.12})$$

then satisfies the functional relation

$$l(\lambda)l(\lambda + i) = 1. \quad (\text{B.3.13})$$

Thus the function $l(\lambda)$ is $2i$ -periodic. This functional equation is solved by

$$l(\lambda) = \prod_{j=1}^{\nu} \tanh\left(\frac{\pi}{2}(\lambda - \theta_j)\right) \quad (\text{B.3.14})$$

which can be easily shown using $\tanh(x + i\pi/2) = \coth(x)$. Since all eigenvalues have the asymptotics $\Lambda(\lambda) \propto \lambda^L$ for $|\lambda| \rightarrow \infty$, we have $l(\lambda) \rightarrow 1$ for $\lambda \rightarrow \pm\infty$. This is only satisfied if ν is even, i.e. all excitations appear in pairs. This is not surprising since we have already seen that the elementary excitations are spinons.

The corresponding energy and momentum of the excitations are given by

$$\epsilon(\lambda) = 2Ji \frac{\partial}{\partial \lambda} \ln\left(\tanh\left(\frac{\pi}{2}(\lambda - \theta_j)\right)\right) \Big|_{\lambda=i/2} = \frac{2\pi J}{\cosh(\pi\theta)}, \quad (\text{B.3.15})$$

$$p(\lambda) = i \ln\left(\tanh\left(\frac{\pi}{2}\left(\frac{i}{2} - \theta_j\right)\right)\right) \quad (\text{B.3.16})$$

which yields the spinon dispersion

$$\epsilon(p) = 2\pi J |\sin p| \quad (\text{B.3.17})$$

since $p(\lambda) \in [-\pi, 0]$.

Another important application of these functional equations is the calculation of thermodynamic properties without using the string hypothesis [34]. The idea is first to use the Trotter-Suzuki decomposition to map the quantum problem to a two-dimensional classical problem. The partition function can then be obtained from the largest eigenvalue of an appropriate transfer matrix. The calculation is based on the use of an inversion relation. In contrast to the thermodynamics based on the string hypothesis one only obtains one integral equation instead of an infinite number. However, this equation is nonlinear and in general has to be solved numerically although analytical results can be obtained in some limits (e.g. $T \rightarrow 0$ or $T \rightarrow \infty$).

Bibliography

- [1] J. Hubbard: Proc. Roy. Soc. **A276**, 238 (1963)
- [2] M.C. Gutzwiller: Phys. Rev. Lett. **10**, 159 (1963)
- [3] J. Kanamori: Prog. Theor. Phys. **30**, 275 (1963)
- [4] W. Heisenberg: Z. Phys. **49**, 619 (1928)
- [5] R.J. Baxter: Ann. Phys. **70**, 323 (1972); **76**, 1, 25, 48 (1973)
- [6] R.J. Baxter: *Exactly Solved Models in Statistical Mechanics*, Academic Press (1982)
- [7] P. Jordan, E. Wigner: Z. Phys. **47**, 631 (1928)
- [8] E. Lieb, T. Schultz, D. Mattis: Ann. Phys. **16**, 407 (1961)
- [9] S. Katsura: Phys. Rev. **127**, 1508 (1962)
- [10] O. Derzhko: [de.arxiv.org/abs/cond-mat/0101188](https://arxiv.org/abs/cond-mat/0101188)
- [11] H. Bethe: Z. Phys. **71**, 205 (1931)
- [12] R. Orbach: Phys. Rev. **112**, 309 (1958)
- [13] L.R. Walker: Phys. Rev. **116**, 1089 (1959)
- [14] C.N. Yang, C.P. Yang: Phys. Rev. **150**, 327 (1966)
- [15] L. Onsager: Phys. Rev. **65**, 117 (1944)
- [16] V.F.R. Jones: Scientific American, November 1990, p. 52
- [17] M. Wadati, T. Deguchi, Y. Akutsu: Phys. Rep. **180**, 247 (1989)
- [18] V.E. Korepin, N.M. Bogoliubov, A.G. Izergin: *Quantum Inverse Scattering Method and Correlation Functions* (Cambridge University Press, 1993)
- [19] M. Karbach, G. Müller: Comp. in Phys. **11**, 36 (1997) [[cond-mat/9809162](https://arxiv.org/abs/cond-mat/9809162)]
M. Karbach, K. Hu, G. Müller: Comp. in Phys. **12**, 565 (1998) [[cond-mat/9809163](https://arxiv.org/abs/cond-mat/9809163)]
M. Karbach, K. Hu, G. Müller: [cond-mat/0008018](https://arxiv.org/abs/0008018)

- [20] L. Hulthen: Arkiv Mat., Astr. Fys. **26A**, 1 (1938)
- [21] J. des Cloiseaux, J.J. Pearson: Phys. Rev. **128**, 2131 (1962)
- [22] A.A. Ovchinnikov: Sov. Phys. JETP **29**, 727 (1969)
- [23] L.D. Faddeev, L.A. Takhtajan: Phys. Lett. **85**, 375 (1981)
- [24] J.D. Johnson, S. Krinsky, B.M. McCoy: Phys. Rev. **A8**, 2526 (1973)
- [25] P.W. Anderson: Science **235**, 1196 (1987)
- [26] M. Arai, M. Fujita, M. Motokawa, J. Akimitsu, S.M. Bennington: Phys. Rev. Lett. **77**, 3649 (1996)
- [27] M. Takahashi: *Thermodynamics of One-Dimensional Solvable Models*, Cambridge University Press (1999)
- [28] A.A. Vladimirov: Phys. Lett. **A105**, 418 (1984)
- [29] F.H.L. Eßler, V.E. Korepin, K. Schoutens: J. Phys. **A25**, 4115 (1992)
- [30] C. Destri, J.H. Lowenstein: Nucl. Phys. **B205**, 369 (1982)
- [31] O. Babelon, H.J. de Vega, C.M. Viallet: Nucl. Phys. **B220**, 13 (1983)
- [32] F. Woynarovich: J. Phys. **A15**, 2985 (1982)
- [33] F. Woynarovich: J. Phys. **C15**, 6397 (1982)
- [34] A. Klümper: Z. Phys. **B91**, 507 (1993)
- [35] R. Siddharthan: [cond-mat/9804210](https://arxiv.org/abs/cond-mat/9804210)
- [36] P.A. Pearce: Phys. Rev. Lett. **58**, 1502 (1987)
- [37] A. Klümper, J. Zittartz: Z. Phys. **B71**, 495 (1988) and **B75**, 371 (1989)
- [38] A. Klümper, A. Schadschneider, J. Zittartz: Z. Phys. **B76**, 247 (1989)